# FURTHER INVESTIGATION OF A KINETIC MODEL TO ACCURATELY PREDICT EVAPORATION OF GASOLINE

By

Natasha Kimberley Eklund

## A THESIS

Submitted to
Michigan State University
in partial fulfillment of the requirements
for the degree of

Forensic Science – Master of Science

#### ABSTRACT

# FURTHER INVESTIGATION OF A KINETIC MODEL TO ACCURATELY PREDICT EVAPORATION OF GASOLINE

By

#### Natasha Kimberley Eklund

In fire debris analysis, analysts compare chromatograms of extracts of fire debris to a database containing chromatograms of ignitable liquid reference standards. Typically, the database will contain chromatograms of experimentally evaporated liquids. Unfortunately, experimentally evaporating ignitable liquids can be a time-consuming process. Previously, a mathematical model was developed with diesel that predicts the evaporation rate constant of compounds as a function of retention index ( $I^T$ ). The model can be used to generate predicted chromatograms of evaporated liquids. In comparing predicted to experimental chromatograms, predictive accuracy was high for comparisons using diesel, torch fuel, and marine fuel stabilizer.

This research aims to improve the predictive accuracy of the model with respect to gasoline and to test the feasibility of developing correlation coefficient ranges for the classification of an ignitable liquid residue as gasoline. Improvement of the predictive accuracy of the model involved changes to the instrumental parameters and data analysis procedures. The feasibility of development of PPMC coefficient ranges involved comparisons of predicted reference collections of a non-gasoline ignitable liquid to chromatograms of experimentally evaporated gasoline

#### **ACKNOWLEDGMENTS**

I would like to first and foremost thank my advisor, Dr. Ruth Smith, for the opportunity to join this program and for her continued guidance throughout the process. I would also like to thank Dr. Victoria McGuffin for support and feedback with my research, and for serving on my committee. I would also like to thank Dr. Mahesh Nalla for volunteering his time and energy to serve on my committee, especially on such short notice.

Additionally, I'd like to extend gratitude to the members of the forensic chemistry group for providing feedback on both my thesis document and presentation, specifically Amanda Setser, Becca Boyea, Emma Stuhmer, Otyllia Abraham, Amber Gerheart, Briana Capistran, Hannah Clause, Lizzie Ritter, Andrew Sacha, Caroline Colpoys, and Breanna Koslowski. I also appreciate Alex Anstett and Trevor Curtis for introducing me to the laboratory and Michigan State as a whole, as well as providing feedback on early presentations.

My mom, Sandy, was always ready with a fun story about the past when I was having a rough time and always tried to understand my research, despite all that was happening with her. My dad, Daniel, as well as Laura Hendrick, Alex Eklund, and Rebecca Bourlier have been a joy to return to on the weekends and have provided a solid foundation through this process. My friends who lived nearby, specifically Jonathan Quirke, Nicole Fricke, and Emily Rogers, have been pillars of strength for me with both my research and personal life. Finally, my love and gratitude to Josh Parker, for always being there for me and doing all he could to help, including write some programs used in this thesis.

# TABLE OF CONTENTS

LIST OF TABLES	vii
LIST OF FIGURES	ix
I. Introduction	1
1.1. Fire Debris Analysis	1
1.2 Gas Chromatography-Mass Spectrometry (GC-MS)	1
1.2.1. Gas Chromatography	1
1.2.2. Mass Spectrometry	
1.3 Identification and Classification of Ignitable Liquids	12
1.4. Evaporation of Ignitable Liquids	
1.5. Modeling the Evaporation of Ignitable Liquids	16
1.6. Research Objectives	
REFERENCES	25
II. Materials and Methods	28
2.1 Ignitable Liquid Sample Collection	
2.2 Evaporation and Preparation of Ignitable Liquids	
2.3 GC-MS Instrument Parameters	
2.4 Data Analysis	
2.5 Python Programs Developed to Automate Calculation of <i>t</i>	
2.5.1 Predicting Chromatograms Corresponding to Specified FR <sub>total</sub>	
2.5.2 Comparison of Experimental Chromatograms to Predicted Chromatograms to	
Determine Highest Possible Correlation	
APPENDICES	
APPENDIX A: Python Code to Predict Chromatograms Corresponding to Specified APPENDIX B: Python Code to Compare Experimental Chromatograms to Predicted	
Chromatograms to Determine Highest Possible Correlation	
REFERENCES	41
III. Instrument and Method Modifications to Improve Accuracy in Predicting Evaporat	ion of
Gasoline	
3.1 Experimental Evaporation of Gasoline	
3.2 Current Limitations in Predicting Chromatograms Corresponding to Evaporated	
3.3 Refinement of Instrumental and Data Processing Parameters to Improve Correlation	
between Experimental and Predicted Chromatograms	
3.4 Changing the Method of Calculation of F <sub>total</sub>	
3.5. Changing the Method of Calculation of F <sub>total</sub> with Torch Fuel	
3.6 Summary	
APPENDICES	69

APPENDIX A: Mean PPMC coefficients calculated between experimental ch (n=3) and chromatograms predicted using different methods of calculating F <sub>tc</sub>	
extension and background subtraction.	
APPENDIX B: F <sub>total</sub> of experimental chromatograms (n=3) calculated using d	
for gasoline samples, after I <sup>T</sup> range extension and background subtraction	
APPENDIX C: Differences in F <sub>total</sub> of experimental chromatograms (n=3) cale	
different methods for gasoline samples after I <sup>T</sup> range extension and backgroun	
REFERENCES	
XEFERENCES	•••••
IV: Application of a Kinetic Model to Generate an Ignitable Liquid Reference C	Collection for
Identification Purposes	
4.1 Gasoline Samples	
4.2 Comparison of Chromatograms of Experimentally Evaporated Gasoline to	o Chromatogran
Predicted Using Unevaporated Gasoline of the Same Source	
4.3 Comparison of Chromatograms of Experimentally Evaporated Gasolines	to
Chromatograms Predicted Using Gasolines of Different Sources	
4.4 Comparison of Chromatograms of Experimentally Evaporated Gasoline to	o Chromatograi
Predicted Using Ignitable Liquids of Other ASTM Classes	
4.5. Summary	
APPENDICES	
APPENDIX A. Maximum PPMC coefficients ± standard deviation and the co	orresponding
F <sub>total</sub> , calculated between experimental chromatograms and (a) the gasoline A	reference
collection and (b) the optimized predicted chromatogram using unevaporated	•
APPENDIX B. Maximum PPMC coefficients ± standard deviation and the co	1 0
F <sub>total</sub> , calculated between experimental chromatograms and (a) the gasoline B	reference
collection and (b) the optimized predicted chromatogram using unevaporated	gasoline B1
APPENDIX C. Maximum PPMC coefficients ± standard deviation and the co	orresponding
F <sub>total</sub> , calculated between experimental chromatograms and (a) the gasoline C	reference
collection and (b) the optimized predicted chromatogram using unevaporated	gasoline C1
APPENDIX D. Maximum PPMC coefficients ± standard deviation and the co	orresponding
F <sub>total</sub> , calculated between experimental chromatograms and (a) the gasoline E	reference
collection and (b) the optimized predicted chromatogram using unevaporated	gasoline E1
APPENDIX E. Maximum PPMC coefficients ± standard deviation and the co	rresponding
F <sub>total</sub> , calculated between experimental chromatograms and (a) the gasoline F	reference
collection and (b) the optimized predicted chromatogram using unevaporated	gasoline F1
APPENDIX F. Maximum PPMC coefficients ± standard deviation and the co	rresponding
F <sub>total</sub> , calculated between experimental chromatograms and (a) the gasoline G	reference
collection and (b) the optimized predicted chromatogram using unevaporated	gasoline G1
APPENDIX G. Maximum PPMC coefficients ± standard deviation and the co	orresponding
F <sub>total</sub> , calculated between experimental chromatograms and (a) the gasoline H	
collection and (b) the optimized predicted chromatogram using unevaporated	
APPENDIX H. Maximum PPMC coefficients and standard deviation compar	
chromatograms to reference chromatogram predicted from unevaporated char	~ 1
APPENDIX I. Maximum PPMC coefficients and standard deviation comparis	
chromatograms to reference chromatogram predicted from unevaporated pain	

APPENDIX J. Maximum PPMC coefficients and standard deviation comparing chromatograms to reference chromatogram predicted from the unevaporated adh	
remover	116
APPENDIX K. Maximum PPMC coefficients and standard deviation comparing chromatograms to reference chromatogram predicted from unevaporated marine	
stabilizer.	118
V. Conclusions and Future Directions	120
5.1. Conclusions	120
5.2. Future Directions	122
REFERENCES	126

## LIST OF TABLES

Table 1.1. Ignitable liquid classification scheme used in ASTM E1618-14.612
Table 2.1. Sources of gasoline used in this research
Table 2.2. Non-gasoline ignitable liquids used in this research
Table 3.1. Mean PPMC coefficients calculated between experimental and predicted chromatograms using original GC-MS parameters (predicted and compared over $I^T = 700-1385$ ). The $\pm$ indicates standard deviation, calculated based on n=3
Table 3.2. List of compounds observed with $I^T < 700$ (plus toluene) using the 100-m and 30-m DB-1 columns
Table 3.3. Mean PPMC coefficients calculated between experimental and predicted gasoline A chromatograms before and after $I^T$ range extension and with background subtraction (n=3). In this and all subsequent tables, gasolines will be abbreviated in the form Gas @-#-0.1 where Gas @ is the source of gasoline being analyzed, # is the day analyzed, and 0.1 is the approximate experimental $F_{total}$ calculated by mass.
Table 3.4. Mean PPMC coefficients calculated between experimental gasoline B and C chromatograms (n=3) and corresponding predicted chromatograms before and after I <sup>T</sup> range extension and after subsequent background subtraction.
Table 3.5. Mean PPMC coefficients calculated between experimental chromatograms (n=3) and chromatograms predicted using different methods of calculating F <sub>total</sub> , after I <sup>T</sup> range extension and background subtraction, for a subset of gasoline samples tested. Corresponding F <sub>total</sub> values can be found in Table 3.6
Table 3.6. F <sub>total</sub> of experimental chromatograms (n=3) calculated using different methods for gasoline samples, after I <sup>T</sup> range extension and background subtraction, for a subset of gasolines.
Table 3.7. Differences in $F_{total}$ of experimental chromatograms (n=3) calculated using different methods for gasoline samples after $I^T$ range extension and background subtraction, for a subset of gasolines.
Table 3.8. Mean PPMC coefficients calculated between experimental chromatograms (n=3) and chromatograms predicted using optimization of F <sub>total</sub> for gasoline samples with varying degrees of refinement of analysis.

Table 3.9. PPMC coefficients calculated between experimental chromatograms (n=3) of gasolines B and C and chromatograms predicted using $F_{total}$ calculated by mass and area with varying degrees of refinement of analysis.
Table 3.10. F <sub>total</sub> calculated by mass and area for experimental chromatograms (n=3) of gasolines B and C after varying degrees of refinement of analysis
Table 3.11. Experimental F <sub>total</sub> of torch fuel calculated by mass and by area and corresponding representative PPMC coefficients (n=3)
Table 4.1. Mean PPMC coefficients calculated between injections of the same unevaporated gasoline on the same day and on different days. The $\pm$ indicates standard deviation80
Table 4.2. PPMC coefficients calculated for comparisons of unevaporated gasoline samples from different sources (Gasoline A-H).
Table 4.3. Mean PPMC coefficients calculated for comparisons of experimental chromatograms ( $F_{total} = 0.1, 0.3$ , and 0.5 by mass) to a predicted reference collection developed using gasoline of the same source as the experimentally evaporated gasoline, gasoline A set 1 here85
Table 4.4. Maximum PPMC coefficients calculated for comparisons of experimental chromatograms ( $F_{total} = 0.1, 0.3, \text{ and } 0.5 \text{ by mass}$ ) to a predicted reference collection developed using gasoline of the same source as the experimentally evaporated gasoline86
Table 4.5. Predicted reference collection $F_{total}$ values corresponding to the maximum PPMC coefficients calculated for comparisons of experimental chromatograms ( $F_{total} = 0.1, 0.3, \text{ and } 0.5$ by mass) to a predicted reference collection developed using gasoline of the same source as the experimentally evaporated gasoline.
Table 4.6. Maximum PPMC coefficients between gasolines E and F, set 1, and the gasoline A reference collection, with the F <sub>total</sub> of the corresponding reference collection chromatogram90

## LIST OF FIGURES

Figure 1.1. Diagram of a gas chromatography instrument
Figure 1.2. Chromatogram of a gasoline sample4
Figure 1.3. Chromatogram of a mixture of <i>n</i> -alkane reference standards5
Figure 1.4. Diagram of an electron ionization source, where M represents a neutral analyte molecule, e- represents an electron, and + represents any positively charged molecular or fragment analyte ions.
Figure 1.5. Side view of a quadrupole mass analyzer7
Figure 1.6. Diagram of an electron multiplier tube
Figure 1.7. Mass spectra of a) compound at retention time 3.159 min from the gasoline chromatogram in Figure 1.2, b) heptane at retention time 3.159 min from the chromatogram of standards in Figure 1.3, and c) heptane standard from the NIST Chemistry Webbook.99
Figure 1.8. Mass spectra of <i>o</i> -, <i>m</i> -, and <i>p</i> -dimethylbenzene (also known as xylene)11
Figure 1.9. Experimental decay curves for <i>n</i> -octane (a) and <i>n</i> -decane (b). Abundances were normalized to the peak height of heneicosane in the extracted ion chromatogram at $m/z$ 57. First-order rate equations for <i>n</i> -octane: $C_t = 0.448 \ exp(-0.226t)$ , for <i>n</i> -decane: $C_t = 5.926 \ exp(-0.0201t)^5$ .
Figure 1.10. Natural logarithm of evaporation rate constant versus retention index on 100% dimethylpolysiloxane GC column for compound classes: normal alkanes (square), branched and cyclic alkanes (circle), alkyl benzenes (diamond), and polycyclic hydrocarbons (triangle). Linear regression equation: $ln(k) = -0.0104 I^T + 6.70^5$ .
Figure 2.1. Example optimization curve generated using the Python script34
Figure 3.1. Chromatogram of unevaporated gasoline A, normalized to n-tetradecane (not shown).
Figure 3.2. Comparison of chromatograms of unevaporated (blue), F <sub>total</sub> = 0.5 (yellow), and F <sub>total</sub> = 0.1 (green) by mass of gasoline A

Figure 3.3. Comparison of a chromatogram of experimentally evaporated $F_{total} = 0.5$ by mass gasoline A (orange) with the corresponding predicted chromatogram (blue)48
Figure 3.4. Comparison of a chromatogram of experimentally evaporated $F_{total} = 0.3$ by mass gasoline A (orange) with the corresponding predicted chromatogram (blue)49
Figure 3.5. Comparison of a chromatogram of experimentally evaporated $F_{total} = 0.1$ by mass gasoline A (orange) with the corresponding predicted chromatogram (blue)49
Figure 3.6. Chromatogram of unevaporated gasoline A analyzed on the 100-m column.  Compound identities are listed in Table 3.2
Figure 3.7. Chromatogram of unevaporated gasoline A analyzed on the 30-m column with the extended I <sup>T</sup> range. Compound identities are listed in Table 3.2
Figure 3.8. Gasoline A with $F_{total} = 0.1$ by mass (orange) analyzed on the 30-m column with corresponding predicted chromatogram (blue). Cyclohexene and chloroform are solvent impurities.
Figure 3.9. Workflow used to determine optimized F <sub>total</sub>
Figure 4.1. Chromatograms of unevaporated gasoline samples A-H83
Figure 4.2. Workflow used to compare chromatograms of experimentally evaporated gasoline to reference collections.
Figure 4.3. Overlay of the aromatic product predicted to $F_{total} = 0.2$ (blue) and Gas C-2-0.3 (orange). The $I^T$ range is such that all compounds in the aromatic product are shown93
Figure 4.4. Chromatograms of unevaporated gasoline A, adhesive remover (aromatic class), charcoal lighter (petroleum distillate) marine fuel stabilizer (naphthenic-paraffinic), paint thinner (isoparaffinic), and gasoline A evaporated to F <sub>total</sub> 0.1 by mass

#### I. Introduction

#### 1.1. Fire Debris Analysis

Arson is defined by the Federal Bureau of Investigation's Uniform Crime Reporting (UCR) Program as the willful or malicious burning or attempted burning of property<sup>1</sup>. In 2010, over 15,000 law enforcement agencies reported 56,825 arson cases total to the UCR program, with reporting time period ranging from 1-12 months depending on the agency. More recent data from the United States Bomb Data Center's 2017 Arson Incident Report notes that arson incidents accounted for 31% of all fires reported, with 20% of arson incidents reported to involve an accelerant, such as an ignitable liquid. Use of ignitable liquids such as gasoline or lighter fluid as accelerants leads to increased damage due to increased speed and spread of the fire. Gasoline is the most common ignitable liquid used in arson cases, likely due to its wide availability and effectiveness as an accelerant<sup>2</sup>.

When arson is suspected, fire investigators collect debris from the site to test for the presence of an ignitable liquid. While ignitable liquids may be present at a scene for benign reasons and not as a result of an intentional fire, the presence is an indication that the fire may have been intentionally set. Analysis for the presence of ignitable liquids consists of a solvent extraction or headspace sampling process to remove ignitable liquid residue from fire debris. The extracted sample is then analyzed by gas chromatography-mass spectrometry (GC-MS).

### 1.2 Gas Chromatography-Mass Spectrometry (GC-MS)

#### 1.2.1. Gas Chromatography

Gas-liquid chromatography consists of a liquid stationary phase coated on the inside of a fused-silica capillary column, through which carrier gas (*e.g.*, He, H<sub>2</sub>, or N<sub>2</sub>) flows as the mobile phase<sup>3</sup> (Figure 1.1). The liquid sample to be tested is injected into an injection port, which is

kept at a high temperature, such as 250 °C, in order to vaporize the sample. The vaporized sample then condenses on the column, held in the oven at a cooler temperature, to create a concentrated plug of sample. The column is held in an oven, which can be held isothermal or programmed to increase the temperature as a function of time. Under temperature programmed conditions, the compounds within the sample stay at the start of the column until the oven temperature reaches the boiling point of a compound. As the oven temperature increases, the boiling points of various compounds within the sample are reached, the compounds enter the gas phase and move through the column, eventually elute, and are transferred to the detector.

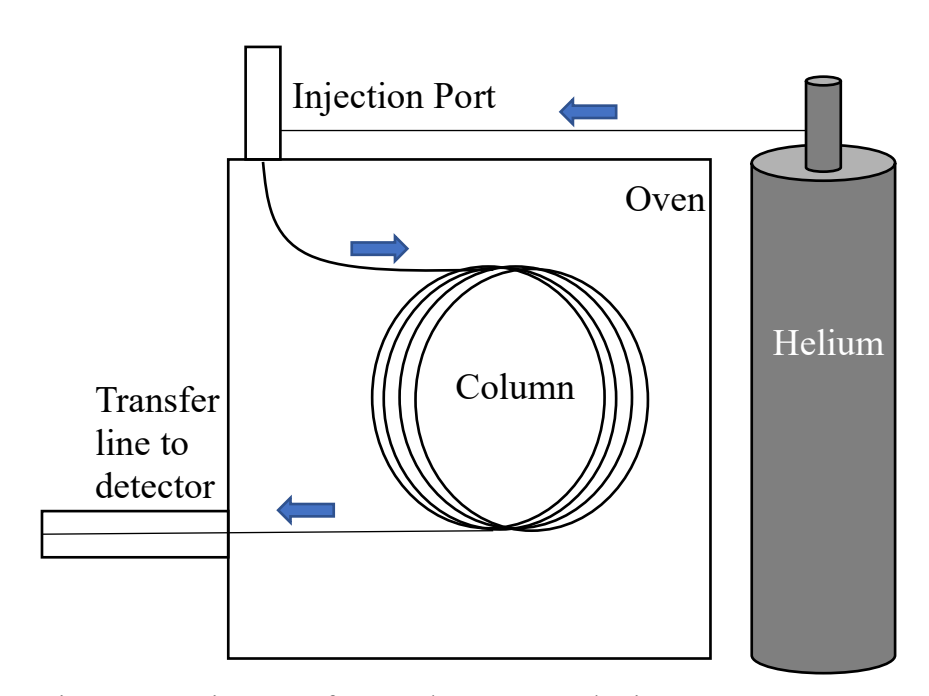


Figure 1.1. Diagram of a gas chromatography instrument.

Under temperature-programmed conditions, the temperature change of the oven, and therefore column, causes compounds to elute based on a combination of boiling point and interaction with the stationary phase. Elution under isothermal conditions is also based on a combination of boiling point of compounds and interaction with the stationary phase. A 100%

dimethylpolysiloxane stationary phase is highly nonpolar and consistent with the type of column used to analyze ignitable liquids for the Ignitable Liquids Reference Collection (ILRC) by the National Center for Forensic Science (NCFS)<sup>4</sup>. While there is the possibility of interaction between this stationary phase and the sample components, the similarity of polarity of compounds common to fire debris and the 100% dimethylpolysiloxane stationary phase leads separation to be based primarily on boiling point of the compounds.

Retention time ( $t_r$ ), the time a compound takes to elute from the GC column, can be converted to retention index ( $I^T$ ), a more robust measure of elution. Retention index is dependent only on the composition of the GC stationary phase and, thus, is independent of other parameters such as column dimensions and oven temperature program<sup>5</sup>. Retention index ( $I^T$ ) is calculated from retention time using a series of normal alkanes. Each alkane is defined by 100n, where n is the number of carbons in the alkane. For example, hexane ( $C_6$ ) is defined as  $I^T = 600$  and nonane ( $C_9$ ) is defined as  $I^T = 900$ . The retention index for each retention time between the alkanes is calculated for temperature-programmed conditions using

$$I_{\chi}^{T} = 100n + 100 \frac{(t_{\chi} - t_{n})}{(t_{(n+1)} - t_{n})}$$
(1.1)

where  $t_x$  is the retention time of the compound of interest, n is the number of carbons in the closest alkane with a lower retention time than  $t_x$ ,  $t_n$  is the retention time of the normal alkane with n carbons,  $t_{(n+1)}$  is the retention time of the normal alkane with n+1 carbons, and  $I_x^T$  is the retention index corresponding to  $t_x^5$ .

After traveling through the column, compounds are transferred to the mass spectrometer for detection. The transfer line is typically kept at a high temperature, such as 280 °C, as compounds need to enter the detector in the gaseous phase. Many different types of detectors are available for gas chromatography; however, in forensic analyses, and particularly fire debris

analysis, a mass spectrometer is the most common detector used. The total abundance as recorded by the mass spectrometer is plotted against retention time  $(t_r)$  to produce a total ion chromatogram (Figure 1.2). In this work, all chromatograms are total ion chromatograms and will be referred to as chromatograms. The identity of a compound can be determined by the comparison of the  $t_r$  in the sample to the  $t_r$  in a reference standard analyzed under equivalent conditions. For instance, the labeled compound in the gasoline chromatogram (Figure 1.2) can be preliminarily identified as n-heptane due to elution at the same time as the n-heptane reference standard in Figure 1.3. However, GC alone is not a confirmatory technique, as multiple compounds may elute at the same  $t_r$  for a given set of conditions. Mass spectrometry (MS) on the other hand, is considered a confirmatory technique due to the structural elucidation abilities of the technique.

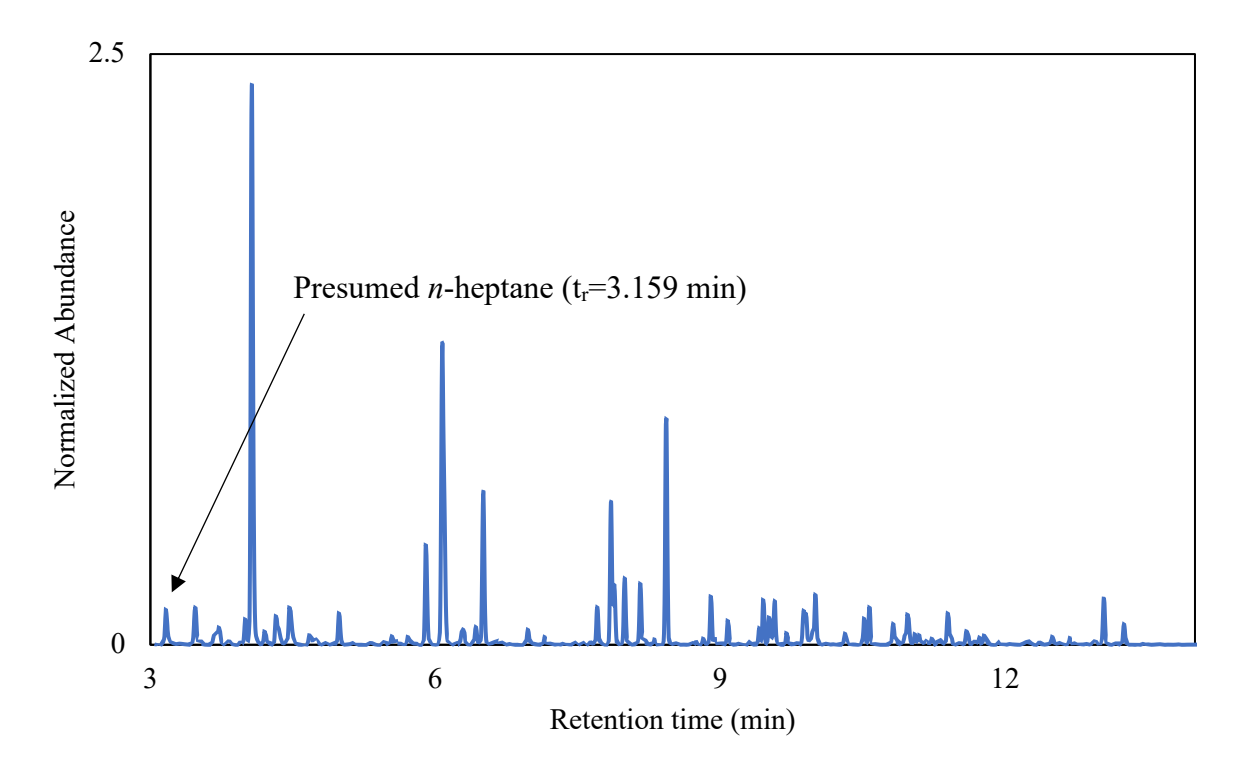


Figure 1.2. Chromatogram of a gasoline sample.

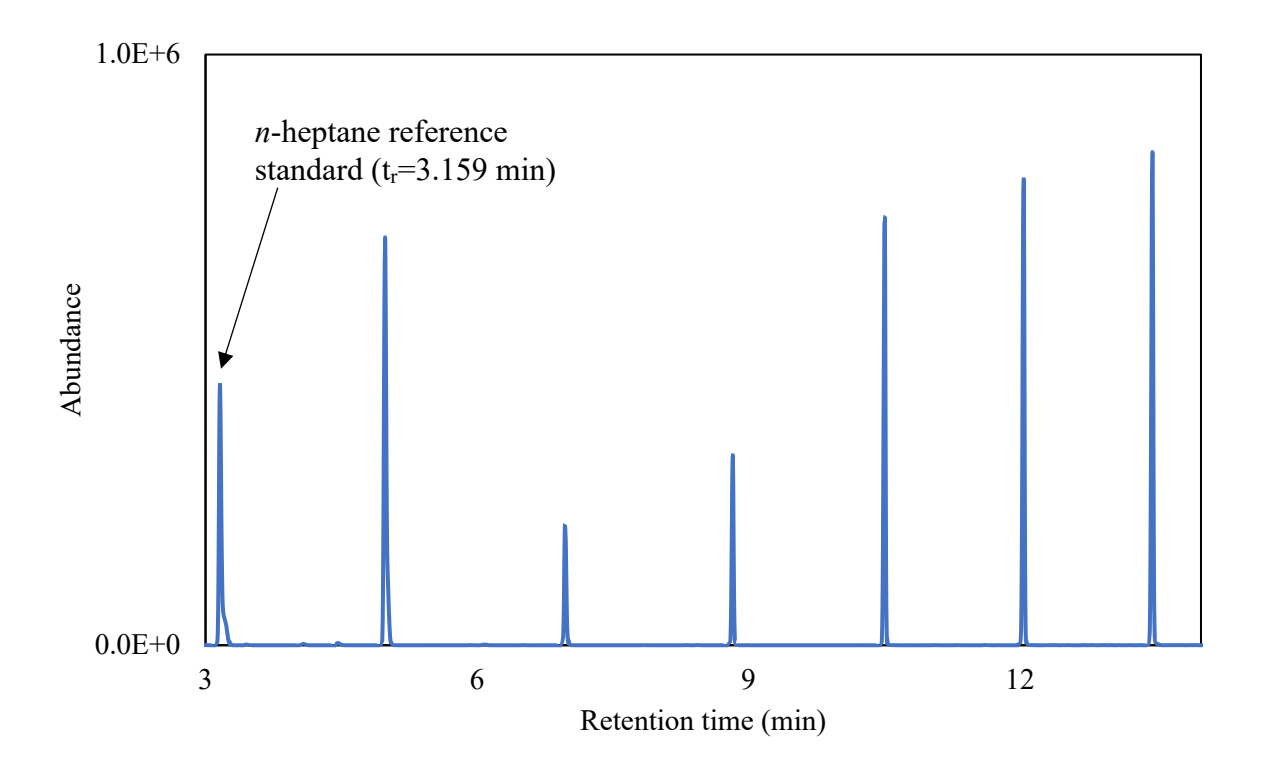


Figure 1.3. Chromatogram of a mixture of *n*-alkane reference standards.

### 1.2.2. Mass Spectrometry

The American Society for Testing and Materials (ASTM) has developed guidelines for testing fire debris samples, with specific guidelines for analyzing extracted ignitable liquid residues by GC-MS (ASTM E1618-14)<sup>6</sup>. The only specification for a mass spectrometer (MS) is unit resolution or better, a requirement that is fulfilled by a single-quadrupole mass analyzer. For benchtop GC-MS instruments, the MS is typically a single quadrupole with an electron ionization source and an electron multiplier detector.

In electron ionization, a positive charge is imparted on the gaseous phase neutral analyte molecule through loss of an electron. A heated tungsten filament emits electrons with 70 eV, which are accelerated towards an anodic electron trap, crossing the path of the neutral analyte<sup>7</sup>. Magnets are placed above the electron trap and below the filament to ensure electrons travel in a

curved trajectory in order to maximize the probability of interactions between the electrons and the analyte molecules (Figure 1.4). Upon interaction with the sample, some of the kinetic energy the electron is carrying is transferred to the analyte molecule, overcoming the first ionization potential and causing ejection of an electron from the molecule. After ionization, there is typically sufficient excess energy for fragmentation of the molecular analyte ion to occur. Ions resulting from electron ionization are typically singly charged. After ionization, a repeller with a positive charge repels the positively charged molecular and fragment analyte ions and is placed such that the ions will be pushed towards accelerating and focusing lenses, which lead to the mass analyzer.

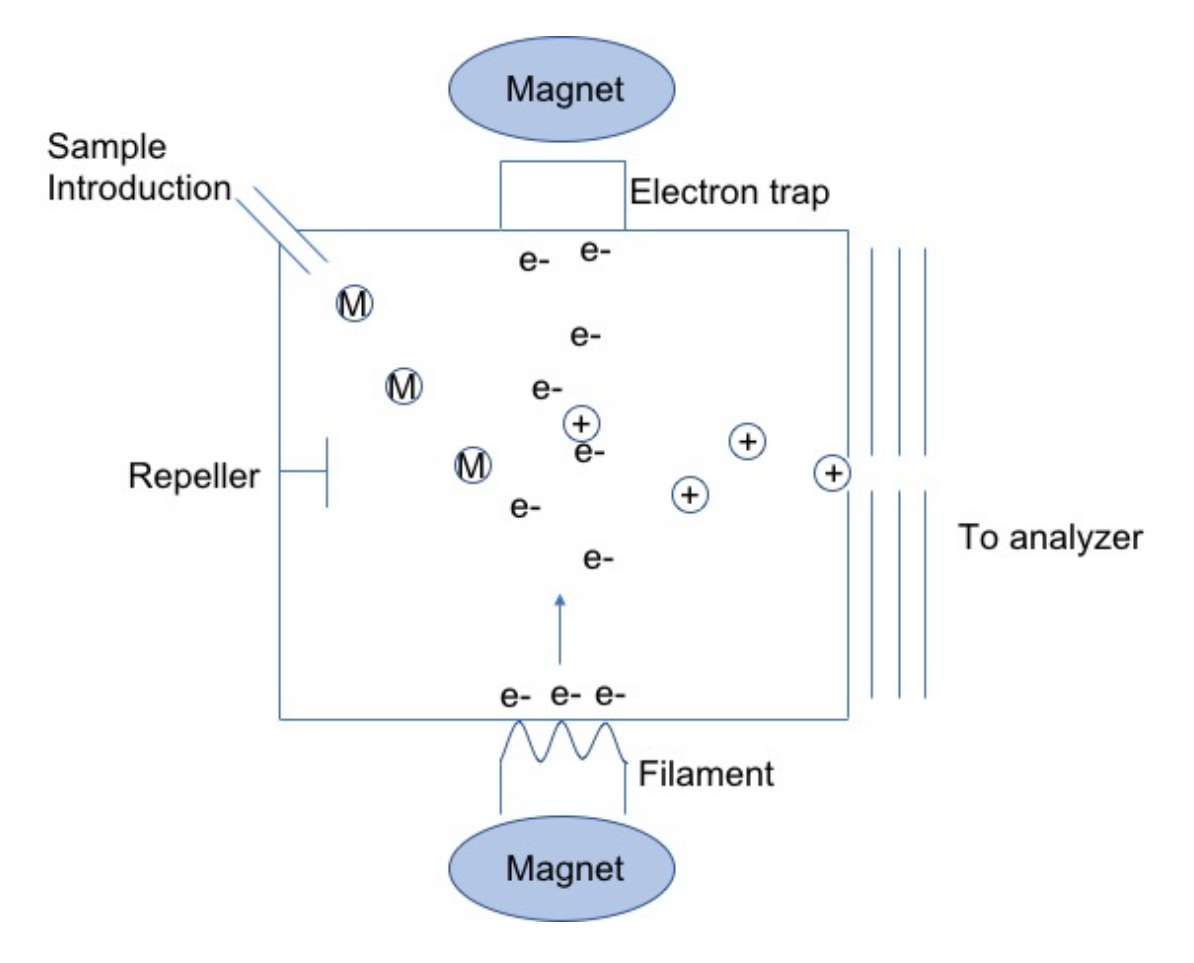


Figure 1.4. Diagram of an electron ionization source, where M represents a neutral analyte molecule, e- represents an electron, and + represents any positively charged molecular or fragment analyte ions.

The mass analyzer commonly used in fire debris analysis is a single quadrupole due to the low cost and unit resolution, which is sufficient according to ASTM guidelines<sup>6</sup>. The quadrupole consists of four rods, with either circular or hyperbolic cross-sections, that are perfectly parallel. Opposing rods have the same charge as determined by a direct current (DC), with one set being positively charged and the other negatively charged (Figure 1.5)<sup>8</sup>. These charges are switched continuously in order to allow ions to pass through the quadrupole. A radiofrequency (RF) voltage is also applied, which in combination with the DC voltage, allows a stable trajectory through the quadrupole for ions of a certain mass-to-charge (m/z) value or range. After passing through the quadrupole, the ion will be transferred to the detector. If the m/z value of the ion is not selected for by the DC/RF ratio, the trajectory through the quadrupole will not be stable and the ion will be annihilated on one of the rods. When the quadrupole is operated in scan mode, the DC/RF ratio is held constant and the magnitudes are changed. While other mass analyzers are capable of better resolution, quadrupoles are noticeably cheaper while still sufficient for analysis of fire debris evidence. The mass analyzer of choice for many forensic science laboratories, therefore, is the quadrupole.

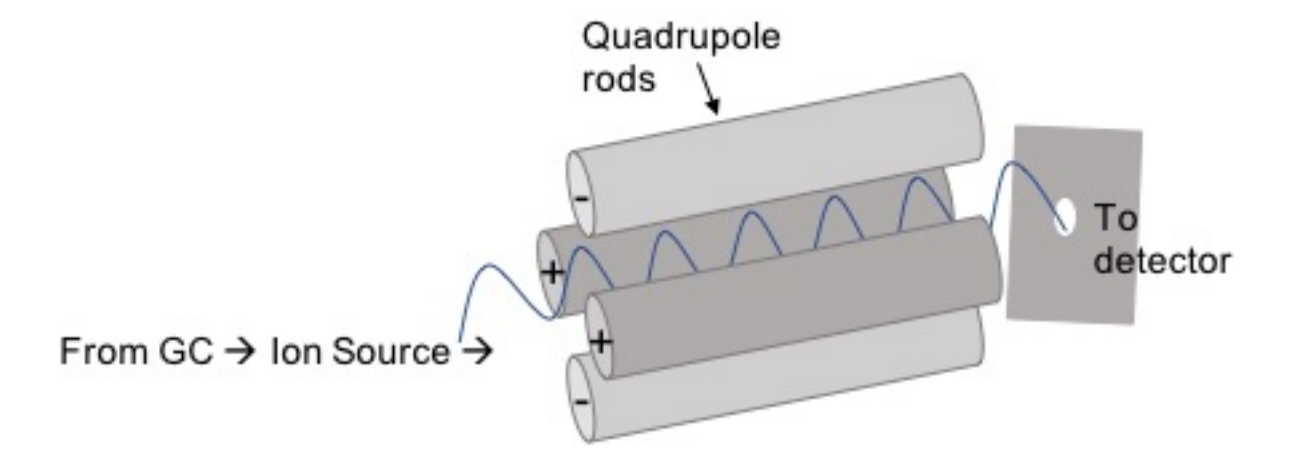


Figure 1.5. Side view of a quadrupole mass analyzer.

After being separated by m/z value, ions must be detected and counted. In benchtop GC-MS instruments, the common detector is an electron multiplier. In an electron multiplier, the positively charged ions from the quadrupole are accelerated to a high velocity toward an initial electrode at a high negative potential. When the ion strikes the electrode, secondary electrons are emitted. These secondary electrons then hit the multiplier tube to emit further secondary electrons (Figure 1.6). The multiplier tube has a uniform electric resistance, allowing an applied voltage to produce an accelerating field down the tube. The secondary electron cascade continues down the electron multiplier tube, amplifying the signal, until collection at an anode where a current is measured<sup>8</sup>. The current is related to abundance of the ion, which leads to a mass spectrum via a data analysis system as the m/z value is scanned by the quadrupole mass analyzer.

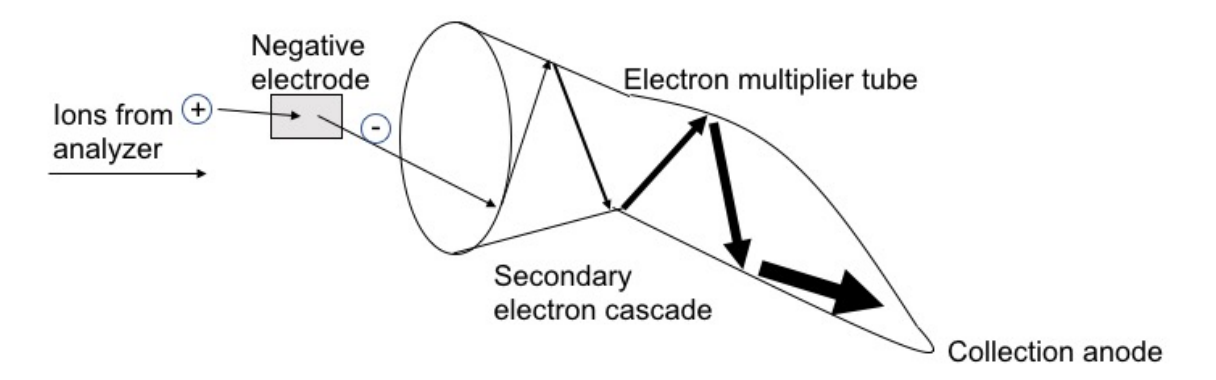


Figure 1.6. Diagram of an electron multiplier tube.

The mass spectrum is characteristic of a compound and, as such, can be compared to a library of mass spectra of known compounds for identification purposes. For instance, the labeled compound in Figure 1.2 discussed earlier as being presumptively identified as heptane based on comparison to a reference standard using GC retention time alone can be confirmed by reviewing the mass spectrum. The mass spectrum has ions at m/z 43, 57, 71, and 100, and the m/z values as well as the pattern in abundance ratios is consistent with that found in the standard

analyzed under the same conditions (Figure 1.7 a, b). The molecular ion is useful for identification purposes, in the case of n-heptane the molecular ion is at m/z 100. Since all n-alkanes contain the ions at m/z 43, 57, and 71, the additional ion at m/z 100, with no ions present at higher m/z values, identifies this mass spectrum as n-heptane as opposed to a different n-alkane. The mass spectrum of the sample can be compared to an in-house library or an outside source such as the National Institute for Standards and Technology (NIST) chemistry webbook if standards are not available (Figure 1.7 c). Fragmentation patterns and fragments are unique for a set of isomeric compounds under specific MS conditions, and can therefore be used to help identify the compound. In many cases isomeric compounds cannot be distinguished by fragmentation pattern. For example, the o-, m-, and p-dimethylbenzenes have nearly identical fragmentation (Figure 1.8). If desired, distinction between the compounds can be achieved using comparison of GC  $t_r$  to that of standards.

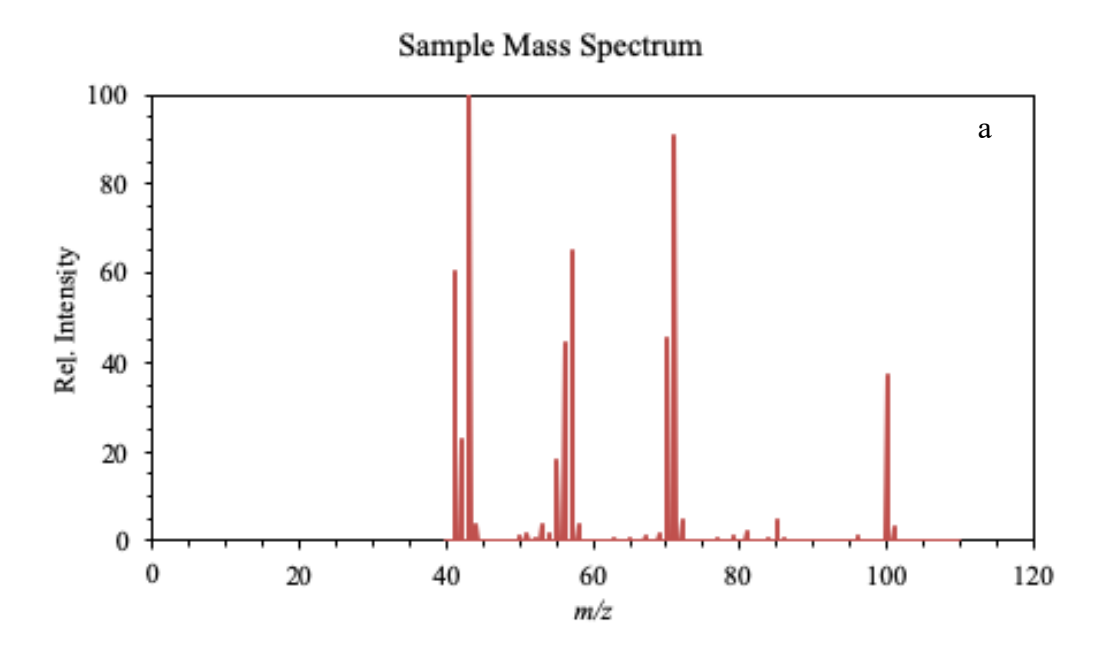
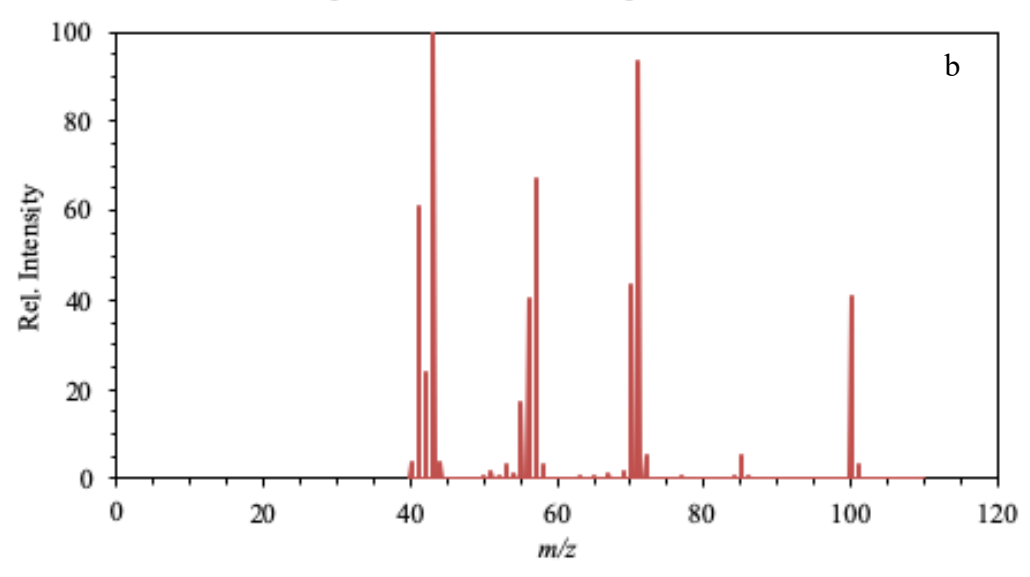
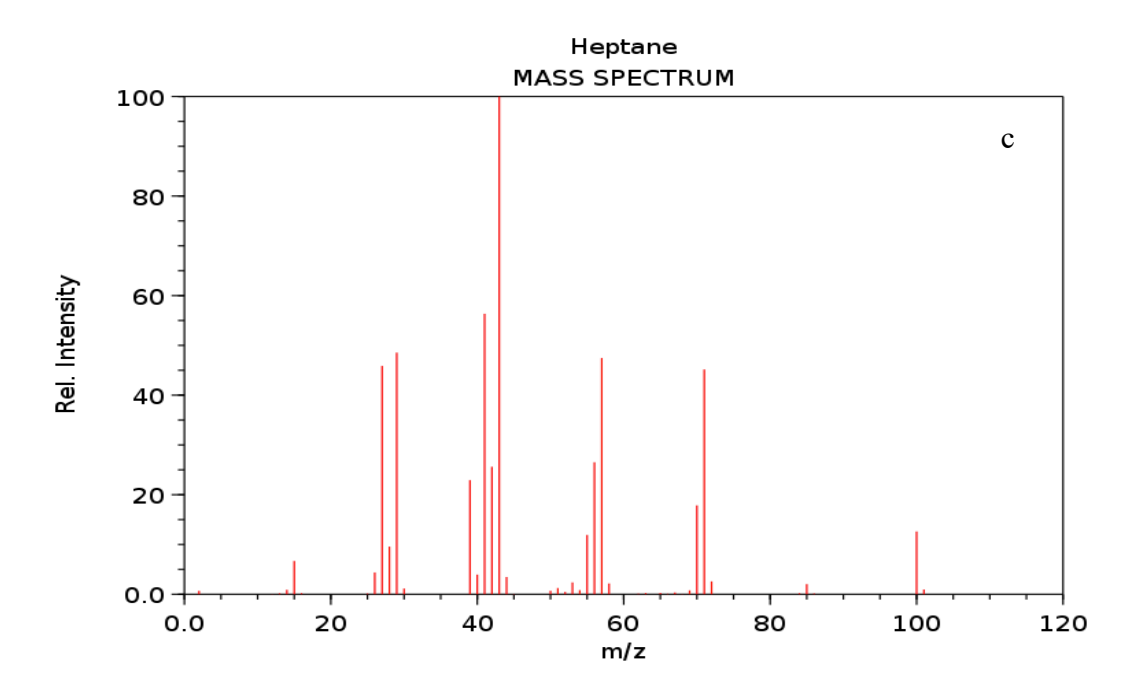


Figure 1.7. Mass spectra of a) compound at retention time 3.159 min from the gasoline chromatogram in Figure 1.2, b) heptane at retention time 3.159 min from the chromatogram of standards in Figure 1.3, and c) heptane standard from the NIST Chemistry Webbook.<sup>9</sup>

Figure 1.7 (cont'd)







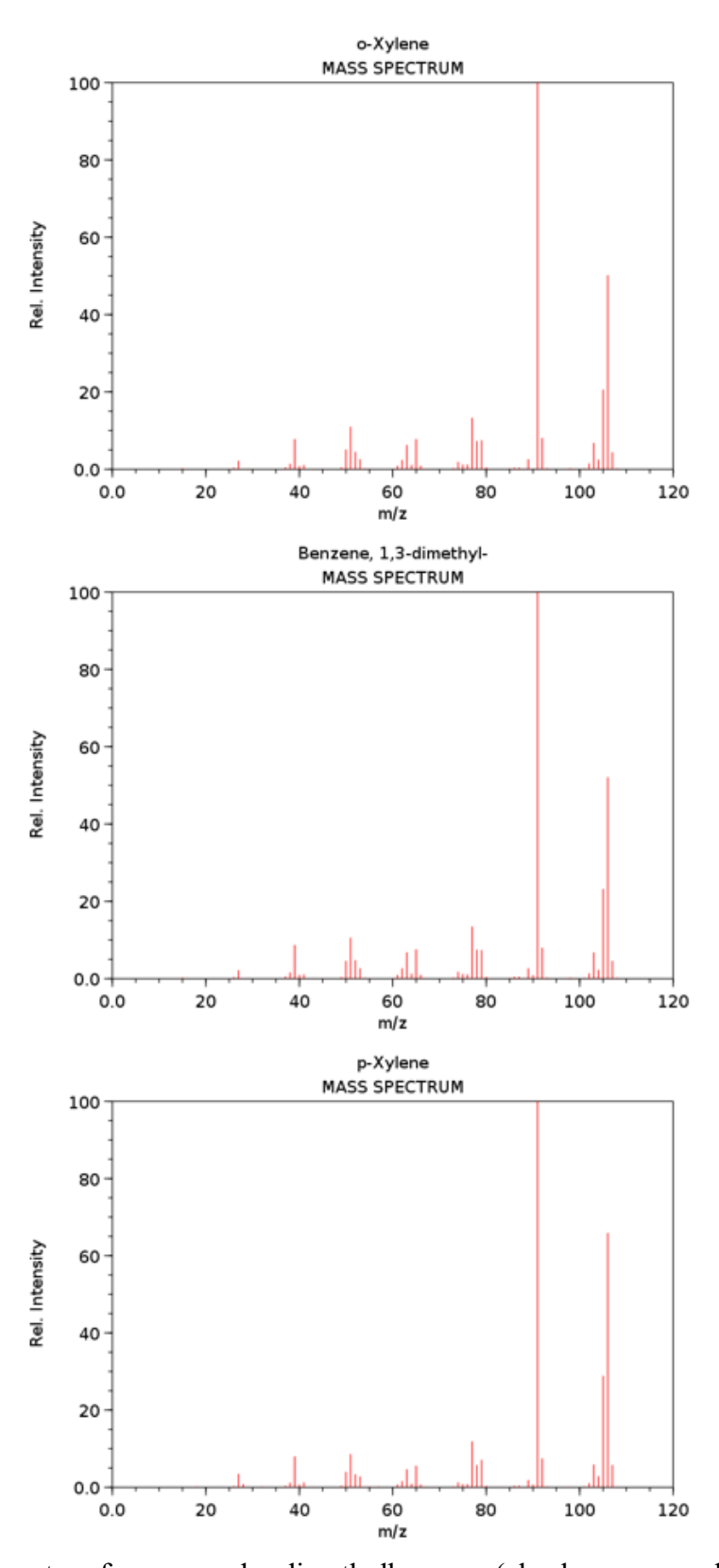


Figure 1.8. Mass spectra of o-, m-, and p-dimethylbenzene (also known as xylene).

### 1.3 Identification and Classification of Ignitable Liquids

The identification of major compounds present in a liquid by GC-MS can be used in conjunction with guidelines set by the ASTM to determine the chemical class of the liquid. There are seven major ignitable liquid classes identified by ASTM E1618-14, as well as a miscellaneous category for liquids that do not fall into any of the major classes<sup>6</sup>. Within each class, aside from gasoline, there is also a breakdown by alkane range: light (C<sub>4</sub>-C<sub>9</sub>), medium (C<sub>8</sub>-C<sub>13</sub>), and heavy (C<sub>9</sub>-C<sub>20+</sub>) (Table 1.1). The guidelines in ASTM E1618-14 include an initial comparison of the total ion chromatograms of samples to reference chromatograms. The overall chromatographic pattern as well as relative abundances of the six major compound classes (normal and branched alkanes, cycloalkanes, aromatics, polynuclear aromatics, and oxygenates) are considered.

Table 1.1. Ignitable liquid classification scheme used in ASTM E1618-14.6

Class	Light (C4-C9)	Medium (C <sub>8</sub> -C <sub>13</sub> )	Heavy (C <sub>9</sub> -C <sub>20+</sub> )
Gasoline - all brands, including gasohol and E85	Fresh gasoline is typically in the range C <sub>4</sub> -C <sub>12</sub>		
Petroleum Distillates including De- Aromatized	Petroleum Ether Some Camping Fuels	Some Charcoal Starters Some Paint Thinners	Kerosene Diesel Fuel
Isoparaffinic Products	Some Specialty Solvents	Some Charcoal Starters Some Paint Thinners	Some Commercial Specialty Solvents
Aromatic Products	Some Paint and Varnish Removers	Some Automotive Parts Cleaners	Industrial Cleaning Solvents
Naphthenic-Paraffinic Products	Cyclohexane Based Solvents/Products	Some Charcoal Starters Some Lamp Oils	Some Lamp Oils Industrial Solvents
Normal-Alkanes Products	Pentane Hexane	Some Candle Oils Some Copier Toners	Some Candle Oils Carbonless Forms
Oxygenated Solvents	Alcohols Some Lacquer Thinners	Some Industrial Solvents	
Miscellaneous	Single Component Products Some Blended Products	Turpentine Products Some Blended Products	Some Blended Products Some Specialty Products

Gasoline classification criteria includes the presence of abundant aromatics, including C2-alkylbenzenes (*o*-, *m*-, and *p*-dimethylbenzene) and C3-alkylbenzenes (1,3,5-trimethylbenzene and 1,2,4-trimethylbenzene), in a pattern similar to that of reference liquids, though no typical abundance ratios for ions are provided. The abundance of aromatics eluting after *n*-heptane should be substantially higher than the alkane abundances. Gasoline is also generally noted to contain naphthalene, methyl-naphthalenes, indanes, and methyl indanes, though they may be absent in some gasolines. ASTM E1618-14 also indicates that the presence of alkylbenzenes alone is not enough to warrant identification as gasoline, but that the pattern must also be consistent with that of known gasolines<sup>6</sup>. This clarification is important because many substrates, including carpet samples, have been known to contain alkylbenzenes and other compounds also found in gasoline after exposure to fire, due to pyrolysis and combustion. The requirement of pattern as well as presence of compounds is an attempt to reduce false positive results due to burned substrates containing no ignitable liquid.

#### 1.4. Evaporation of Ignitable Liquids

While ASTM provides a classification scheme and guidelines, chromatograms of liquids extracted from fire debris do not necessarily reflect the chromatogram of a corresponding reference liquid due to changes that occur as a result of the fire itself. When ignitable liquids are exposed to the conditions of a fire, the composition will change, substantially due to evaporation. Evaporation of the liquid leads to an increase in concentration of compounds of low volatility as more volatile compounds evaporate first. Additional compounds may form due to pyrolysis or combustion of materials at the scene. Based on these changes, ignitable liquid residues at a scene are more similar to ignitable liquids evaporated in a laboratory than unevaporated liquids<sup>6</sup>.

It is important, therefore, that the reference library contains chromatograms from a variety of ignitable liquids at many stages of evaporation, as well as chromatograms of extracts from common substrates found at scenes with no ignitable liquids added. This library may be comprised of chromatograms of liquids that were experimentally evaporated and analyzed in the forensic laboratory. In-house libraries increase the likelihood of reference liquids being analyzed on the same instrument as actual samples, or at least under equivalent conditions. Unfortunately, experimental evaporation of liquids is a lengthy process for an individual laboratory to undertake, with Hetzel noting an average evaporation time of 52 days for a variety of gasoline samples to reach 90% evaporated at room temperature<sup>10</sup>. Gasoline is one of the more volatile ignitable liquids so presumably other liquids would take even longer to evaporate.

An alternate option for procuring reference chromatograms is the ignitable liquids reference collection (ILRC) maintained by the National Center for Forensic Science (NCFS)<sup>4</sup>. This reference collection contains chromatograms of unevaporated and experimentally evaporated or biologically degraded ignitable liquids. Experimental evaporation was performed using 10 mL of ignitable liquid in a graduated microvial. The vial was then placed into a dry bath with nitrogen flowing above the ignitable liquid and a vacuum pump to remove ignitable liquid vapor. The height of the vial and temperature of the dry bath were changed based on desired evaporation level (as determined by volume). Typically, the ILRC contains chromatograms of the unevaporated liquid and only a few evaporation levels (six at most: 25%, 50%, 75%, 90%, 95%, and 99%), if any evaporations were performed at all. For some liquids, the unevaporated and evaporated samples were analyzed years apart with different GC-MS solvent delay parameters. The 100% dimethylpolysiloxane column (HP-1 or DB-1 (Agilent), ZB-1 (Phenomenex), etc.) used by the NCFS is 25 m long with an inner diameter of 0.20 mm

and film thickness of  $0.5~\mu m$ . Differences in stationary phase identity and column dimensions could affect the order in which compounds elute, though the overall pattern may be similar enough for preliminary identification. If an analyst preliminarily identifies a liquid based on comparison to the ILRC, they can request a sample to analyze on their own instrument with similar conditions as the case sample.

Currently, there is no standard method for the experimental evaporation of ignitable liquids<sup>4,5,10,11</sup>. Hetzel evaporated 10-mL samples of gasoline in test tubes at room temperature, while Smith *et al.* evaporated 10-mL samples of gasoline in graduated cylinders with stirring and nitrogen flow, a method similar to that used by the NCFS<sup>10,11</sup>. The method used by Smith *et al.* determined evaporation level based on change in mass. McIlroy *et al.* performed evaporation of petroleum distillates in a temperature- and humidity-controlled chamber<sup>5</sup>. The evaporation level was determined based on the change in mass and the evaporation time. The different evaporation methods may lead to variations in chromatograms of evaporated liquids.

An alternate approach was suggested by Bruno *et al.*, who used distillation and the advanced distillation curve (ADC) method to characterize ignitable liquids and visualize weathering patterns<sup>12</sup>. Samples of the distillate were collected and analyzed by GC-MS for volume fractions from 5 to 90%, in increments of 5%. While fire debris analysis typically concerns the liquid remaining in the distillation flask as opposed to the distillate, Bruno *et al.* suggest that the distillate composition anticipates the composition of the residual liquid in the distillation flask. The ADC is a classic distillation curve (boiling temperature plotted against volume fraction distilled) improved for complex fluids through features such as temperature, volume, and pressure measurements with uncertainties that are suitably low for development of equations of state, trace chemical analysis of distillate fractions and more. The ADC therefore

displays the typical temperature versus volume fraction distillated but with additional chemical information for each fraction. One distillation, from start to distillate volume fraction 90%, including sample preparation for GC-MS analysis, requires approximately 1.5 hours as opposed to the days or weeks needed to obtain similar amounts of information using evaporation methods discussed earlier. Use of this method by analysts would still require distillation of fuel samples and analysis of each distilled fraction. The authors did propose using the ADC method to predict the chemical profile of an evaporated ignitable liquid, though this was not illustrated.

#### 1.5. Modeling the Evaporation of Ignitable Liquids

This idea of predicting the chemical profile of an evaporated ignitable liquid, as opposed to experimental determination, has been investigated to varying degrees of success, though often for environmental purposes such as oil spills as opposed to forensic purposes<sup>5,14,17</sup>. As such, mathematical models developed to predict evaporation often require knowledge of the identity of the liquid, identity of individual compounds, or physical properties of the mixture or components<sup>12-16</sup>. When an oil spill occurs, the composition of the spilled material is usually known. In the case of fire debris, however, the ignitable liquid residue is from an unknown source, so the composition and physical properties of both the bulk liquid and individual compounds are unknown. The requirement of knowledge of individual compounds and/or physical properties makes application of most previously developed models to fire debris difficult, if not impossible.

Birks *et al.* developed a thermodynamic model using a mix of seven compounds found in gasoline, ranging from toluene to eicosane, to attempt to predict the composition of evaporated gasoline at a range of temperatures, with an intention of fire debris analysis application<sup>16</sup>. Vapor

Antoine coefficients. The calculated vapor pressure of the headspace was subjected to losses of 5% to simulate evaporation, after which new partial and total vapor pressures were calculated. This process was repeated, and simulated evaporation results were compared to corresponding experimental evaporations up to 90 °C, with results suggesting the simulations were successful. After conducting modeling at several temperatures, they determined that, for the same extent of evaporation, less volatile compounds have an increased rate of change of vapor pressure with increased temperature. At higher temperatures, therefore, volatile compounds will comprise a larger relative proportion than at lower temperatures. These findings are consistent with patterns seen for ignitable liquid residue from fire scenes. This method unfortunately requires knowledge of individual compounds and separate calculations for each compound, which can again be difficult with a complex mixture.

One group that investigated evaporation as related to the fuel as a single entity for fire debris applications was Okamoto *et al*<sup>13</sup>. While the application was fire debris related, the specific goal was to develop a model to predict the amount of vapor generated from a gasoline spill. Gasoline samples of 100-200 mL were degraded to weight loss fractions from 0 to 0.7 in increments of 0.1 by leaving them in a square pan at 20 °C with no wind or fume hood fan. Vapor pressure was measured in increments of 5 °C from 10-40 °C using an automated vapor pressure tester and evaporation rate was measured using weight loss on an electronic balance with the weight recorded every 10 s. They determined that, at constant temperature, vapor pressure decreased exponentially as weight loss fraction increased. Additionally, the evaporation rate was proportional to vapor pressure and therefore exponentially related to the weight loss fraction of gasoline at a constant temperature. This information was used to develop an equation

predicting the amount of gasoline vapor after an amount of time and was shown to be independent of the area and depth of the gasoline layer. Additionally, the evaporation rate at various temperatures was shown to be capable of estimation using the ratio of vapor pressures, as evaporation rate is nearly proportional to vapor pressure. The relation of evaporation rate to weight loss fraction is intriguing and could potentially be useful in predicting evaporated chromatograms, though this idea was not discussed by the authors. Unfortunately, this model requires knowledge of the vapor pressure of the liquid, which in turn requires knowledge of the liquid being examined, an unknown quality in fire debris analysis.

Regnier and Scott focused on the calculation of evaporation rate constants at various temperatures for individual compounds within diesel<sup>17</sup>. Diesel was experimentally evaporated, analyzed by GC, and the concentration of each normal alkane was determined from the chromatogram. The logarithm of the concentration of alkane remaining was plotted against time, a linear fit was performed, and the slope of that line was determined to be the evaporation rate constant. This process was repeated at multiple temperatures to ascertain the relationship between evaporation rate constant and temperature, determined to be increased evaporation rate constant with increased temperature. Vapor pressures were calculated using standard equations at multiple temperatures and it was determined that the evaporation rate constant at any temperature could be calculated if the evaporation rate constant was known at 30 °C and the vapor pressure was known at 30 °C and the temperature in question. While useful when investigating individual compounds or mixtures with a few compounds, the identification of compounds and subsequent calculations required to predict evaporation for a fuel with many compounds, such as gasoline, would be extensive and time consuming. Additionally, this method is only applicable to individual compounds as opposed to a total fuel sample.

A kinetic model was previously developed by McIlroy *et al.* that predicts evaporation rate constant based on retention index as opposed to vapor pressure or other physical properties<sup>5</sup>. Retention index is calculated from retention time (Equation 1.1) and was shown by McIlroy *et al.* to be related to boiling point and vapor pressure when a 100% dimethylpolysiloxane GC stationary phase is used. The model was developed through evaporation of diesel samples in a highly controlled environment. Diesel was evaporated at 25°C for 30 minutes to 300 hours, after which samples were analyzed using GC-MS. Multiple compounds of various compound classes, such as normal alkanes and aromatics, were identified in the chromatograms and the normalized abundance recorded for each. These abundances were plotted against evaporation time to create a decay curve for each compound (Figure 1.9). Evaporation rate constants were calculated from decay curves using Equation 1.2, assuming first-order kinetic decay because evaporation is a first-order process<sup>17</sup>

$$C_t = C_0 \exp\left(-kt\right) \tag{1.2}$$

where  $C_t$  is concentration at time t (h),  $C_\theta$  is initial concentration, and k is the evaporation rate constant (h<sup>-1</sup>).

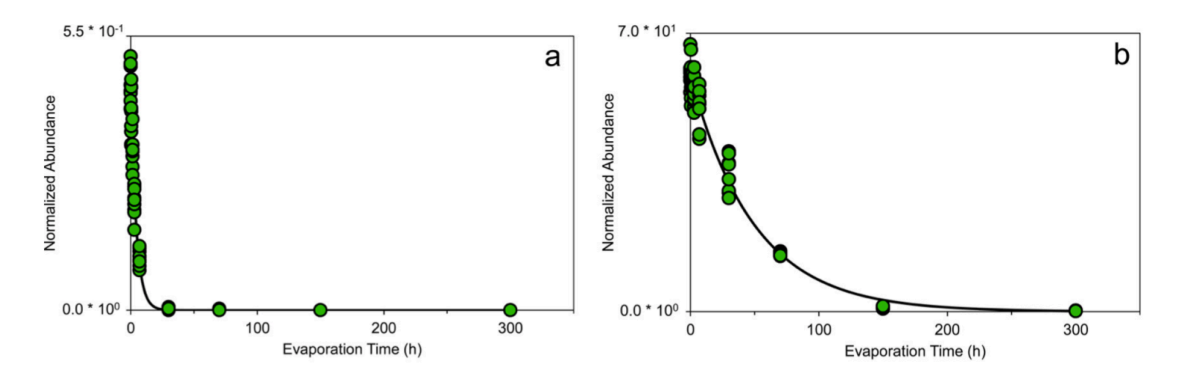


Figure 1.9. Experimental decay curves for *n*-octane (a) and *n*-decane (b). Abundances were normalized to the peak height of heneicosane in the extracted ion chromatogram at m/z 57. First-order rate equations for *n*-octane:  $C_t = 0.448 \ exp(-0.226t)$ , for *n*-decane:  $C_t = 5.926 \ exp(-0.0201t)^5$ .

Evaporation rate constants for all compounds analyzed were then plotted against retention index and a linear fit was performed (Figure 1.10). The linear fit is the model equation, relating retention index ( $I^T$ ) and evaporation rate constant (k,  $h^{-1}$ ) at 25°C<sup>5</sup>.

$$k = \exp(-1.04 \times 10^{-2} I^T + 6.70) \tag{1.3}$$

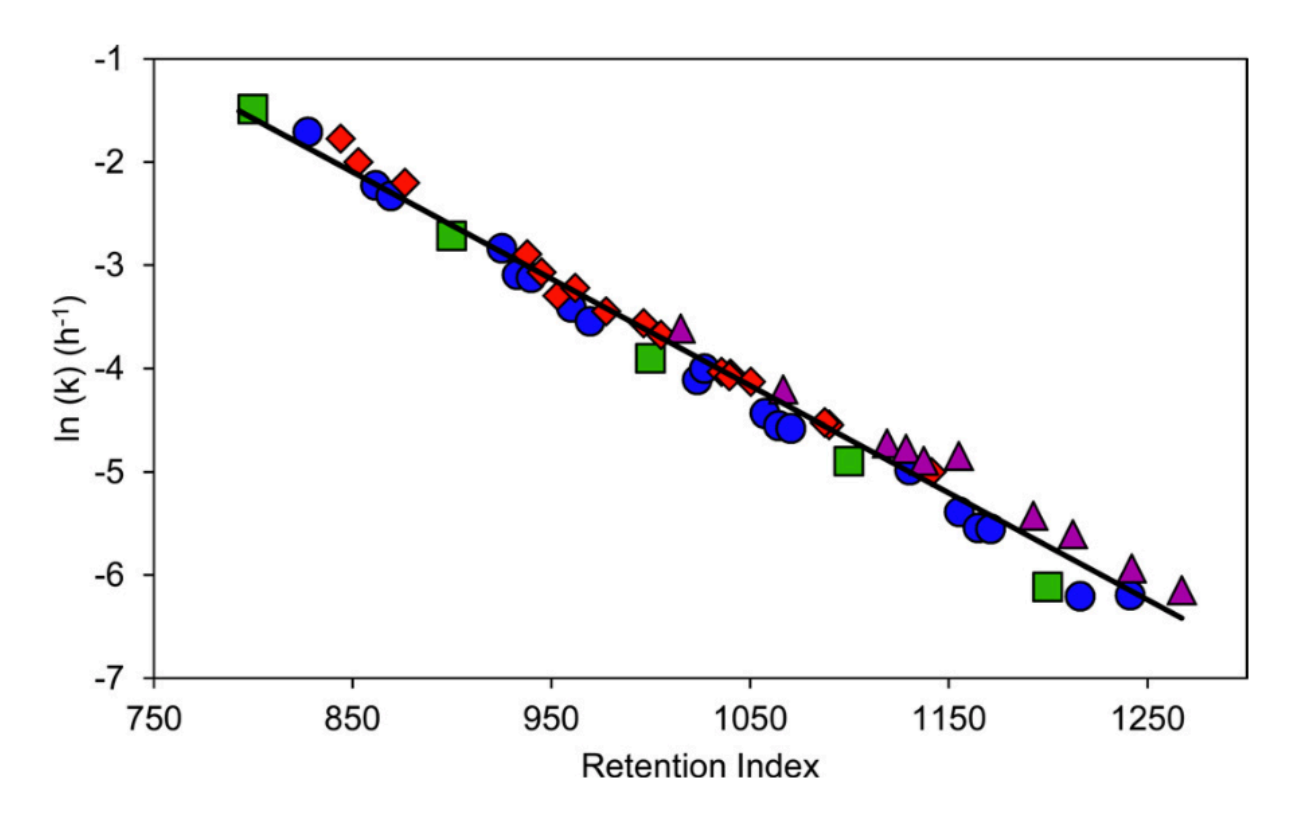


Figure 1.10. Natural logarithm of evaporation rate constant versus retention index on 100% dimethylpolysiloxane GC column for compound classes: normal alkanes (square), branched and cyclic alkanes (circle), alkyl benzenes (diamond), and polycyclic hydrocarbons (triangle). Linear regression equation:  $ln(k) = -0.0104 I^T + 6.70^5$ .

For each  $I^T$ , an evaporation rate constant  $(k, h^{-1})$  is calculated using equation 1.3 and can be used, along with a selected time (t, h), to predict the fraction remaining of the chromatographic abundance at that  $I^T(F_{I^T})$ .

$$F_{I^T} = \exp(-kt) = \frac{c_{I^T t}}{c_{I^T 0}}$$
 (1.4)

where  $C_{I^Tt}$  is the concentration at  $I^T$  for a time t, and  $C_{I^T0}$  is the initial concentration at  $I^T$ . Concentration is related to the GC-MS abundance (A), so  $C_{I^T0}$  refers to the abundance at that  $I^T$  of a sample analyzed prior to any evaporation. The predicted abundance at a given  $I^T$  is the product of the  $F_{I^T}$  and the abundance of a chromatogram of an unevaporated liquid at that same  $I^T$ . The resulting predicted abundances can be plotted as a function of  $I^T$  to produce a predicted chromatogram for a given time t. The total fraction remaining ( $F_{total}$ ) can then be calculated as

$$F_{total} = \frac{\sum_{j=l_i^T}^{l_f^T} F_j A_j}{\sum_{j=l_i^T}^{l_f^T} A_j}$$
 (1.5)

where  $I_i^T$  and  $I_f^T$  are the initial and final retention indices in the retention index range of interest and  $A_j$  is the GC-MS abundance of a chromatogram of an unevaporated liquid at the specified retention index<sup>10</sup>. The  $F_{total}$  is therefore the sum of the abundances of the predicted chromatogram divided by the sum of the abundances of the unevaporated chromatogram. Changing the time changes each  $F_{IT}$  (Equation 1.4), which in turn changes the predicted abundances at each  $I^T$  (Equation 1.5), thereby changing the  $F_{total}$  of the predicted chromatogram.

In terms of application to fire debris analysis, Smith *et al.* demonstrated that this model can be used to quickly predict chromatograms corresponding to evaporated liquids to populate a reference collection for comparison to chromatograms of samples<sup>10</sup>. The accuracy of predicted chromatograms was determined by comparing predicted chromatograms to chromatograms of experimentally evaporated liquids using Pearson product-moment correlation (PPMC) coefficients, calculated using Equation 1.6

$$PPMC = \frac{\sum_{j=I_{\bar{i}}}^{I_{f}^{T}} \{ (A_{I^{T}x} - \bar{A}_{x}) (A_{I^{T}y} - \bar{A}_{y}) \}}{\sqrt{\{ \left[ \sum_{j=I_{\bar{i}}}^{I_{f}^{T}} (A_{I^{T}x} - \bar{A}_{x})^{2} \right] \left[ \sum_{j=I_{\bar{i}}}^{I_{f}^{T}} (A_{I^{T}y} - \bar{A}_{y})^{2} \right] \}}}$$
(1.6)

Where  $I_i^T$  and  $I_f^T$  are the initial and final retention indices of interest,  $A_{I^Tx}$  and  $A_{I^Ty}$  are the abundances at each retention index in chromatograms x and y, and  $\bar{A}_x$  and  $\bar{A}_y$  are the mean abundances of all points in chromatograms x and y. PPMC coefficients range from 0 to  $\pm 1$  with values  $< \pm 0.49$  considered to represent weak correlation between the chromatograms, values between  $\pm 0.50$  and  $\pm 0.79$  representing moderate correlation, and values  $> \pm 0.80$  representing strong correlation<sup>11</sup>. Additionally, the model was proven capable of accurately predicting chromatograms for a variety of petroleum distillates and marine fuel stabilizer (naphthenic-paraffinic class). The comparisons for various petroleum distillates and marine fuel stabilizer resulted in PPMC coefficients ranging from 0.920 to 0.988<sup>11</sup>. Conversely, when predicting and comparing to gasoline samples, the PPMC coefficients ranging from 0.772 to 0.949<sup>11</sup>.

The kinetic model developed by McIlroy *et al.* addresses a major limitation of all previous models in that it does not require any knowledge of the compounds being investigated and in fact can be used to predict entire chromatograms as opposed to individual compounds. There is no experimental evaporation required so there is no concern that different laboratories will be using different methods. Any laboratory can use this model to predict chromatograms using chromatograms of unevaporated liquids analyzed with that laboratory's GC-MS program for fire debris analysis. There is therefore no concern about the reference chromatograms having been produced under different conditions than the sample chromatograms. Unfortunately, the model was less accurate when predicting gasoline evaporation than when predicting diesel evaporation, with lower correlation coefficients representing decreased accuracy<sup>11</sup>. As gasoline is the most common ignitable liquid observed in arson cases, it is important that this model be capable of accurately predicting the evaporation of gasoline in order to be used for forensic purposes.

#### 1.6. Research Objectives

The objectives in this research are:

- 1. To improve the predictive capabilities of the model specifically for gasoline and
- 2. To test the feasibility of developing correlation coefficient ranges for classification of an ignitable liquid residue as gasoline.

As previously discussed, reference collections of evaporated ignitable liquids are used for comparison to a case sample. Reference collections can be privately developed, but this is very time-intensive for analysts. Alternately, analysts can use the ILRC database, containing chromatograms from the unevaporated liquid and a maximum of six evaporation levels, if any evaporations were performed at all. This model could be used to develop predicted reference collections, with chromatograms for any  $F_{total}$ , while only requiring the analysis of a single unevaporated sample. This would be a more time-conscious method of developing a reference collection so as to not overburden analysts.

The kinetic model developed by McIlroy *et al.*, as applied by Smith *et al.*, is incapable of predicting gasoline evaporation to all evaporation levels with a high accuracy, as determined using PPMC coefficients. Gasoline is the most common ignitable liquid used in arson cases, so a mathematical model must be capable of accurately predicting gasoline evaporation in order to be relevant to the forensic science community. Both GC-MS instrument parameters and data analysis methods will be tested to determine the effect they have on predictive accuracy. Gasoline samples will be analyzed on the same GC-MS instrument with varying parameters and data analysis will be performed using multiple methods for samples from each change in instrument parameters. Predictive accuracy for each method change will be determined by

comparing predicted chromatograms to corresponding chromatograms of experimentally evaporated gasoline, using PPMC coefficients.

Current classification of ignitable liquids relies on visual comparison of chromatograms and determination of the presence or absence of compounds, with no statistical basis. It may be possible to determine PPMC coefficient ranges to distinguish whether or not the chromatogram of a case sample is consistent with that of a specific ignitable liquid class. Preliminary testing will be performed for the gasoline class through intra- and inter-class comparisons. Gasoline samples will be collected from multiple service stations on multiple days. Reference collections from one sample will be compared to chromatograms of experimentally evaporated liquids from the other samples to determine the intra-class PPMC coefficient range. Additionally, reference collections will be developed with ignitable liquids of other classes (medium petroleum distillate, aromatic, naphthenic-paraffinic, and isoparaffinic). These reference collections will be compared to chromatograms of experimentally evaporated liquids from the gasoline samples to determine the inter-class PPMC coefficient range. If the highest PPMC coefficient calculated for all inter-class comparisons is lower than the lowest PPMC coefficient calculated for the intra-class comparisons, it may be possible to determine such ranges on a larger scale.

REFERENCES

#### REFERENCES

- 1. Uniform Crime Reporting Program, Federal Bureau of Investigation (2017). <a href="https://www.fbi.gov/services/cjis/ucr">https://www.fbi.gov/services/cjis/ucr</a>
- 2. Ferreiro-Gonzalez, M., Ayuso, J., Alvarez, J.A., Palma, M., Barroso, C.G. Application of an HS-MS for the Detection of Ignitable Liquids from Fire Debris. Talanta 2015, Apr; 142: 150-56.
- 3. Skoog, D.A., Holler, F.J., Crouch, S.R. Principles of Instrumental Analysis. 6<sup>th</sup> ed..; Thomas Brooks/Cole: Belmont, CA, 2007.
- 4. Ignitable Liquids Reference Collection Database, National Center for Forensic Science, University of Central Florida. <a href="http://ilrc.ucf.edu/">http://ilrc.ucf.edu/</a>
- 5. McIlroy, J.W., Jones, A.D., McGuffin, V.L., Gas Chromatographic Retention Index as a Basis for Predicting Evaporation Rates of Complex Mixtures. Anal. Chim. Acta 2014, Sep; 852: 257-66
- 6. ASTM E1618-14, Standard Test Method for Ignitable Liquid Residues in Extracts from Fire Debris Samples by Gas Chromatography–Mass Spectrometry. ASTM International, West Conshohocken, PA, 2014.
- 7. Gross, J.H. Mass Spectrometry: A Textbook. 3<sup>rd</sup> ed.: Springer: Cham, Switzerland 2017.
- 8. deHoffmann, E., Stroobant, V. Mass Spectrometry: Principles and Applications. 3<sup>rd</sup> ed. John Wiley & Sons: West Sussex, England, 2013.
- 9. NIST Chemistry WebBook, National Institute of Standards and Technology. <a href="https://webbook.nist.gov/chemistry/">https://webbook.nist.gov/chemistry/</a>
- 10. Hetzel, S.S., Survey of American Gasolines (2008). J. Forensic Sci. 2015, Jan; 60 (S1): S197-S206.
- 11. Smith, R.W., Brehe, R.J., McIlroy, J.W., McGuffin, V.L., Mathematically Modeling Chromatograms of Evaporated Ignitable Liquids for Fire Debris Applications. Forensic Chemistry 2016, Jan; 2: 37-45.
- 12. Bruno, T.J., Lovestead, T.M., Huber, M.L., Prediction and Preliminary Standardization of Fire Debris Constituents with the Advanced Distillation Curve Method. J. Forensic Sci. 2011, Jan; 56 (S1): S192-S202.
- 13. Okamoto, K., Watanabe, N., Hagimoto, Y., Miwa, K., Ohtani, H. Changes in Evaporation Rate and Vapor Pressure of Gasoline with Progress of Evaporation. Fire Safety Journal 2009, Apr; 44: 47-61

- 14. Fingas, M.F., Modeling Evaporation Using Models that are not Boundary-Layer Regulated. J. Hazard. Mater. 2004; 107: 27-36.
- 15. Hirz, R., Rizzi, A.M. Simulation of the Weathering of Gasolines Using Gas Chromatographic Retention Data. J. Forensic Sci., 1991; 31(3): 309-19.
- 16. Birks, H.L., Cochran, A.R., Williams, T.J., Jackson, G.P. The Surprising Effect of Temperature on the Weathering of Gasoline. Forensic Chemistry 2017, Feb; 4: 32-40.
- 17. Regnier, Z.R., Scott, B.F. Evaporation Rates of Oil Components. Environmental Science and Technology 1975; 9: 469-72.
- 18. Brown, T.L., LeMay, H.E., Bursten, B.E., Murphy, C.J., Woodward, P.M. Chemistry: The Central Science 12<sup>th</sup> edition, Prentice Hall: Glenview, IL, 2012.

### II. Materials and Methods

## 2.1 Ignitable Liquid Sample Collection

Initial analysis was performed using approximately one gallon of gasoline collected from a Marathon service station in East Lansing, MI (Gasoline A). Gasoline A was stored in a 4-L amber bottle, with an approximately 450-mL aliquot transferred to a smaller 500-mL amber bottle. Seven additional gasoline samples were collected at later dates from gasoline service stations in or near East Lansing, MI and stored in 250-mL amber bottles (Table 2.1). Gasoline D was collected and analyzed but eliminated from consideration due to errors in the analysis. All collected gasolines were unleaded with minimum octane rating 87 using the (R+M)/2 method. Octane rating is a measure of anti-knocking capacity of the engine and not a measure of the concentration of octane in the gasoline. Ignitable liquids from other classes were obtained from various stores prior to September of 2016 (Table 2.2).

Table 2.1. Sources of gasoline used in this research.

Gasoline designation	Service station	Service station	Collection date
		location	
A	Marathon	1198 S. Harrison	11/5/17
В	Shell	1831 E. Grand River	4/2/18
C	Marathon	1435 E. Grand River	5/15/18
D	Citgo	N. Foster Ave.	4/9/18
E	Speedway	3201 E. Saginaw	4/9/18
F	Admiral	1120 E. Grand River	3/20/18
	Petroleum		
G	Speedway	1923 E. Michigan Ave.	5/21/18
Н	Sunoco	2818 E. Kalamazoo St.	5/21/18

Table 2.2. Non-gasoline ignitable liquids used in this research.

Ignitable	Ace Charcoal	Crown Paint	Goof Off	Marine Fuel	Tiki
Liquid	Lighter	Thinner	Adhesive	Stabilizer	Torch
			Remover		Fuel
Ignitable	Medium	Isoparaffinic	Aromatic	Napthenic-	Heavy
Liquid Class	Petroleum			Paraffinic	Petroleum
	Distillate				Distillate

### 2.2 Evaporation and Preparation of Ignitable Liquids

Evaporation of each liquid was performed in a 10-mL graduated cylinder with agitation via a stir bar and nitrogen flow. The process involved weighing 10 mL of gasoline in a 10-mL graduated cylinder with a stir bar and aluminum foil cap, evaporating to various levels, and then reweighing the remaining gasoline.

The evaporation was performed to specific total fraction remaining ( $F_{total}$ ) increments, with  $F_{total}$  determined by mass.  $F_{total}$  by mass was calculated as the mass of the gasoline after evaporation divided by the mass of the gasoline before evaporation. Evaporation to each  $F_{total}$  increment was performed in triplicate.

After evaporation, samples were diluted to 10 mL using ACS-grade dichloromethane (CH<sub>2</sub>Cl<sub>2</sub>) (Macron Fine Chemicals, Darmstadt, Germany) and the diluted sample was transferred to a labeled conical vial, capped, and refrigerated at 0-5 °C. For evaporated gasolines, a 10-μL aliquot of the diluted sample was added to 20 μL of *n*-tetradecane (0.051 M, Acros, NJ) as an internal standard and diluted to 2 mL with DCM in a volumetric flask. This 2-mL diluted sample was placed in a gas chromatography (GC) vial for analysis. For samples of unevaporated gasoline, a 10-μL aliquot of unevaporated gasoline was added to 20 μL of *n*-tetradecane (0.051 M) internal standard and diluted to 2 mL with DCM in a volumetric flask. For the other ignitable liquids, the same procedure as that of the unevaporated gasoline was used, with the exception of marine fuel stabilizer having 20 μL of *n*-octadecane (0.010 M, Sigma, St. Louis, MO) as an internal standard.

To determine retention index ( $I^{T}$ ), an alkane ladder was prepared containing all normal alkanes from n-pentane to n-tetradecane using mixed and individual standards diluted approximately 300:1 using DCM. The time corresponding to the peak apex of each n-alkane was

used to determine the alkane retention indices. Retention index was calculated for all other retention times using Equation 1.1 in Microsoft Excel (Redmond, WA, Version 16.20). While concentrations of the alkanes could not be accurately determined, concentrations were estimated to be between 0.001 and 0.003 M for all alkanes. The lack of accurate determination stems from the lack of information about concentrations within the mixed standard sources.

#### 2.3 GC-MS Instrument Parameters

All unevaporated and evaporated liquids were analyzed using an Agilent 6890N gas chromatograph (GC) with an Agilent 5975C mass spectrometer (MS) equipped with an Agilent 7683B autosampler (Agilent Technologies, Santa Clara, CA). Two columns were used in this research: both were 100% polydimethylsiloxane capillary columns with a difference in length and film thickness (HP-1ms, 30-m x 0.25 mm x 0.25  $\mu$ m and HP-1ms, 100-m x 0.25 mm x 0.50 μm, Agilent Technologies). The longer column with increased film thickness was only used to determine what compounds, if any, were not visualized with the 30-m column. Ultra-high purity helium (Airgas, Independence, OH) was used as the carrier gas at a nominal flow rate of 1 mL/min. A 1-μL aliquot of liquid was injected in the pulsed splitless mode with a pulse pressure of 15 psi for 0.25 min and with the gas saver turned off. The injector temperature was maintained at 250 °C and the oven temperature program was equivalent to that used by the National Center for Forensic Science (NCFS): 40 °C with a hold time of 3 min, followed by a 10 °C/min ramp to 280 °C, with a final hold time of 4 min<sup>1</sup>. The transfer line was held at 280 °C while the electron ionization source (70 eV) was held at 230 °C and the quadrupole was held at 150 °C. The scan range was mass-to-charge (m/z) 40-550 and 2.86 scans/sec. Some of the analyses used a 3-min solvent delay while others were performed with the detector turned off

during the solvent elution, as discussed in Chapter 3. Injections were performed in triplicate with a DCM blank analyzed between each different sample.

### 2.4 Data Analysis

Data were collected with ChemStation (Enhanced ChemStation, MSD ChemStation E.01.00.237, Copyright 1989-2007, Agilent Technologies Inc.) and were transferred to Excel for further visualization and processing. Chromatographic data for gasoline samples were normalized to the height of the appropriate internal standard using Excel, with the height of the internal standard set to 1.0.

The kinetic model was used to predict chromatograms of evaporated liquids based on the corresponding unevaporated sample analyzed on the same day, using procedures outlined in Section 1.5. Predicted chromatograms were calculated over an I<sup>T</sup> range of either 700-1385 or 500-1385 depending on the truncation of the unevaporated chromatogram.

The predicted and experimental chromatograms were compared using Pearson product-moment correlation (PPMC) coefficients (Equation 1.6) to assess the accuracy of the model. High PPMC coefficients are considered to be those above  $\pm 0.8$  and indicate strong correlation between the predicted and experimental chromatograms, coefficients between  $\pm 0.5$  and  $\pm 0.79$  indicate moderate correlation, and those below  $\pm 0.49$  indicate poor or no correlation<sup>2</sup>. PPMC coefficients discussed in this work are an average of the PPMC coefficients obtained by comparing the predicted chromatogram to experimental chromatograms from the three replicate injections of a sample.

### 2.5 Python Programs Developed to Automate Calculation of t

## 2.5.1 Predicting Chromatograms Corresponding to Specified FRtotal

To change the  $F_{total}$  of a predicted chromatogram, the variable t must be changed in Equation 1.4. Previously, this was done manually through a trial-and-error method until the required  $F_{total}$  was reached. To automate this calculation of t, and thereby reduce the man hours required, a program was developed by Joshua Parker (private communication, East Lansing, MI, 2017) using Python. Python is a free, easily accessible programming language with additional free resources, such as NumPy, a library package which is used for scientific computing such as calculating PPMC coefficients. The Python program used in this research was developed to quickly determine the value of t that, when input into the model, results in a user-selected  $F_{total}$  for the predicted chromatogram.

The normalized abundance and calculated rate constant at each retention index for the chromatogram of the unevaporated liquid, as well as the selected  $F_{total}$ , a time range, and a time step size, are inputs for the developed Python program. For each time step, the program calculates a predicted chromatogram using the model. In this research, a time step of 0.001 h was used, meaning a predicted chromatogram, and corresponding  $F_{total}$ , was calculated for every 0.001 h within the time range specified. The  $F_{total}$  is calculated as the sum of the abundances of the predicted chromatogram divided by the sum of the abundances of the chromatogram of the corresponding unevaporated liquid. The calculated  $F_{total}$  is then compared to the selected  $F_{total}$  using the difference in  $F_{total}$  between the calculated and selected values. If the  $F_{total}$  difference is less than the previous smallest  $F_{total}$  difference, this new calculated  $F_{total}$  becomes the "best". This process is repeated for each time step given. After calculating  $F_{total}$  for all time points, the program reports the "best"  $F_{total}$  (the one corresponding to the smallest  $F_{total}$  difference) and the

time required to reach that F<sub>total</sub>. The full, commented code can be found in Appendix 2A. The program was validated against the trial-and-error method through comparison of results of both methods. In all cases the result of the program was the same, or more accurate, than the result of the trail-and-error method. This program was subsequently used throughout Chapters 3 and 4.

# 2.5.2 Comparison of Experimental Chromatograms to Predicted Chromatograms to Determine Highest Possible Correlation

To determine the F<sub>total</sub> of a predicted chromatogram that results in the highest PPMC coefficient when the predicted chromatogram is compared with experimental chromatograms, the variable *t* must be changed in Equation 1.4. As the variable *t* changes, chromatograms are predicted with different F<sub>total</sub>. These predicted chromatograms are compared to the experimental chromatograms and an average PPMC coefficient is calculated. The user then analyzes the results of the initial comparisons and alters the time accordingly to produce F<sub>total</sub> values that correspond to predict chromatograms with higher PPMC coefficients. This process continues until a maximum PPMC coefficient is reached. The entire process is time-consuming and so a second program was developed in Python by Joshua Parker to automate the process. This program is similar to one previously developed by McIlroy using MatLab<sup>3</sup>.

The inputs for this program include rate constant and normalized abundance at each  $I^T$  of the chromatogram of the unevaporated liquid, a time range and a time step size, as well as the normalized abundance at each  $I^T$  from the chromatograms of the replicate injections of an experimentally evaporated liquid. For each time step, the program calculates a predicted chromatogram and corresponding  $F_{total}$ , and then calculates an average PPMC coefficient between the predicted chromatogram and experimental chromatograms. This process is repeated at every time step. After every time step has been analyzed, the program reports the highest

PPMC coefficient, as well as the model time required to reach that PPMC coefficient and the F<sub>total</sub> at that time. The program then provides a plot of PPMC coefficients versus the corresponding F<sub>total</sub>, with each time step providing a point on the curve. The maximum PPMC coefficient point is indicated as a red dot on the same curve, which is blue, allowing easy visualization (Figure 2.1). The full, commented code can be found in Appendix 2B. The program was validated against the manual method through comparison of the results of both methods. In all cases the result of the program was the same, or more accurate, than the result of the trail-and-error method. This program was subsequently used throughout Chapters 3 and 4.

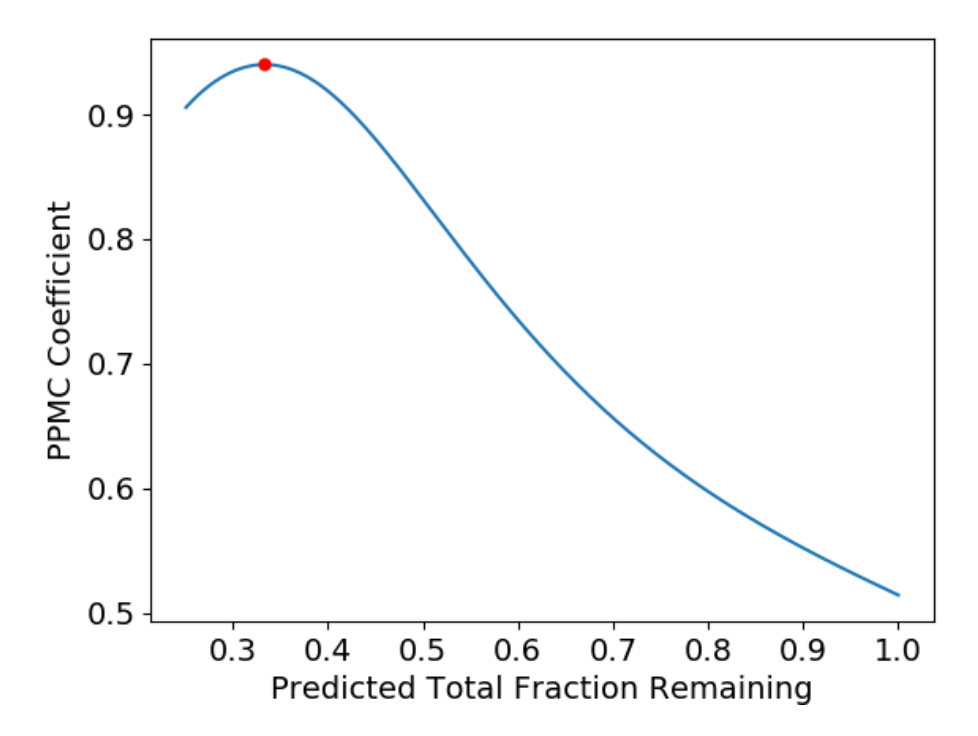


Figure 2.1. Example optimization curve generated using the Python script.

APPENDICES

APPENDIX A: Python Code to Predict Chromatograms Corresponding to Specified FRtotal

```
import csv
import math
import numpy
#Method for calculating new TFR. Takes in two lists, then sums and divides
def formulaTFR(fColumn,eColumn):
  sum 1 = 0
  sum2 = 0
  for a in fColumn:
    sum1 += a
  for b in eColumn:
    sum2 += b
  return sum1/sum2 #This method will/should return a single number
#Given a list and time, outputs a new list
def buildDColumn(cColumn,time):
  newColumn = []
  for i in cColumn:
    newColumn.append(math.exp(-i*time))
  return newColumn #This will be a list.
#Given 2 lists, create a new list which is the product of the 2.
def buildFColumn(dColumn,eColumn):
  newColumn = []
  for i in range(0,len(dColumn)):
    newColumn.append(dColumn[i]*eColumn[i])
  return newColumn #This will be a list.
#Main method.
if name ==' main ':
  goal = 0.1 #Here is where you change the desired goal
  bestTime = 0
  bestScore = 0
  #Here is where you change file name if necessary
  with open('FRCalcProgramInput.csv') as csvfile:
    readCSV = csv.reader(csvfile, delimiter=',')
    RC = []
    NTIC = []
    skip = 0
    for row in readCSV:
       if skip == 1 and row[0]!= "": #Because sometimes the NTIC column is longer than the
RC column
         RC.append(float(row[0]))
         #FR.append(float(row[1]))
```

```
NTIC.append(float(row[2]))
else:
    skip = 1
for t in numpy.arange(82,84,0.001):
    FR = buildDColumn(RC,t)
    RTIC = buildFColumn(FR,NTIC)
    score = formulaTFR(RTIC,NTIC)
    if math.fabs(score-goal) < math.fabs(bestScore-goal):
        bestScore = score
        bestTime = t
print("best TFR was: "+str(bestScore))
print("the time was: "+str(bestTime))
```

## APPENDIX B: Python Code to Compare Experimental Chromatograms to Predicted Chromatograms to Determine Highest Possible Correlation

```
import csv
import math
import scipy.stats
import numpy
import matplotlib
from mpl toolkits.mplot3d import Axes3D
import matplotlib.pyplot as plt
#Method for calculating new TFR. Takes in two lists, then sums and divides
def formulaTFR(fColumn,eColumn):
  sum1 = 0
  sum 2 = 0
  for a in fColumn:
    sum1 += a
  for b in eColumn:
    sum2 += b
  return sum1/sum2 #This method will/should return a single number
#Given a list and time, outputs a new list
def buildFRColumn(cColumn,time):
  newColumn = []
  for i in cColumn:
    newColumn.append(math.exp(-i*time))
  return newColumn #This will be a list.
#Given 2 lists, create a new list which is the product of the 2.
def buildRTICColumn(dColumn,eColumn):
  newColumn = []
  for i in range(0,len(dColumn)):
    newColumn.append(dColumn[i]*eColumn[i])
  return newColumn #This will be a list.
#Main method.
if name ==' main ':
  #goal = 0.9096 #Here is where you change the desired goal
  bestTime = 0
  bestScore = 0
  maxPPMC = 0
  #Here is where you change file name if necessary
  with open('PPMC Optimization Input.csv') as csvfile:
    readCSV = csv.reader(csvfile, delimiter=',')
    RC = []
    NTIC = []
```

```
exp1 = []
     exp2 = []
     exp3 = []
     avg ppmcs = []
     TFRs = []
     skip = 0
     for row in readCSV:
       if skip == 1 and row[0]!= "" and row[2]!= "": #In case of unequal column lengths
         RC.append(float(row[0]))
         #FR.append(float(row[1]))
         NTIC.append(float(row[2]))
         expl.append(float(row[3]))
         \exp 2.append(float(row[4]))
         exp3.append(float(row[5]))
       else:
         skip = 1
     for t in numpy.arange(0,10,0.001):
       FR = buildFRColumn(RC,t)
       RTIC = buildRTICColumn(FR,NTIC)
       first ppmc = scipy.stats.pearsonr(RTIC,exp1)[0]
       second ppmc = scipy.stats.pearsonr(RTIC,exp2)[0]
       third ppmc = scipy.stats.pearsonr(RTIC,exp3)[0]
       ppmc = (first ppmc+second ppmc+third ppmc)/3
       avg ppmcs.append(ppmc)
       score = formulaTFR(RTIC,NTIC)
       TFRs.append(score)
       if ppmc > maxPPMC:
         maxPPMC = ppmc
         bestScore = score
         bestTime = t
     fig, ax = plt.subplots()
     ax.plot(TFRs,avg ppmcs)
     # c refers to the color of the point. marker lets you change the symbol used to denote the
maximum.
     # markersize refers to how large that point/symbol will be.
     # see https://matplotlib.org/api/markers api.html#module-matplotlib.markers for marker
options.
     # see one of {'b', 'g', 'r', 'c', 'm', 'y', 'k', 'w'}; for color options.
     # For additional color options (there are a LOT): https://matplotlib.org/api/colors api.html
     ax.plot(bestScore,maxPPMC,c='r',marker='.',markersize=10)
     #ax.plot(bestScore,pinpoint,c='r',marker='* or . or ,')
     ax.set xlabel("Modeled Total Fraction Remaining", fontsize=18)
     ax.set ylabel("PPMC Coefficient", fontsize=4)
     # Hide the right and top spines
```

```
ax.spines['right'].set visible(True)
ax.spines['top'].set visible(True)
plt.xticks(fontsize=14)
# Only show ticks on the left and bottom spines
ax.yaxis.set ticks position('left')
ax.xaxis.set ticks position('bottom')
print("max ppmc was: " +str(maxPPMC) )
print("best TFR was: "+str(bestScore))
print("the time was: "+str(bestTime))
view = raw input("Do you wish to see the graph?") #For Python 2.x
#view = input("Do you wish to see the graph?") #For Python 3.x
if view == "yes" or view == "y" or view == "Yes" or view == "YES":
  plt.show()
else:
  view = False
save = raw input("Do you wish to save this image?") #For Python 2.x
#save = input("Do you wish to save this image?") #For Python 3.x
if save == "yes" or save == "y" or save == "Yes" or save == "YES":
 name = raw input("What do you want to save it as?") #For Python 2.x
 #name = input("What do you want to save it as?") #For Python 3.x
 fig.savefig( "%s"%(name)) #No periods in the filename!
 print("saved!")
print("Program End")
plt.close()
```

REFERENCES

### **REFERENCES**

- 1. Ignitable Liquids Reference Collection Database, National Center for Forensic Science, University of Central Florida. <a href="http://ilrc.ucf.edu/">http://ilrc.ucf.edu/</a>
- 2. Smith, R.W., Brehe, R.J., McIlroy, J.W., McGuffin, V.L., Mathematically Modeling Chromatograms of Evaporated Ignitable Liquids for Fire Debris Applications. Forensic Chemistry 2016, Jan; 2: 37-45.
- 3. McIlroy, J.W., Kinetic Models for the Prediction of Weathering of Complex Mixtures on Natural Waters, 2014.

III. Instrument and Method Modifications to Improve Accuracy in Predicting Evaporation of Gasoline

A kinetic model was previously developed to predict evaporation rate constants for compounds in diesel as a function of retention index ( $I^T$ )<sup>1</sup>. The evaporation rate constants can then be used to predict the fraction remaining at each  $I^T$  ( $F_{I^T}$ ). The predicted  $F_{I^T}$  is multiplied by the abundance of an unevaporated liquid at that  $I^T$  to calculate a predicted abundance, which can be used to generate a predicted chromatogram corresponding to a specific total fraction remaining ( $F_{total}$ ). In this research, the  $F_{total}$  is typically that of the experimentally evaporated liquid. To begin validating the model, Pearson product-moment correlation (PPMC) coefficients (Equation 1.6) were calculated between predicted chromatograms and corresponding experimentally evaporated chromatograms.

In previous work with petroleum distillates, PPMC coefficients between predicted and experimental chromatograms were greater than 0.9 for F<sub>total</sub> levels of 0.7, 0.5, 0.3, and 0.1 by mass<sup>1</sup>. Coefficients above 0.8 represent strong correlation, with higher coefficients representing stronger correlation and coefficients of 1 representing identical chromatograms. Model performance to predict gasoline evaporation was poorer, with PPMC coefficients ranging from 0.772-0.949<sup>2</sup>. For forensic applications, it is important that the kinetic model accurately predict evaporation of all ignitable liquid classes and, as gasoline is the most common ignitable liquid observed in arson cases, predicting evaporation of gasoline must be improved. This chapter focuses on improving the prediction of evaporation of gasoline by (1) modifying the gas chromatography-mass spectrometry (GC-MS) procedures and (2) further investigating the method by which the experimental F<sub>total</sub> is calculated.

### 3.1 Experimental Evaporation of Gasoline

Gasoline was evaporated as described in Section 2.2 and both unevaporated and evaporated samples were analyzed by GC-MS, using instrument parameters described in Chapter 2 (i.e., 3-min solvent delay and no background subtraction). Gasoline contains normal, branched, and cyclic alkanes, alkylbenzenes, and naphthalenes in the carbon range of butane (C<sub>4</sub>) to tridecane (C<sub>13</sub>) with aromatics comprising the highest abundance<sup>3</sup>. A representative chromatogram of unevaporated gasoline A is shown in Figure 3.1. Toluene (I<sup>T</sup> = 750) is the first characteristic compound to elute, followed by C<sub>2</sub>-alkylbenzenes (I<sup>T</sup> = 850-880), C<sub>3</sub>-alkylbenzenes (I<sup>T</sup> = 940-980), C<sub>4</sub>-alkylbenzenes (I<sup>T</sup> = 1040-1150), naphthalene (I<sup>T</sup> = 1160), and methyl-naphthalenes (I<sup>T</sup> = 1270-1300). Normal alkanes observed included heptane (I<sup>T</sup> = 700), octane (I<sup>T</sup> = 800), and nonane (I<sup>T</sup> = 900). Compounds eluting earlier than heptane are not seen due to the 3 min solvent delay employed.

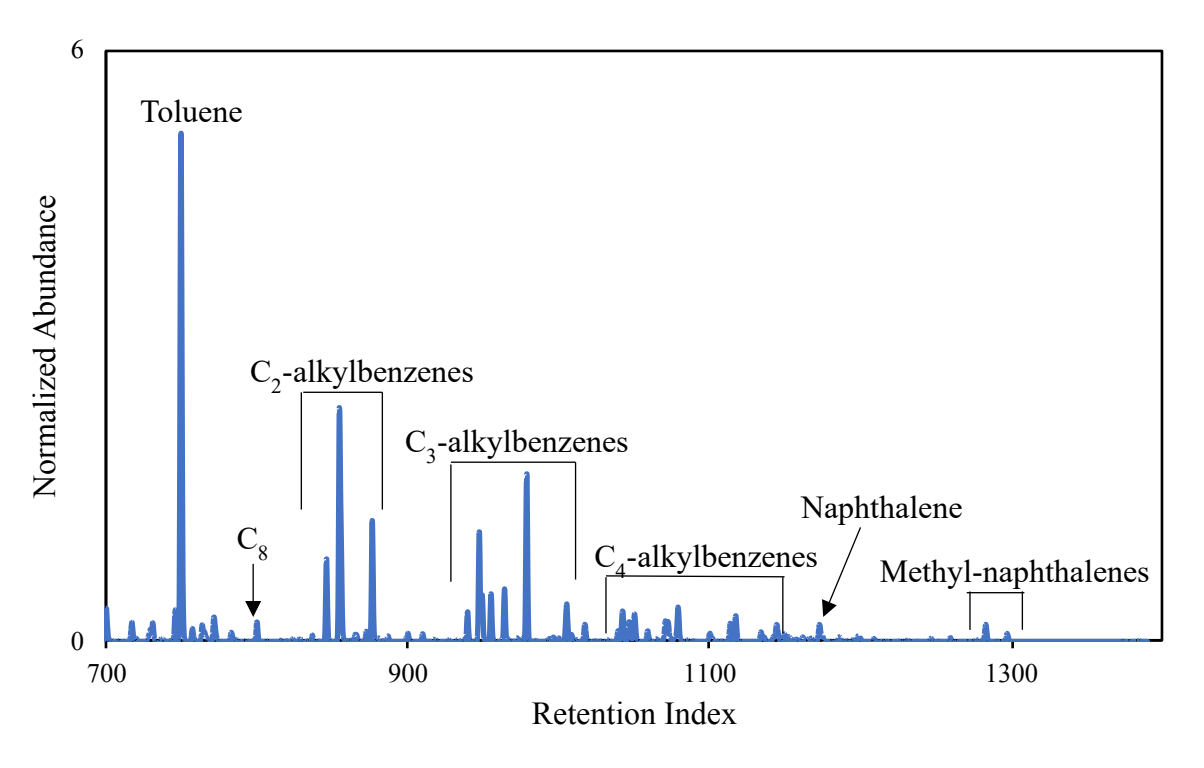


Figure 3.1. Chromatogram of unevaporated gasoline A, normalized to n-tetradecane (not shown).

Gasoline was evaporated to different levels (0.7, 0.5, 0.3, and 0.1) by mass and analyzed by GC-MS, again using parameters in Chapter 2. Figure 3.2 shows a chromatogram of unevaporated gasoline A overlaid with chromatograms of approximate  $F_{\text{total}} = 0.5$  (50%) evaporated) and  $F_{total} = 0.1$  (90% evaporated) by mass of gasoline A. The chromatogram of  $F_{total}$ = 0.5 gasoline contains the same compounds as the unevaporated gasoline, but with lower abundances for compounds eluting with  $I^T < 900$ . While abundances are lower, the abundance of compounds eluting with  $I^T < 900$  still accounts for about 55% of the total abundance of the chromatogram, as opposed to approximately 60% for the unevaporated gasoline. At  $I^T > 900$ , the normalized abundances of the unevaporated and F<sub>total</sub> 0.5 gasolines are similar. As evaporation continues, later-eluting compounds decrease in abundance in addition to further depletion of the early eluting compounds. At F<sub>total</sub> 0.1 by mass, the abundance of compounds eluting with I<sup>T</sup> < 900 accounts for < 6% of the total abundance of the chromatogram, again opposed to approximately 60% for the unevaporated gasoline. In fact, toluene is fully evaporated and  $C_2$ -alkylbenzenes are at least 95% evaporated at  $F_{total} = 0.1$  by mass. At this F<sub>total</sub>, C<sub>3</sub>-alkylbenzenes and naphthalenes are still present, although abundance of C<sub>3</sub>-

alkylbenzenes decrease by approximately a third while naphthalene and methyl-naphthalenes remain largely unchanged.

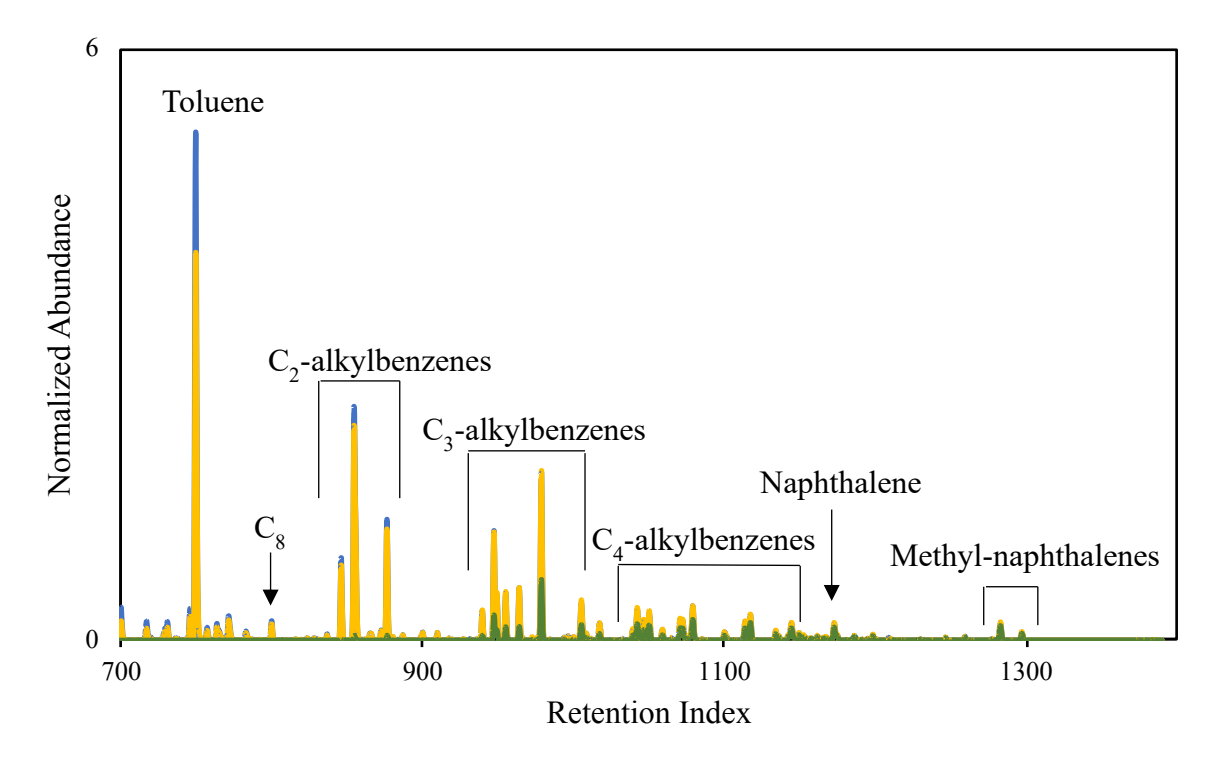


Figure 3.2. Comparison of chromatograms of unevaporated (blue),  $F_{total} = 0.5$  (yellow), and  $F_{total} = 0.1$  (green) by mass of gasoline A.

Compounds of higher volatility have higher evaporation rate constants than their lower volatility counterparts. As gasoline evaporates, more volatile compounds are preferentially lost first. As these more volatile compounds have lower boiling points, they elute first from the GC using temperature-programmed conditions. As a result, as F<sub>total</sub> decreases, abundance of these early-eluting compounds in the chromatogram decreases. This is consistent with the pattern observed in Figure 3.2.

### 3.2 Current Limitations in Predicting Chromatograms Corresponding to Evaporated Gasoline

Chromatograms of unevaporated gasoline (analyzed as described in Chapter 2) were used to predict chromatograms corresponding to different  $F_{total}$  by mass. The predicted

chromatograms were then compared to experimental chromatograms corresponding to the same level. Using these analysis parameters, the retention index range that was visible started at  $I^T = 700$  and the range used for prediction purposes spanned  $I^T = 700$ -1385. The upper limit of  $I^T = 1385$  was selected to exclude tetradecane ( $C_{14}$ ), the internal standard, from modeling. Normalization to the internal standard was performed by setting the height of the internal standard to 1.0.

The predicted chromatograms consistently underpredicted the  $F_{IT}$  (overpredicted the extent of evaporation) over the I<sup>T</sup> range 700-1200 when compared to corresponding experimental chromatograms (Figures 3.3-3.5). This underprediction of  $F_{I}^{T}$  is reflected in the chromatogram as a lower abundance of the predicted chromatogram as compared to experimental chromatogram, with the extent of underprediction at each I<sup>T</sup> varying with each F<sub>total</sub> level. For instance, the underprediction is most prominent in the range 700-1200 in the  $F_{total} = 0.1$  sample, while the range for the  $F_{total} = 0.5$  sample shows the most prominent underprediction over the  $I^{T}$ range 700-1000. Consistent underprediction of  $F_{IT}$  at many retention indices led to consistently lower abundances in the predicted chromatograms, with the discrepancy between predicted and experimental abundance being more prominent as I<sup>T</sup> decreased. Experimentally, at F<sub>total</sub> values of 0.7, 0.5, and 0.3, chromatographic peaks were visible at the same I<sup>T</sup> with abundances decreasing with decreased F<sub>total</sub>, as expected. In predicted chromatograms, however, some of these shared chromatographic peaks that were visible experimentally were predicted to have an abundance at or near zero for both  $F_{\text{total}} = 0.5$  and 0.3 (Figures 3.3 and 3.4). For chromatographic peaks that were predicted to have non-zero abundance at  $I^T \le 1000$ , namely toluene and the  $C_2$ and C<sub>3</sub>-alkylbenzenes, the ratio of predicted-to-experimental abundance decreased as F<sub>total</sub> decreased. PPMC coefficients were < 0.82 for all samples with  $F_{total} = 0.5$ , 0.3, and 0.1 by mass

(Table 3.1). Table 3.1 includes samples from multiple gasoline sources, defined as A, B, and C. Detail on the sources can be found in Table 2.1.

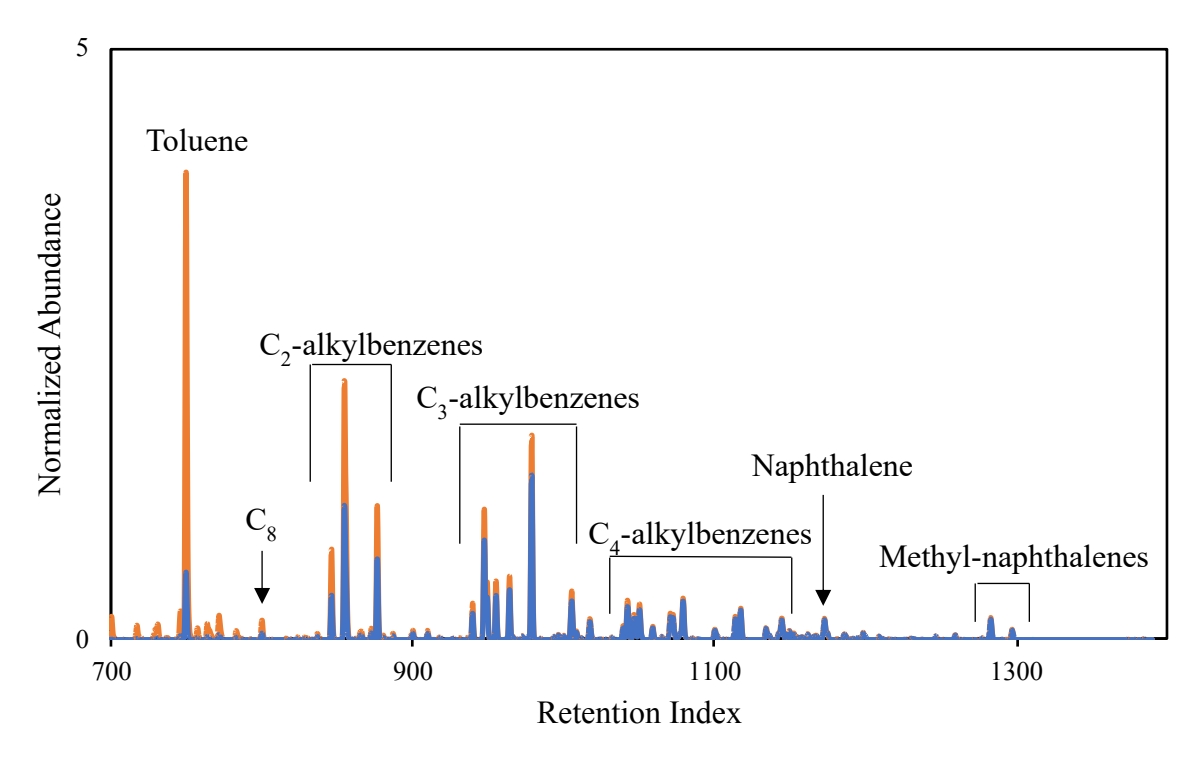


Figure 3.3. Comparison of a chromatogram of experimentally evaporated  $F_{total} = 0.5$  by mass gasoline A (orange) with the corresponding predicted chromatogram (blue).

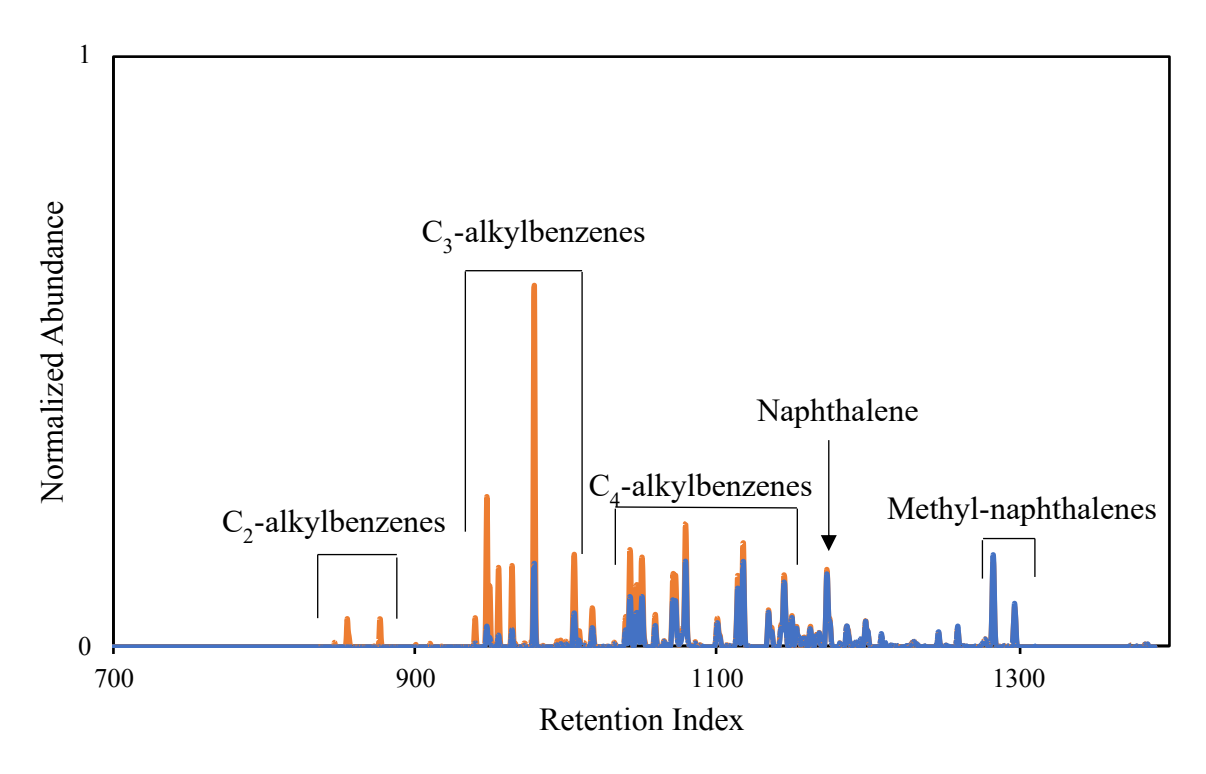


Figure 3.4. Comparison of a chromatogram of experimentally evaporated  $F_{total} = 0.3$  by mass gasoline A (orange) with the corresponding predicted chromatogram (blue).

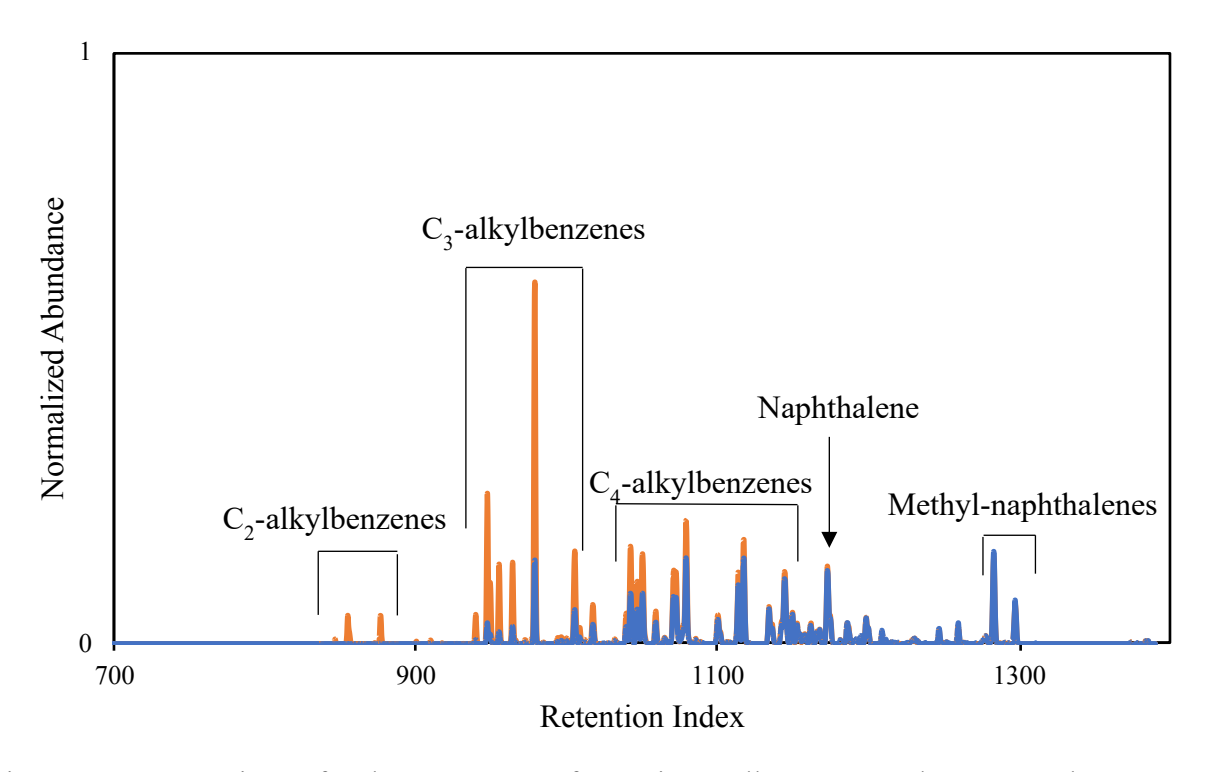


Figure 3.5. Comparison of a chromatogram of experimentally evaporated  $F_{total} = 0.1$  by mass gasoline A (orange) with the corresponding predicted chromatogram (blue).

Table 3.1. Mean PPMC coefficients calculated between experimental and predicted chromatograms using original GC-MS parameters (predicted and compared over  $I^T = 700-1385$ ). The  $\pm$  indicates standard deviation, calculated based on n=3.

	Gasoline A	Gasoline B	Gasoline C
$F_{total} = 0.1$ by mass	$0.818 \pm 0.001$	$0.765 \pm 0.002$	$0.726 \pm 0.002$
$F_{total} = 0.3$ by mass	$0.708 \pm 0.003$	$0.713 \pm 0.004$	$0.6685 \pm 0.0003$
$F_{total} = 0.5 \text{ by mass}$	$0.811 \pm 0.003$	$0.77 \pm 0.02$	$0.817 \pm 0.003$
$F_{total} = 0.7$ by mass	$0.950 \pm 0.002$	Not analyzed	Not analyzed

The PPMC coefficient range calculated using this GC-MS method is wide (0.6685-0.950), with many coefficients falling in the moderate correlation category (0.5-0.8) (Table 3.1). Comparisons of predicted and experimental chromatograms with F<sub>total</sub> of 0.5 result in not only an increased PPMC coefficient when compared to F<sub>total</sub> 0.3 comparisons of the same gasoline, but also higher abundance ratios of predicted-to-experimental over much of the I<sup>T</sup> range. The higher abundance ratios mean the abundances of the predicted chromatogram are closer to those of the experimental chromatogram. The exception to this trend is  $F_{total} = 0.1$  by mass. The comparison between experimental and predicted chromatograms with  $F_{total} = 0.1$  consistently results in higher PPMC coefficients than the comparison of chromatograms with  $F_{\text{total}} = 0.3$  (Figures 3.4 and 3.5, Table 3.1). For instance, with gasoline A, the PPMC coefficient between experimental and predicted chromatograms with an approximate  $F_{total} = 0.3$  is 0.708, while the PPMC coefficient for chromatograms with an approximate  $F_{total} = 0.1$  is 0.818. This increase in correlation results from a decreased number of compounds and, therefore, a decreased number of non-zero points of correlation. While there is still some discrepancy in abundance of the earlier eluting compounds in experimental  $F_{total} = 0.1$ , the number of points with discrepancy and the extent of the discrepancy is lower than with  $F_{\text{total}} = 0.3$ .

3.3 Refinement of Instrumental and Data Processing Parameters to Improve Correlation between Experimental and Predicted Chromatograms

Gasoline is a very volatile liquid and the kinetic model appears to be overpredicting the extent of evaporation. An investigation was started to determine whether there were more compounds present in the liquid that were not being observed under the original GC-MS parameters, as this could be contributing to the overprediction of evaporation. A limitation of the original GC-MS parameters that likely contributed to the lower PPMC coefficients with gasoline is the limited I<sup>T</sup> range. The GC-MS parameters were selected to be consistent with those used in model development, however, while the range starting at  $I^{T} = 700$  is sufficient for petroleum distillates, gasoline contains compounds with  $I^T < 700$ . These compounds are not observed in the experimental chromatograms due to the GC-MS parameters selected. To determine the identity of these compounds, gasoline was analyzed using the same GC-MS method as described in Chapter 2 and Sections 3.1 and 3.2, but using a 100-m column, rather than a 30-m column, with the same stationary phase. The longer column resulted in compounds being more retained, resulting in later elution and separation from the solvent. This later elution allowed visualization of compounds with  $I^T < 700$  (Figure 3.6), such as pentane ( $I^T = 500$ ), hexane ( $I^T = 600$ ), methylpentanes ( $I^T = 560-580$ ), methylhexane ( $I^T = 667$ ), and benzene ( $I^T = 600$ ) 641). A full list of compounds with  $I^T < 700$ , plus toluene, observed on the 100-m and 30-m columns is given in Table 3.2.

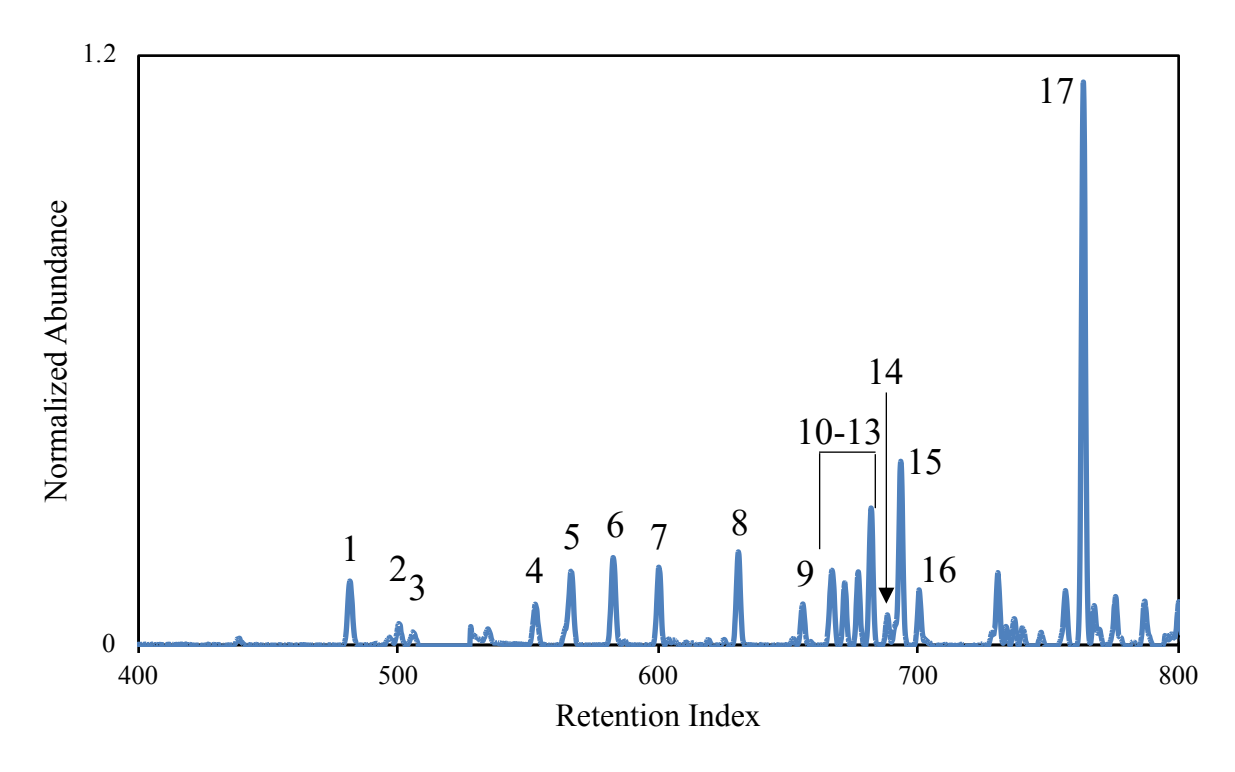


Figure 3.6. Chromatogram of unevaporated gasoline A analyzed on the 100-m column. Compound identities are listed in Table 3.2.

Table 3.2. List of compounds observed with  $I^T \le 700$  (plus toluene) using the 100-m and 30-m DB-1 columns.

Compound #	Retention Index (30- m, with solvent delay)	Retention Index (100-m, no solvent delay)	Retention Index (30-m, no solvent delay)	Compound
1	Not observed	481	490	Methylbutane
2	Not observed	500	500	<i>n</i> -pentane
3	Not observed	505	Not observed	Methylbutene
4	Not observed	552	Not observed	Dichloroethylene
5	Not observed	566	561	Methylpentane
6	Not observed	582	578	Methylpentane
7	Not observed	600	600	<i>n</i> -hexane
8	Not observed	630	619	Methylcyclopentane
9	Not observed	655	641	Benzene
10	Not observed	666	649	Cyclohexane
11	Not observed	671	659	Dimethylpentane
12	Not observed	676	667	Methylhexane
13	Not observed	681	Not observed	Cyclohexene
14	Not observed	688	680	Dimethylcyclopentane
15	Not observed	693	685	Tetramethylbutane
16	700	700	700	<i>n</i> -heptane
17	750	763	750	Toluene

The compounds with  $I^T$  < 700 observed using the 100-m column were likely eluting during the solvent delay when using the original method on the 30-m column. To be forensically relevant, the 30-m column was re-installed, and the 3-min solvent delay was eliminated to detect these early eluting compounds. Instead of a solvent delay, the detector was turned off between 1.65 and 1.88 min during the solvent elution. With this modification, compounds with  $I^T$  as low as 500 were observed (Figure 3.7). Further, most compounds observed (before  $I^T$  = 700) using the 100-m column were also observed using the 30-m column with the solvent delay eliminated (Table 3.2). There were a few compounds visible with the 100-m column that were not visible

with the 30-m column. These compounds likely co-eluted with the solvent based on their position ( $I^T = 505$  and 552) relative to other compounds that were visible with the 30-m column with no solvent delay directly before and after the detector was turned off ( $I^T = 500$  and 560). Cyclohexene is another compound visible only in the chromatogram from the 100-m column, but this compound was attributed to solvent impurities. A different solvent bottle, without the cyclohexene impurity, was used to prepare the samples analyzed on the 30-m column.

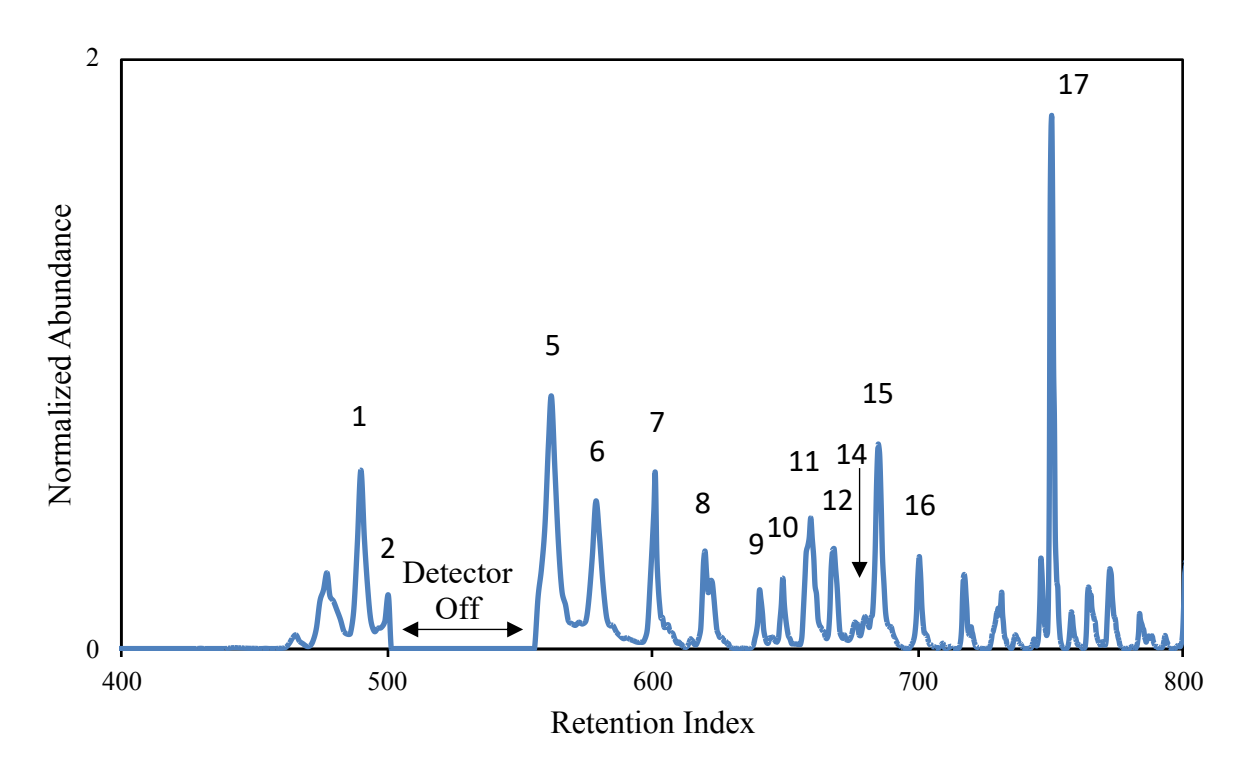


Figure 3.7. Chromatogram of unevaporated gasoline A analyzed on the 30-m column with the extended  $I^T$  range. Compound identities are listed in Table 3.2.

To predict retention indices more accurately over the whole range of compounds observed in gasoline, an alkane ladder was prepared containing all normal alkanes from n-pentane ( $I^T = 500$ ) to n-tetradecane ( $I^T = 1400$ ). The alkane ladder was analyzed at the start of each day when samples were analyzed and used to determine retention indices. Ideally, the alkane ladder would be included in the sample for the most accurate determination of  $I^T$ , however, this was not deemed feasible for this research and so an external alkane ladder was

employed. The  $I^T$  range extension and addition of the alkane ladder led to greater similarity between predicted and experimental chromatograms for  $F_{total} = 0.3$  and 0.5 by mass. This increased similarity is reflected by increased PPMC coefficients when compared to comparisons made using chromatograms predicted with the original parameters (Table 3.3, columns 1 and 2).

Table 3.3. Mean PPMC coefficients calculated between experimental and predicted gasoline A chromatograms before and after I<sup>T</sup> range extension and with background subtraction (n=3). In this and all subsequent tables, gasolines will be abbreviated in the form Gas @-#-0.1 where Gas @ is the source of gasoline being analyzed, # is the day analyzed, and 0.1 is the approximate experimental F<sub>total</sub> calculated by mass.

	Original Parameters	Extended I <sup>T</sup> Range	Extended IT Range
	$I^{T} = 700 - 1385$	$I^{T} = 500 - 1385$	$I^{T} = 500 - 1385$
	No Background	No Background	Background
	Subtraction	Subtraction	Subtraction
Gas A-0-0.1	$0.818 \pm 0.001$	$0.59 \pm 0.02$	$0.7740 \pm 0.0007$
Gas A-0-0.3	$0.708 \pm 0.003$	$0.841 \pm 0.007$	$0.825 \pm 0.007$
Gas A-0-0.5	$0.811 \pm 0.003$	$0.914 \pm 0.009$	$0.91 \pm 0.02$
Gas A-0-0.7	$0.950 \pm 0.002$	$0.953 \pm 0.004$	$0.954 \pm 0.006$

The decreased PPMC coefficient for  $F_{total} = 0.1$  after  $I^T$  range extension was due to the solvent (dichloromethane) and solvent impurities, which are labeled in Figure 3.8. The solvent itself was visible in the chromatogram during a tailing portion starting at  $I^T = 553$ . The detector was turned on during this portion of the solvent elution due to other compounds eluting at the same time in higher abundance in unevaporated and high  $F_{total}$  samples. Solvent impurities previously eluting with solvent delay were now visible after extending the  $I^T$  range. Impurities in the solvent included chloroform ( $I^T = 602$ ), a co-product of the reaction used to make  $CH_2Cl_2$ , and cyclohexene ( $I^T = 665$ ). Solvent peaks are not part of the sample and, therefore, should not be subjected to modeling. A simple background subtraction was performed using the Agilent GC-MS Data Analysis software to minimize solvent peaks, when visible. This method subtracts the spectrum of a selected retention time, or the average mass spectrum of a range of retention times, from the mass spectra of every retention time. Following background subtraction, PPMC

coefficients between experimental and predicted chromatograms increased for  $F_{total} = 0.1$  by mass, and did not significantly change for  $F_{total} = 0.3$ , 0.5, and 0.7 by mass (Table 3.3).

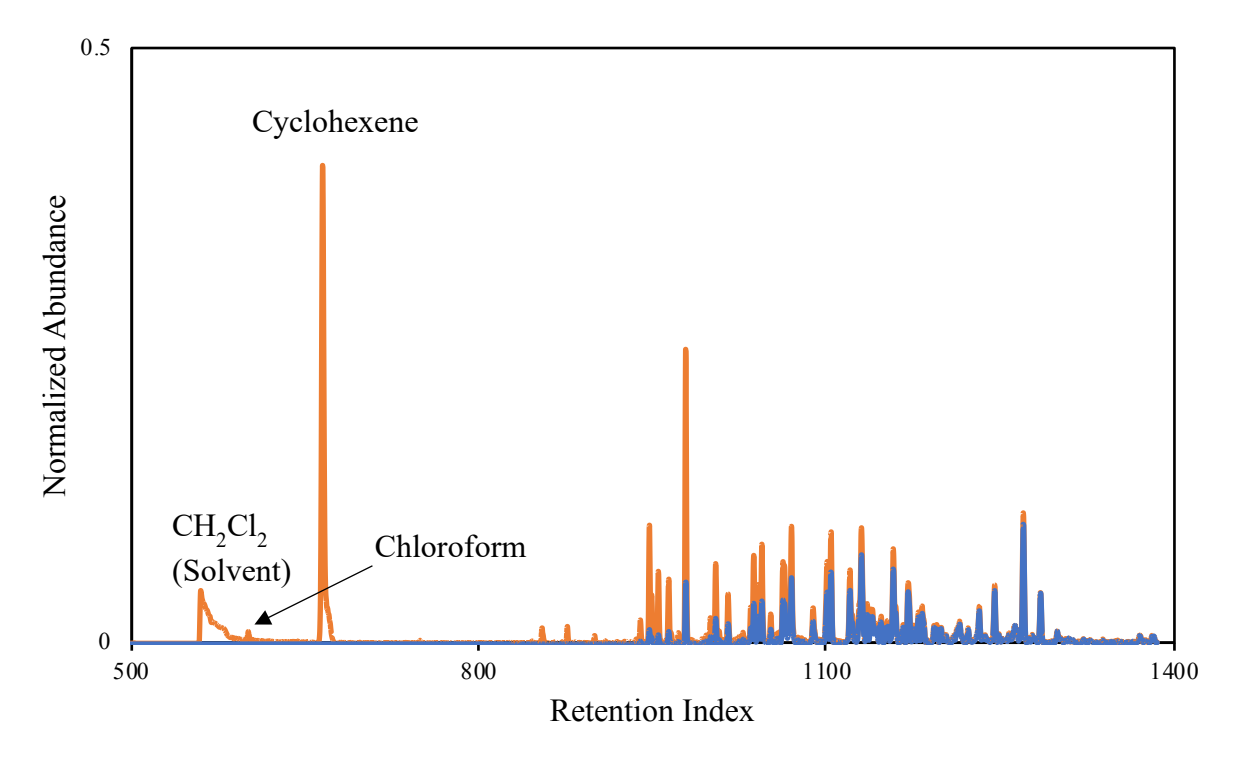


Figure 3.8. Gasoline A with  $F_{total} = 0.1$  by mass (orange) analyzed on the 30-m column with corresponding predicted chromatogram (blue). Cyclohexene and chloroform are solvent impurities.

As  $F_{total}$  decreased, the fraction of the total abundance contributed by the solvent peaks increased. Removal of the solvent peaks resulted in an increased time variable (Equations 1.4, 1.5) for the predicted chromatogram to reach the same  $F_{total}$ , meaning the  $F_{IT}$  decreased and therefore underpredicted the abundance more than before the background subtraction. For  $F_{total}$  0.7, 0.5, and 0.3, the disadvantage of further underprediction had a similar effect on correlation, as the benefit of removal of a poorly modeled solvent peak caused correlation to be changed only slightly (+0.001 to -0.018). This slight change suggests the background subtraction is not necessary to achieve high correlation at or above  $F_{total} = 0.3$  by mass.

The large PPMC coefficient improvement (0.183) observed with  $F_{total} = 0.1$  by mass is due to the large fraction of total abundance contributed by the solvent peaks. Removal of solvent peaks at this  $F_{total}$  leads to further underprediction of  $F_{I^T}$  across the modeling  $I^T$  range, but that negative effect is outweighed by the benefit of removing those peaks that were poorly modeled. As there are fewer total peaks, a discrepancy to the extent observed between predicted and experimental chromatograms with the solvent peaks has a substantial impact on correlation.

To ensure that extending the I<sup>T</sup> range and performing background subtraction had the same effect on prediction accuracy (as measured with PPMC coefficients), two other gasolines (B and C) were analyzed. Both gasolines were experimentally evaporated, and both evaporated and unevaporated samples were analyzed using the original I<sup>T</sup> range (solvent delay), extended I<sup>T</sup> range (no solvent delay), and extended I<sup>T</sup> range with background subtraction. Prediction and comparison to corresponding experimental chromatograms were performed over the appropriate I<sup>T</sup> range. These gasolines followed the trends in predictive accuracy observed with gasoline A when using the extended I<sup>T</sup> range, as well as background subtraction, for  $F_{total} = 0.3$  and 0.5 by mass. The response to both analysis method changes, however, with  $F_{total} = 0.1$  by mass (Table 3.4). Gasolines A, B, and C all had increased PPMC coefficients for  $F_{total} = 0.3$  and 0.5 when the I<sup>T</sup> range was extended and saw a non-significant change when background subtraction was added. With  $F_{total} = 0.1$ , however, gasoline A had PPMC coefficient increases with both the extension of the I<sup>T</sup> range and background subtraction, while gasolines B and C followed the pattern of  $F_{total} = 0.3$  and 0.5. Gasolines B and C were diluted with  $CH_2Cl_2$  from a different bottle than Gasoline A. The CH<sub>2</sub>Cl<sub>2</sub> used to dilute gasoline A contained cyclohexene as an impurity, whereas the CH<sub>2</sub>Cl<sub>2</sub> used to dilute gasolines B and C did not contain this impurity. The lack of this impurity in gasolines B and C led to increased correlation for the  $F_{\text{total}} = 0.1$ 

when the  $I^T$  range was extended and minimal change in correlation (< 0.01) when background subtraction was applied. The importance of background subtraction, therefore, depends on the relative abundance of solvent impurity peaks. Additionally, if the solvent peaks are present in low relative abundance, extension of the  $I^T$  range is an effective method of increasing correlation for all  $F_{total}$  levels.

Table 3.4. Mean PPMC coefficients calculated between experimental gasoline B and C chromatograms (n=3) and corresponding predicted chromatograms before and after I<sup>T</sup> range extension and after subsequent background subtraction.

	Original Parameters $I^T = 700 - 1385$ No Background Subtraction	Extended I <sup>T</sup> Range I <sup>T</sup> = 500 – 1385 No Background Subtraction	Extended I <sup>T</sup> Range I <sup>T</sup> = 500-1385 Background Subtraction
Gas B-1-0.1	$0.765 \pm 0.002$	$0.833 \pm 0.003$	$0.838 \pm 0.001$
Gas B-1-0.3	$0.713 \pm 0.004$	$0.824 \pm 0.004$	$0.826 \pm 0.004$
Gas B-1-0.5	$0.77 \pm 0.02$	$0.86 \pm 0.02$	$0.87 \pm 0.02$
Gas C-1-0.1	$0.726 \pm 0.002$	$0.833 \pm 0.004$	$0.842 \pm 0.002$
Gas C-1-0.3	$0.6685 \pm 0.0003$	$0.8362 \pm 0.0004$	$0.839 \pm 0.001$
Gas C-1-0.5	$0.817 \pm 0.003$	$0.925 \pm 0.004$	$0.934 \pm 0.005$

After I<sup>T</sup> range extension and background subtraction, the experimental chromatograms were more accurate representations of the actual composition of the gasoline than those collected using the original GC-MS parameters and without background subtraction. In turn, the more accurate experimental unevaporated and evaporated chromatograms resulted in more representative predicted chromatograms with higher predictive accuracy. Chromatograms are predicted using unevaporated chromatograms and compared to chromatograms of experimentally evaporated liquids, so more accurate chromatograms of unevaporated and evaporated liquids necessarily lead to higher predictive accuracy. The increased PPMC coefficients reflect this increased accuracy; however, there are still comparisons for which coefficients were below 0.9, the lowest PPMC coefficient calculated using petroleum distillates, indicating further improvement is necessary.

## 3.4 Changing the Method of Calculation of F<sub>total</sub>

Until this point, the F<sub>total</sub> of predicted chromatograms has been equal to the F<sub>total</sub> of the experimentally evaporated liquid as calculated by mass. To further investigate the accuracy of predicted chromatograms, using the revisions discussed in Section 3.3, the time variable, and resulting F<sub>total</sub> of the predicted chromatogram, was calculated instead to result in the predicted chromatogram with the highest PPMC coefficient upon comparison to triplicate experimental chromatograms. Each predicted chromatogram was compared to the corresponding experimental chromatograms and PPMC coefficients were calculated. A Python program was written to change time, in equation 1.3, in increments of 0.001 hours, to generate predicted chromatograms with different F<sub>total</sub> values (Figure 3.9). Previous optimization of F<sub>total</sub> required using a manual trial-and-error method, a process which was more time-intensive. The Python program was written to report the time and corresponding F<sub>total</sub> that led to the predicted chromatogram with the highest PPMC coefficient when compared to the experimental chromatograms. More detail on this program can be found in Section 2.5.2 and the full, commented code can be found in Appendix 2B. The F<sub>total</sub> calculated using this method will be referred to as the optimized F<sub>total</sub>.

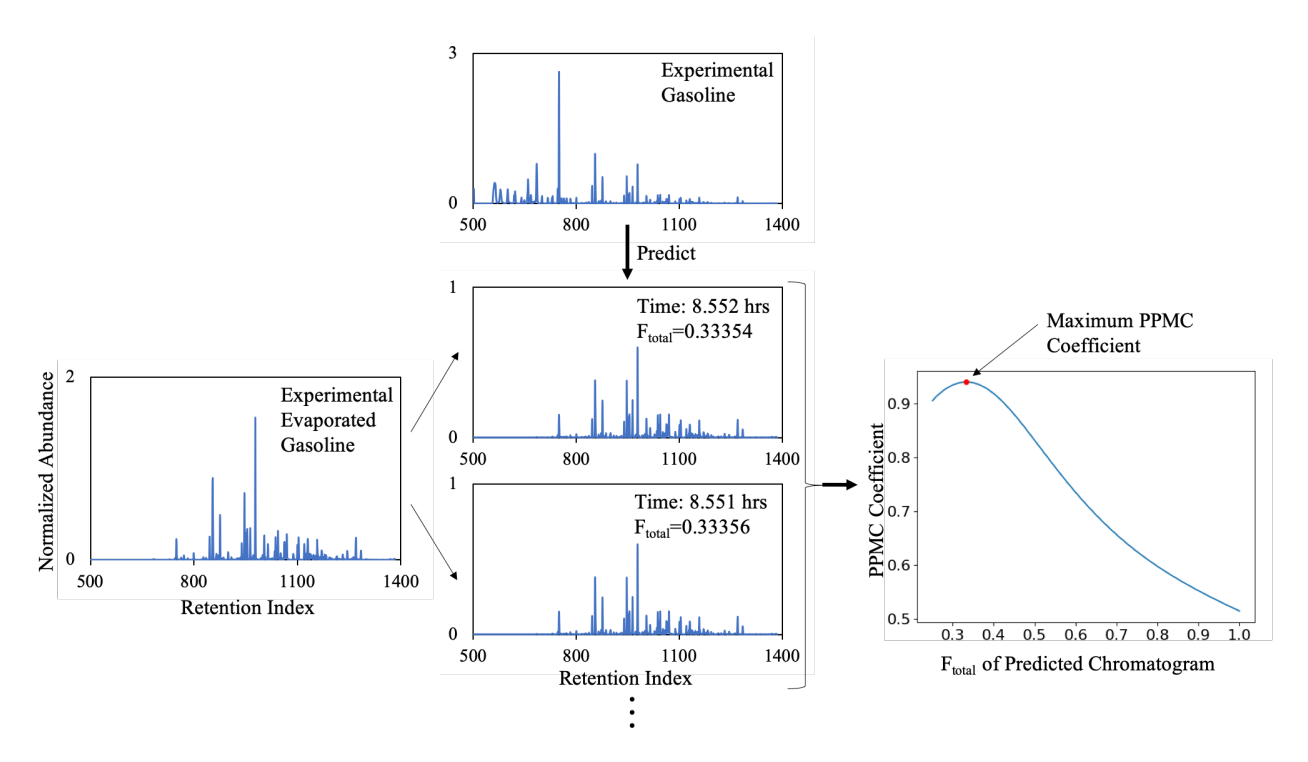


Figure 3.9. Workflow used to determine optimized F<sub>total</sub>.

This procedure, in addition to predicting chromatograms with a  $F_{total}$  equal to the  $F_{total}$  by mass of an experimentally evaporated sample, was performed using gasoline from seven different sources (Table 2.1). A source is defined here as a single pump from a single gasoline service station on a given day. Gasoline from each source was evaporated to approximate  $F_{total}$  = 0.5, 0.3, and 0.1 by mass, with these evaporations performed over a period of three days. Unevaporated gasoline from the same source was analyzed at the start of the day and used for prediction purposes.

Determination of  $F_{total}$  by optimization led to increased correlation (PPMC coefficients) between experimental and predicted chromatograms, as opposed to comparisons using chromatograms predicted to  $F_{total}$  by mass (subset in Table 3.5, full set in Appendix 3A). The optimized  $F_{total}$  values were greater than the  $F_{total}$  by mass values, with differences in  $F_{total}$  more pronounced at higher  $F_{total}$  by mass levels for samples from the same source and day (subsets in Tables 3.6, 3.7, full sets in Appendix 3B, 3C). Increased  $F_{total}$  values of predicted

chromatograms led to higher  $F_{I^T}$ , which addressed the problem of underprediction of  $F_{I^T}$  that was observed when chromatograms were predicted using  $F_{total}$  by mass. PPMC coefficients calculated using this method were above 0.95 for comparisons for all seven gasoline samples (Appendix 3A).

Table 3.5. Mean PPMC coefficients calculated between experimental chromatograms (n=3) and chromatograms predicted using different methods of calculating  $F_{total}$ , after  $I^T$  range extension and background subtraction, for a subset of gasoline samples tested. Corresponding  $F_{total}$  values can be found in Table 3.6.

	PPMC Coefficient (F <sub>total</sub> by mass)	PPMC Coefficient (Optimized F <sub>total</sub> )	PPMC Coefficient (F <sub>total</sub> by area)
Gas A-1-0.1	$0.923 \pm 0.003$	$0.974 \pm 0.004$	$0.974 \pm 0.004$
Gas A-1-0.3	$0.926 \pm 0.005$	$0.990 \pm 0.003$	$0.985 \pm 0.005$
Gas A-1-0.5	$0.935 \pm 0.008$	$0.988 \pm 0.002$	$0.988 \pm 0.002$
Gas B-1-0.1	$0.838 \pm 0.001$	$0.995 \pm 0.001$	$0.943 \pm 0.001$
Gas B-1-0.3	$0.826 \pm 0.004$	$0.990 \pm 0.003$	$0.941 \pm 0.004$
Gas B-1-0.5	$0.87 \pm 0.02$	$0.98 \pm 0.01$	$0.93 \pm 0.02$
Gas C-1-0.1	$0.842 \pm 0.002$	$0.990 \pm 0.003$	$0.988 \pm 0.003$
Gas C-1-0.3	$0.8389 \pm 0.0006$	$0.9974 \pm 0.0006$	$0.9965 \pm 0.0006$
Gas C-1-0.5	$0.934 \pm 0.005$	$0.983 \pm 0.008$	$0.983 \pm 0.008$

Table 3.6. F<sub>total</sub> of experimental chromatograms (n=3) calculated using different methods for gasoline samples, after I<sup>T</sup> range extension and background subtraction, for a subset of gasolines.

gasonne sampres, arter r	range extension and background subtraction, for a subset of gasonnes.			
	F <sub>total</sub> by mass	Optimized F <sub>total</sub>	F <sub>total</sub> by area	
Gas A-1-0.1	0.0801	0.1207	$0.12 \pm 0.01$	
Gas A-1-0.3	0.2945	0.4220	$0.49 \pm 0.03$	
Gas A-1-0.5	0.4967	0.7093	$0.70 \pm 0.02$	
Gas B-1-0.1	0.0984	0.1871	$0.136 \pm 0.003$	
Gas B-1-0.3	0.3010	0.5469	$0.404 \pm 0.005$	
Gas B-1-0.5	0.5051	0.8106	$0.59 \pm 0.02$	
Gas C-1-0.1	0.0876	0.1575	$0.147 \pm 0.003$	
Gas C-1-0.3	0.3036	0.5415	$0.520 \pm 0.009$	
Gas C-1-0.5	0.5110	0.7188	$0.690 \pm 0.004$	

Table 3.7. Differences in  $F_{total}$  of experimental chromatograms (n=3) calculated using different methods for gasoline samples after  $I^T$  range extension and background subtraction, for a subset of gasolines.

	Optimized F <sub>total</sub> - F <sub>total</sub> by mass	F <sub>total</sub> by area - F <sub>total</sub> by mass	Optimized F <sub>total</sub> - F <sub>total</sub> by area
Gas A-1-0.1	0.0406	0.04	0.00
Gas A-1-0.3	0.1475	0.20	-0.05
Gas A-1-0.5	0.2126	0.20	0.01
Gas B-1-0.1	0.0887	0.038	0.051
Gas B-1-0.3	0.2459	0.103	0.143
Gas B-1-0.5	0.3055	0.08	0.22
Gas C-1-0.1	0.0699	0.059	0.011
Gas C-1-0.3	0.2379	0.216	0.022
Gas C-1-0.5	0.2078	0.179	0.029

Determination of optimized  $F_{total}$  was also performed on a subset of gasoline samples with partial or no refinement (extension of  $I^T$  range, background subtraction). PPMC coefficients were similar whether a sample had been analyzed by initial GC-MS conditions, the extended  $I^T$  range, or extended  $I^T$  range and background subtraction (Table 3.8). PPMC coefficients were > 0.978 when using original GC-MS parameters, indicating that the calculation of  $F_{total}$  using optimization eliminates the need to extend the retention index range or perform background subtraction. Though not necessary for the sake of increased correlation, the solvent delay was removed and background subtraction was performed in all further testing due to the increased number of compounds visualized and more representative chromatograms produced.

Table 3.8. Mean PPMC coefficients calculated between experimental chromatograms (n=3) and chromatograms predicted using optimization of  $F_{total}$  for gasoline samples with varying degrees of refinement of analysis.

	$I^{T} = 700-1385$	$I^{T} = 500-1385$	$I^{T} = 500-1385$
	No Background	No Background	Background
	Subtraction	Subtraction	Subtraction
Gas B-1-0.1	$0.986 \pm 0.002$	$0.996 \pm 0.002$	$0.995 \pm 0.001$
Gas B-1-0.3	$0.991 \pm 0.003$	$0.992 \pm 0.003$	$0.990 \pm 0.003$
Gas B-1-0.5	$0.98 \pm 0.01$	$0.99 \pm 0.01$	$0.98 \pm 0.01$
Gas C-1-0.1	$0.979 \pm 0.005$	$0.991 \pm 0.004$	$0.990 \pm 0.003$
Gas C-1-0.3	$0.9978 \pm 0.0006$	$0.9984 \pm 0.0006$	$0.9974 \pm 0.0006$
Gas C-1-0.5	$0.983 \pm 0.009$	$0.985 \pm 0.008$	$0.983 \pm 0.008$

Optimization of  $F_{total}$  led to high PPMC coefficients (> 0.95) for all gasoline samples tested, yet PPMC coefficients were lower for all comparisons using chromatograms predicted using  $F_{total}$  equal to the experimental  $F_{total}$  by mass. The lower PPMC coefficients can be directly related to the lower  $F_{total}$ . The method of calculation of  $F_{total}$  by mass for experimentally evaporated gasoline is different from the method used to calculate  $F_{total}$  of predicted chromatograms and may account for some of the discrepancy in  $F_{total}$  by mass and by optimization. The  $F_{total}$  of predicted chromatograms is calculated using area, by summing the normalized abundances of the predicted chromatogram and dividing that sum by the sum of the normalized abundances of the unevaporated chromatogram (Equation 1.5).

To investigate if this difference in calculation method led to a discrepancy in the  $F_{total}$ , the  $F_{total}$  by area was calculated for chromatograms of experimentally evaporated gasolines that were analyzed with the extended  $I^T$  range and subjected to background subtraction.  $F_{total}$  by area was consistently higher than  $F_{total}$  by mass for all gasoline samples tested, with changes ranging from 0.011 to 0.533 (Tables 3.6, 3.7), implying an underlying issue in the way the chromatogram represents gasoline. The difference between  $F_{total}$  by mass and by area generally increases from  $F_{total} = 0.1$  by mass to  $F_{total} = 0.3$  by mass (in 96% of gasoline samples) for a given set of

evaporations (single gasoline sample on a single day). This trend continues and leads to  $F_{total}$  = 0.5 by mass resulting in the highest difference between  $F_{total}$  by mass and by area in 71% of gasoline samples analyzed.

This is likely due to the relation of detector response to carbon number. Gorocs *et al.* found that relative molar response (relative to naphthalene) increased with increasing carbon number at a slope of 0.220 for *n*-alkanes (from *n*-octane to *n*-heptadecane) and 0.221 for alkylbenzenes (from ethylbenzene to *n*-pentadecylbenzene)<sup>4</sup>. This means that later eluting compounds are more heavily weighted in determination of total area of the chromatogram. Loss of early eluting compounds will therefore be less impactful than if all compounds were evenly weighted, leading to a higher  $F_{total}$  by area than by mass. At  $F_{total} = 0.1$ , compounds with higher relative molar responses are lost, bringing the  $F_{total}$  by area closer to the  $F_{total}$  by mass. No such trend was observed with other  $F_{total}$  by mass levels. At  $F_{total} = 0.5$  and 0.3 by mass, the differences lie more in the changing concentrations of early eluting compounds than the actual complete loss of these compounds. Since  $F_{total} = 0.3$  by mass still contains compounds with low relative molar response, the discrepancy between  $F_{total}$  by mass and by area is still similar to  $F_{total} = 0.5$  by mass.

The increase in  $F_{total}$ , when using area as opposed to mass, results in the same trend of increased correlation between predicted and experimental chromatograms observed when  $F_{total}$  was optimized. This increase in correlation is once again due to increased predicted  $F_{I^T}$ , bringing the predicted abundance closer to that of the experimental chromatogram at each  $I^T$ . The PPMC coefficients and corresponding  $F_{total}$  values can be seen in Tables 3.5 and 3.6, respectively. PPMC coefficients calculated using the  $F_{total}$  by area were all greater than those calculated by mass, with improvements ranging from 0.006-0.258 for all samples tested (Tables

3.6, 3.7). While an increase of 0.006 is small, a change of 0.258 could, and did, change the meaning of the correlation from moderate to strong. The extent of evaporation was not indicative of the PPMC coefficient calculated between a chromatogram predicted to  $F_{total}$  by area and the corresponding experimental chromatogram for samples of the same source evaporated and analyzed on the same day. Additionally, there was no pattern observed relating the magnitude of PPMC coefficient increase between comparisons made using chromatograms predicted to  $F_{total}$  by mass or by area as related to the extent of evaporation.

The gasoline sample with the PPMC coefficient increase of 0.258 between comparisons to chromatograms predicted using  $F_{total}$  by area and by mass was gasoline F, with a  $F_{total} = 0.1$  by mass, evaporated and analyzed on day 3. Chromatograms of experimentally evaporated Gasoline F with  $F_{total} = 0.1$  by mass from days 2 and 3 both had lower PPMC coefficients (0.67 and 0.69, respectively) when compared to the chromatogram predicted to  $F_{total}$  by mass than the same type of comparisons for  $F_{total} = 0.1$  by mass samples from other gasoline sources (PPMC coefficients of 0.831-0.937). The difference between  $F_{total}$  by area and by mass for these samples are the highest of all  $F_{total} = 0.1$  by mass samples. The differences are 0.2205 and 0.1784 for days 2 and 3 respectively, while the next highest difference for any  $F_{total} = 0.1$  by mass sample is 0.0787. Additionally, the actual  $F_{total}$  by area is the highest of  $F_{total}$  0.1 by mass samples from all sources (0.32 and 0.28 for days 2 and 3).

Gasoline F was analyzed on the same day as gasoline A, yet these inconsistencies are not present with gasoline A, therefore the instrument was likely functioning as expected and so instrument changes are unlikely to be responsible for this variation. Alternately, if the sample was prepared to be more concentrated than intended, the higher abundances could account for the discrepancy. Once again, however, gasoline A did not show these inconsistencies and was

prepared on the same day, so it seems unlikely this was the reasoning. It is also possible that the samples were at some point exposed to open air for a long enough period of time to become more concentrated, leading to the discrepancy. Overall, the source of the error is unknown but likely due to concentration of the samples prior to injection.

To determine if calculating  $F_{\text{total}}$  by area for modeling eliminates the need for all other refinement (background subtraction, retention index range extension), predicted chromatograms were recalculated using F<sub>total</sub> by area with data collected according to the original collection parameters (Chapter 2). Calculating F<sub>total</sub> by area did increase PPMC coefficients when compared to F<sub>total</sub> by mass for all samples tested (Table 3.9). The largest increase observed in Table 3.9 occurs with the  $F_{total} = 0.3$  by mass of gasoline C. In this case, the PPMC coefficient using  $F_{total}$  by mass (0.3036) for prediction was  $0.6685 \pm 0.0003$  and the coefficient using  $F_{total}$  by area (0.54) for prediction was  $0.9459 \pm 0.0005$ , resulting in a difference of 0.277 and a change in classification from moderate to strong correlation. When calculating F<sub>total</sub> by area as opposed to  $F_{\text{total}}$  by mass for the original collection parameters, the  $F_{\text{total}}$  increases, leading to higher  $F_{IT}$ , and therefore higher abundance, at each individual I<sup>T</sup> (Table 3.10). This higher abundance is closer to the abundance found in experimental chromatograms and is reflected in higher PPMC coefficients. However, the coefficients are still mostly lower than those calculated between experimental and predicted chromatograms with the extended IT range and background subtraction, with predicted chromatograms calculated using F<sub>total</sub> by area (Table 3.9).

Table 3.9. PPMC coefficients calculated between experimental chromatograms (n=3) of gasolines B and C and chromatograms predicted using F<sub>total</sub> calculated by mass and area with varying degrees of refinement of analysis.

	PPMC calculated using F <sub>total</sub> by mass for prediction I <sup>T</sup> = 700-1385 No Background Subtraction	PPMC calculated using $F_{total}$ by area for prediction $I^T = 700\text{-}1385$ No Background Subtraction	PPMC calculated using $F_{total}$ by area for prediction $I^T = 500\text{-}1385$ Background Subtraction
Gas B-1-0.1	$0.765 \pm 0.002$	$0.889 \pm 0.002$	$0.943 \pm 0.001$
Gas B-1-0.3	$0.713 \pm 0.004$	$0.888 \pm 0.004$	$0.941 \pm 0.004$
Gas B-1-0.5	$0.77 \pm 0.02$	$0.86 \pm 0.02$	$0.93 \pm 0.02$
Gas C-1-0.1	$0.726 \pm 0.002$	$0.930 \pm 0.003$	$0.988 \pm 0.004$
Gas C-1-0.3	$0.6685 \pm 0.0003$	$0.9459 \pm 0.0005$	$0.9965 \pm 0.0006$
Gas C-1-0.5	$0.817 \pm 0.003$	$0.939 \pm 0.004$	$0.983 \pm 0.008$

Table 3.10. F<sub>total</sub> calculated by mass and area for experimental chromatograms (n=3) of gasolines B and C after varying degrees of refinement of analysis.

	F <sub>total</sub> by mass I <sup>T</sup> = 700-1385 No Background Subtraction	F <sub>total</sub> by area I <sup>T</sup> = 700-1385 No Background Subtraction	$F_{total} \ by \ area \\ I^T = 500-1385 \\ Background \ subtraction$
Gas B-1-0.1	0.0984	$0.143 \pm 0.004$	$0.136 \pm 0.003$
Gas B-1-0.3	0.3010	$0.437 \pm 0.004$	$0.404 \pm 0.005$
Gas B-1-0.5	0.5051	$0.60 \pm 0.01$	$0.59 \pm 0.02$
Gas C-1-0.1	0.0876	$0.151 \pm 0.003$	$0.147 \pm 0.003$
Gas C-1-0.3	0.3036	$0.54 \pm 0.01$	$0.520 \pm 0.009$
Gas C-1-0.5	0.5110	$0.680 \pm 0.002$	$0.690 \pm 0.004$

## 3.5. Changing the Method of Calculation of F<sub>total</sub> with Torch Fuel

To determine if calculation of  $F_{total}$  by area results in greater correlation than  $F_{total}$  by mass when using an ignitable liquid from a different ASTM class, predicted chromatograms were generated for torch fuel using  $F_{total}$  based on mass and area. These predicted chromatograms were then compared to corresponding experimentally evaporated chromatograms. The  $F_{total}$  calculated by mass and by area were similar (differences of 0.01 and 0.036) and corresponding PPMC coefficients based on  $F_{total}$  by mass and area were also similar

(differences of < 0.04) (Table 3.11). This implies that the reasoning behind the  $F_{total}$  by mass not equaling the  $F_{total}$  by area for gasoline does not apply to torch fuel. Torch fuel spans a narrower  $I^T$  range ( $I^T = 1100\text{-}1400$ ) than gasoline ( $I^T = 500\text{-}1300$ ) and so detector response is likely to be more similar over this smaller range. Changes in number of carbons in terms of volatility and detector response is more significant for lower carbon numbers, for example pentane to hexane as opposed to tridecane to tetradecane. It is also possible that the largest discrepancy in detector response appears with more volatile compounds than those present in torch fuel.

Table 3.11. Experimental F<sub>total</sub> of torch fuel calculated by mass and by area and corresponding representative PPMC coefficients (n=3).

			PPMC calculated	PPMC calculated
F <sub>total</sub> by mass	F <sub>total</sub> by area	using F <sub>total</sub> by	using F <sub>total</sub> by	
		mass for	area for	
			prediction	prediction

 $0.987 \pm 0.004$ 

 $0.89 \pm 0.02$ 

 $0.986 \pm 0.004$ 

 $0.86 \pm 0.02$ 

 $0.61\pm0.02$ 

 $0.067 \pm 0.002$ 

## 3.6 Summary

 $\mathbf{F}_{\text{total}} = \mathbf{0.6}$ 

 $\mathbf{F_{total}} = \mathbf{0.1}$ 

0.62

0.103

Following extension of the  $I^T$  range and background subtraction, the mathematical model previously developed is capable of accurately predicting evaporation of gasoline. While the difference in  $F_{total}$  by mass and area is interesting, the distinction is unnecessary, and likely irrelevant, when considering actual ignitable liquid residues. In a true unknown situation, the  $F_{total}$  by mass will be unknown and so prediction of an unevaporated gasoline will be performed to either a set of standard  $F_{total}$  values or through  $F_{total}$  optimization for comparison to the unknown liquid.

APPENDICES

APPENDIX A: Mean PPMC coefficients calculated between experimental chromatograms (n=3) and chromatograms predicted using different methods of calculating  $F_{total}$ , after  $I^T$  range extension and background subtraction.

extension and backgroun	PPMC (F <sub>mass</sub> )	PPMC (Fopt)	PPMC (Farea)
Gas A-1-0.1	$0.923 \pm 0.003$	$0.974 \pm 0.004$	$0.974 \pm 0.004$
Gas A-1-0.3	$0.925 \pm 0.005$ $0.926 \pm 0.005$	$0.974 \pm 0.004$ $0.990 \pm 0.003$	$0.985 \pm 0.005$
Gas A-1-0.5	$0.920 \pm 0.003$ $0.935 \pm 0.008$	$0.988 \pm 0.002$	$0.988 \pm 0.002$
Gas A-2-0.1	$0.937 \pm 0.007$	$0.976 \pm 0.002$	$0.958 \pm 0.002$
Gas A-2-0.3	$0.937 \pm 0.007$ $0.917 \pm 0.006$	$0.970 \pm 0.003$ $0.982 \pm 0.002$	$0.979 \pm 0.003$
Gas A-2-0.5	$0.934 \pm 0.005$	$0.986 \pm 0.003$	$0.986 \pm 0.003$
Gas A-3-0.1	$0.927 \pm 0.003$	$0.987 \pm 0.003$	$0.979 \pm 0.002$
Gas A-3-0.3	$0.93 \pm 0.01$	$0.983 \pm 0.003$	$0.975 \pm 0.002$ $0.975 \pm 0.008$
Gas A-3-0.5	$0.93 \pm 0.01$	$0.977 \pm 0.007$	$0.95 \pm 0.01$
Gas B-1-0.1	$0.838 \pm 0.001$	$0.995 \pm 0.001$	$0.943 \pm 0.001$
Gas B-1-0.3	$0.826 \pm 0.004$	$0.990 \pm 0.003$	$0.941 \pm 0.004$
Gas B-1-0.5	$0.87 \pm 0.02$	$0.98 \pm 0.01$	$0.93 \pm 0.02$
Gas B-2-0.1	$0.861 \pm 0.001$	$0.990 \pm 0.001$	$0.9360 \pm 0.0006$
Gas B-2-0.3	$0.839 \pm 0.003$	$0.986 \pm 0.006$	$0.943 \pm 0.005$
Gas B-2-0.5	$0.860 \pm 0.001$	$0.998 \pm 0.001$	$0.9612 \pm 0.0004$
Gas B-3-0.1	$0.901 \pm 0.002$	$0.9934 \pm 0.0005$	$0.9787 \pm 0.0004$
Gas B-3-0.3	$0.842 \pm 0.004$	$0.9965 \pm 0.0004$	$0.960 \pm 0.002$
Gas B-3-0.5	$0.88 \pm 0.01$	$0.997 \pm 0.002$	$0.971 \pm 0.007$
Gas C-1-0.1	$0.842 \pm 0.002$	$0.990 \pm 0.003$	$0.988 \pm 0.003$
Gas C-1-0.3	$0.8389 \pm 0.0006$	$0.9974 \pm 0.0006$	$0.9965 \pm 0.0006$
Gas C-1-0.5	$0.934 \pm 0.005$	$0.983 \pm 0.008$	$0.983 \pm 0.008$
Gas C-2-0.1	$0.831 \pm 0.001$	$0.991 \pm 0.005$	$0.987 \pm 0.004$
Gas C-2-0.3	$0.855 \pm 0.002$	$0.995 \pm 0.004$	$0.994 \pm 0.004$
Gas C-2-0.5	$0.922 \pm 0.003$	$0.990 \pm 0.002$	$0.990 \pm 0.002$
Gas C-3-0.1	$0.8595 \pm 0.0002$	$0.9962 \pm 0.0004$	$0.9829 \pm 0.0003$
Gas C-3-0.3	$0.86 \pm 0.01$	$0.990 \pm 0.007$	$0.984 \pm 0.009$
Gas C-3-0.5	$0.92 \pm 0.01$	$0.99 \pm 0.01$	$0.99 \pm 0.01$
Gas E-1-0.1	$0.904 \pm 0.004$	$0.9827 \pm 0.0009$	$0.975 \pm 0.001$
Gas E-1-0.3	$0.888 \pm 0.005$	$0.983 \pm 0.004$	$0.948 \pm 0.009$
Gas E-1-0.5	$0.911 \pm 0.006$	$0.98 \pm 0.01$	$0.97 \pm 0.01$
Gas E-2-0.1	$0.85 \pm 0.01$	$0.955 \pm 0.007$	$0.945 \pm 0.008$
Gas E-2-0.3	$0.906 \pm 0.005$	$0.97 \pm 0.01$	$0.93 \pm 0.02$
Gas E-2-0.5	$0.926 \pm 0.007$	$0.96 \pm 0.02$	$0.94 \pm 0.03$
Gas E-3-0.1	$0.901 \pm 0.002$	$0.982 \pm 0.001$	$0.961 \pm 0.002$
Gas E-3-0.3	$0.922 \pm 0.004$	$0.983 \pm 0.006$	$0.983 \pm 0.006$
Gas E-3-0.5	$0.933 \pm 0.005$	$0.982 \pm 0.002$	$0.980 \pm 0.002$

	PPMC (Fmass)	PPMC (Fopt)	PPMC (Farea)
Gas F-1-0.1	$0.87 \pm 0.01$	$0.985 \pm 0.004$	$0.985 \pm 0.004$
Gas F-1-0.3	$0.870 \pm 0.009$	$0.984 \pm 0.004$	$0.984 \pm 0.004$
Gas F-1-0.5	$0.91 \pm 0.03$	$0.97 \pm 0.01$	$0.97 \pm 0.01$
Gas F-2-0.1	$0.67 \pm 0.01$	$0.9795 \pm 0.0009$	$0.906 \pm 0.004$
Gas F-2-0.3	$0.897 \pm 0.011$	$0.982 \pm 0.003$	$0.982 \pm 0.003$
Gas F-2-0.5	$0.906 \pm 0.003$	$0.976 \pm 0.003$	$0.970 \pm 0.003$
Gas F-3-0.1	$0.69 \pm 0.007$	$0.978 \pm 0.004$	$0.948 \pm 0.002$
Gas F-3-0.3	$0.815 \pm 0.006$	$0.9814 \pm 0.0008$	$0.939 \pm 0.002$
Gas F-3-0.5	$0.88 \pm 0.01$	$0.980 \pm 0.004$	$0.886 \pm 0.004$
Gas G-1-0.1	$0.867 \pm 0.001$	$0.99718 \pm 0.00009$	$0.9936 \pm 0.0002$
Gas G-1-0.3	$0.870 \pm 0.001$	$0.9954 \pm 0.0009$	$0.9950 \pm 0.0008$
Gas G-1-0.5	$0.927 \pm 0.001$	$0.9953 \pm 0.0002$	$0.9953 \pm 0.0002$
Gas G-2-0.1	$0.871 \pm 0.003$	$0.9967 \pm 0.0009$	$0.989 \pm 0.002$
Gas G-2-0.3	$0.85 \pm 0.02$	$0.98 \pm 0.01$	$0.98 \pm 0.01$
Gas G-2-0.5	$0.90 \pm 0.01$	$0.985 \pm 0.009$	$0.984 \pm 0.009$
Gas G-3-0.1	$0.857 \pm 0.004$	$0.973 \pm 0.002$	$0.905 \pm 0.003$
Gas G-3-0.3	$0.878 \pm 0.004$	$0.98 \pm 0.01$	$0.974 \pm 0.007$
Gas G-3-0.5	$0.897 \pm 0.003$	$0.98 \pm 0.01$	$0.97 \pm 0.01$
Gas H-1-0.1	$0.895 \pm 0.004$	$0.995 \pm 0.002$	$0.994 \pm 0.002$
Gas H-1-0.3	$0.886 \pm 0.003$	$0.994 \pm 0.003$	$0.994 \pm 0.003$
Gas H-1-0.5	$0.91 \pm 0.03$	$0.98 \pm 0.02$	$0.97 \pm 0.02$
Gas H-2-0.1	$0.894 \pm 0.004$	$0.9942 \pm 0.0009$	$0.993 \pm 0.001$
Gas H-2-0.3	$0.882 \pm 0.002$	$0.984 \pm 0.005$	$0.983 \pm 0.004$
Gas H-2-0.5	$0.93 \pm 0.01$	$0.99 \pm 0.01$	$0.99 \pm 0.01$
Gas H-3-0.1	$0.865 \pm 0.005$	$0.979 \pm 0.001$	$0.913 \pm 0.004$
Gas H-3-0.3	$0.89 \pm 0.01$	$0.988 \pm 0.009$	$0.98 \pm 0.01$
Gas H-3-0.5	$0.92 \pm 0.01$	$0.983 \pm 0.007$	$0.983 \pm 0.007$

APPENDIX B:  $F_{total}$  of experimental chromatograms (n=3) calculated using different methods for gasoline samples, after  $I^T$  range extension and background subtraction.

for gasonne samples, and	F <sub>total</sub> by mass	Optimized F <sub>total</sub>	F <sub>total</sub> by area
Gas A-1-0.1	0.0801	0.1207	$0.12 \pm 0.01$
Gas A-1-0.3	0.2945	0.4220	$0.49 \pm 0.03$
Gas A-1-0.5	0.4967	0.7093	$0.70 \pm 0.02$
Gas A-2-0.1	0.089	0.1233	$0.10 \pm 0.01$
Gas A-2-0.3	0.2893	0.4431	$0.48 \pm 0.02$
Gas A-2-0.5	0.5021	0.7087	$0.70 \pm 0.06$
Gas A-3-0.1	0.1107	0.1578	$0.138 \pm 0.004$
Gas A-3-0.3	0.2653	0.3945	$0.34 \pm 0.01$
Gas A-3-0.5	0.4998	0.6923	$0.55 \pm 0.03$
Gas B-1-0.1	0.0984	0.1871	$0.136 \pm 0.003$
Gas B-1-0.3	0.3010	0.5469	$0.404 \pm 0.005$
Gas B-1-0.5	0.5051	0.8106	$0.59 \pm 0.02$
Gas B-2-0.1	0.0940	0.1742	$0.123 \pm 0.003$
Gas B-2-0.3	0.3027	0.5251	$0.397 \pm 0.008$
Gas B-2-0.5	0.4812	0.7930	$0.616 \pm 0.002$
Gas B-3-0.1	0.0830	0.1495	$0.123 \pm 0.004$
Gas B-3-0.3	0.3063	0.5404	$0.418 \pm 0.003$
Gas B-3-0.5	0.5013	0.8041	$0.645 \pm 0.001$
Gas C-1-0.1	0.0876	0.1575	$0.147 \pm 0.003$
Gas C-1-0.3	0.3036	0.5415	$0.520 \pm 0.009$
Gas C-1-0.5	0.5110	0.7188	$0.690 \pm 0.004$
Gas C-2-0.1	0.1017	0.1880	$0.171 \pm 0.003$
Gas C-2-0.3	0.3113	0.5346	$0.52 \pm 0.02$
Gas C-2-0.5	0.5102	0.7697	$0.796 \pm 0.008$
Gas C-3-0.1	0.0837	0.1534	$0.130 \pm 0.003$
Gas C-3-0.3	0.3189	0.5503	$0.498 \pm 0.004$
Gas C-3-0.5	0.5059	0.7614	$0.68 \pm 0.01$
Gas E-1-0.1	0.1013	0.1567	$0.18 \pm 0.03$
Gas E-1-0.3	0.3224	0.5167	$0.676 \pm 0.004$
Gas E-1-0.5	0.4972	0.7325	$0.82 \pm 0.05$
Gas E-2-0.1	0.112	0.1886	$0.16 \pm 0.01$
Gas E-2-0.3	0.3096	0.4571	$0.595 \pm 0.005$
Gas E-2-0.5	0.4822	0.6435	$0.81 \pm 0.03$
Gas E-3-0.1	0.1047	0.1614	$0.13 \pm 0.01$
Gas E-3-0.3	0.3145	0.4627	$0.45 \pm 0.04$
Gas E-3-0.5	0.5069	0.7081	$0.66 \pm 0.02$
Gas F-1-0.1	0.1017	0.1737	$0.17 \pm 0.02$

	F <sub>total</sub> by mass	Optimized F <sub>total</sub>	F <sub>total</sub> by area	
Gas F-1-0.3	0.2956	0.5214	$0.54 \pm 0.07$	
Gas F-1-0.5	0.5019	0.7473	$0.75 \pm 0.09$	
Gas F-2-0.1	0.0995	0.2234	$0.32 \pm 0.01$	
Gas F-2-0.3	0.2955	0.4981	$0.48 \pm 0.09$	
Gas F-2-0.5	0.5083	0.7792	$0.7 \pm 0.1$	
Gas F-3-0.1	0.1016	0.2223	$0.28 \pm 0.04$	
Gas F-3-0.3	0.3162	0.5589	$0.73 \pm 0.06$	
Gas F-3-0.5	0.4761	0.7231	$1.1 \pm 0.1$	
Gas G-1-0.1	0.1071	0.1868	$0.17 \pm 0.03$	
Gas G-1-0.3	0.3031	0.5002	$0.488 \pm 0.007$	
Gas G-1-0.5	0.5230	0.7521	$0.76 \pm 0.02$	
Gas G-2-0.1	0.1070	0.1853	$0.162 \pm 0.004$	
Gas G-2-0.3	0.3119	0.5300	$0.49 \pm 0.01$	
Gas G-2-0.5	0.5186	0.7887	$0.75 \pm 0.01$	
Gas G-3-0.1	0.1061	0.1803	$0.121 \pm 0.004$	
Gas G-3-0.3	0.3148	0.4935	$0.45 \pm 0.02$	
Gas G-3-0.5	0.4928	0.7240	$0.810 \pm 0.004$	
Gas H-1-0.1	0.0921	0.1507	$0.143 \pm 0.003$	
Gas H-1-0.3	0.2554	0.4326	$0.44 \pm 0.01$	
Gas H-1-0.5	0.4813	0.7389	$0.70 \pm 0.02$	
Gas H-2-0.1	0.0990	0.1637	$0.153 \pm 0.005$	
Gas H-2-0.3	0.3138	0.5285	$0.499 \pm 0.008$	
Gas H-2-0.5	0.5080	0.7681	$0.75 \pm 0.02$	
Gas H-3-0.1	0.1001	0.1703	$0.1135 \pm 0.0006$	
Gas H-3-0.3	0.2942	0.4832	$0.430 \pm 0.005$	
Gas H-3-0.5	0.4874	0.7410	$0.76 \pm 0.01$	

APPENDIX C: Differences in  $F_{total}$  of experimental chromatograms (n=3) calculated using different methods for gasoline samples after  $I^T$  range extension and background subtraction.

any er ent memous jor gan	F <sub>opt</sub> - F <sub>mass</sub>	F <sub>area</sub> - F <sub>mass</sub>	F <sub>opt</sub> - F <sub>area</sub>
Gas A-1-0.1	0.0406	0.04	0.00
Gas A-1-0.3	0.1475	0.20	-0.05
Gas A-1-0.5	0.2126	0.20	0.01
Gas A-2-0.1	0.0343	0.01	0.02
Gas A-2-0.3	0.1538	0.19	-0.04
Gas A-2-0.5	0.2066	0.20	0.01
Gas A-3-0.1	0.0471	0.027	0.020
Gas A-3-0.3	0.1292	0.07	0.05
Gas A-3-0.5	0.1925	0.05	0.14
Gas B-1-0.1	0.0887	0.038	0.051
Gas B-1-0.3	0.2459	0.103	0.143
Gas B-1-0.5	0.3055	0.08	0.22
Gas B-2-0.1	0.0802	0.029	0.051
Gas B-2-0.3	0.2224	0.094	0.128
Gas B-2-0.5	0.3118	0.135	0.177
Gas B-3-0.1	0.0665	0.040	0.027
Gas B-3-0.3	0.2341	0.112	0.122
Gas B-3-0.5	0.3028	0.144	0.159
Gas C-1-0.1	0.0699	0.059	0.011
Gas C-1-0.3	0.2379	0.216	0.022
Gas C-1-0.5	0.2078	0.179	0.029
Gas C-2-0.1	0.0863	0.069	0.017
Gas C-2-0.3	0.2233	0.21	0.01
Gas C-2-0.5	0.2595	0.286	-0.026
Gas C-3-0.1	0.0697	0.046	0.023
Gas C-3-0.3	0.2314	0.179	0.052
Gas C-3-0.5	0.2555	0.17	0.08
Gas E-1-0.1	0.0554	0.08	-0.02
Gas E-1-0.3	0.1943	0.354	-0.159
Gas E-1-0.5	0.2353	0.32	-0.09
Gas E-2-0.1	0.0766	0.05	0.03
Gas E-2-0.3	0.1475	0.285	-0.138
Gas E-2-0.5	0.1613	0.33	-0.17
Gas E-3-0.1	0.0567	0.03	0.03
Gas E-3-0.3	0.1482	0.14	0.01
Gas E-3-0.5	0.2012	0.15	0.05
Gas F-1-0.1	0.0720	0.07	0.00
Gas F-1-0.3	0.2258	0.24	-0.02
Gas F-1-0.5	0.2454	0.25	0.00

	Fopt - Fmass	Farea - Fmass	F <sub>opt</sub> - F <sub>area</sub>
Gas F-2-0.1	0.1239	0.22	-0.10
Gas F-2-0.3	0.2026	0.18	0.02
Gas F-2-0.5	0.2709	0.2	0.1
Gas F-3-0.1	0.1207	0.18	-0.06
Gas F-3-0.3	0.2427	0.41	-0.17
Gas F-3-0.5	0.2470	0.6	-0.4
Gas G-1-0.1	0.0797	0.063	0.017
Gas G-1-0.3	0.1971	0.185	0.012
Gas G-1-0.5	0.2291	0.24	-0.01
Gas G-2-0.1	0.0783	0.055	0.023
Gas G-2-0.3	0.2181	0.18	0.04
Gas G-2-0.5	0.2701	0.23	0.04
Gas G-3-0.1	0.0742	0.015	0.059
Gas G-3-0.3	0.1787	0.14	0.04
Gas G-3-0.5	0.2312	0.317	-0.086
Gas H-1-0.1	0.0586	0.051	0.008
Gas H-1-0.3	0.1772	0.18	-0.01
Gas H-1-0.5	0.2576	0.22	0.04
Gas H-2-0.1	0.0647	0.054	0.011
Gas H-2-0.3	0.2147	0.185	0.030
Gas H-2-0.5	0.2601	0.24	0.02
Gas H-3-0.1	0.0702	0.0134	0.0568
Gas H-3-0.3	0.1890	0.136	0.053
Gas H-3-0.5	0.2536	0.27	-0.02

REFERENCES

#### **REFERENCES**

- McIlroy, J.W., Jones, A.D., McGuffin, V.L., Gas Chromatographic Retention Index as a Basis for Predicting Evaporation Rates of Complex Mixtures. Anal. Chim. Acta 2014, Sep; 852: 257-66
- 2. Smith, R.W., Brehe, R.J., McIlroy, J.W., McGuffin, V.L., Mathematically Modeling Chromatograms of Evaporated Ignitable Liquids for Fire Debris Applications. Forensic Chemistry 2016, Jan; 2: 37-45.
- 3. ASTM E1618-14, Standard Test Method for Ignitable Liquid Residues in Extracts from Fire Debris Samples by Gas Chromatography–Mass Spectrometry. ASTM International, West Conshohocken, PA, 2014.
- 4. Gorocs, N., Bek, B., Bozsik, J., Matyasi, J., Balla, J. The Determination of GC-MS Relative Molar Responses of Benzene and Biphenyl Derivatives. Journal of Analytical Chemistry 2014; 69 (11): 1112-21.

IV: Application of a Kinetic Model to Generate an Ignitable Liquid Reference Collection for Identification Purposes

After modifications discussed in Chapter 3, the kinetic model was demonstrated to accurately predict the evaporation of gasoline. Predictive accuracy was determined through comparing predicted chromatograms to corresponding chromatograms of experimentally evaporated gasoline using Pearson product-moment correlation (PPMC) coefficients (Equation 1.6). In combination with previous work, the model has now been demonstrated to accurately predict the evaporation of ignitable liquids from the petroleum distillate and gasoline classes, as well as marine fuel stabilizer (naphthenic-paraffinic class)<sup>1</sup>. However, to this point, the accuracy of the model has been determined based on comparisons of experimentally evaporated liquids to chromatograms predicted using an unevaporated liquid from the same source. In this context, 'same source' indicates a single collection of gasoline from a service station on a specific day. In reality, the source of the original liquid in a fire debris sample is unknown. That is, the chromatogram of an ignitable liquid residue recovered from fire debris is compared to reference chromatograms that, in all likelihood, originate from a different source than the submitted sample.

While the accuracy of the mathematical model has been demonstrated, the capabilities with respect to predicting evaporation using an unevaporated chromatogram of a liquid from a different source have not yet been tested. To continue validating the model prior to implementation in forensic laboratories, these capabilities were assessed and are described in this chapter. The model was used to predict chromatograms of gasoline from one source and the predicted chromatograms were then compared to experimental chromatograms of gasoline from a different source. Comparisons were also performed between experimental gasoline

chromatograms and chromatograms predicted using ignitable liquids from four different ASTM classes.

# 4.1 Gasoline Samples

Gasoline samples were collected from seven sources over the course of two months, with one exception of Gasoline A collected four months before the rest, and each source was evaporated in triplicate to  $F_{total} = 0.5$ , 0.3, and 0.1 by mass (Table 2.1).  $F_{total}$  by mass is calculated as the mass of the evaporated gasoline divided by the mass of the gasoline prior to evaporation. One set of evaporations to  $F_{total} = 0.5$ , 0.3, and 0.1 by mass for a given gasoline was analyzed in a day. Five of the seven gasoline samples were evaporated and analyzed on consecutive days, with gasolines A and F evaporated and analyzed on non-consecutive days within one week. Unevaporated gasoline from a given source was analyzed on each day that corresponding experimentally evaporated samples were analyzed, with all unevaporated and evaporated samples analyzed in triplicate. For each unevaporated gasoline, the chromatograms of the triplicate injections analyzed on the same day were compared using PPMC coefficients. A few unevaporated gasoline samples (Gasoline E sets 1 and 3 and gasoline F set 2) were found to have one injection that was significantly different from the other two and, thus, were not considered in comparisons. The resulting PPMC coefficient range of 0.901-0.999 (Table 4.1) is indicative of error in the instrument replicates. The error was not due to retention time misalignments but rather discrepancies in abundance.

Table 4.1. Mean PPMC coefficients calculated between injections of the same unevaporated gasoline on the same day and on different days. The  $\pm$  indicates standard deviation.

	A	В	C	E	F	G	Н
Mean PPMC coefficient between injections day 1	0.985 ± 0.003	0.9985± 0.0008	0.984 ± 0.006	0.970*	0.98 ± 0.01	0.98 ± 0.02	0.97 ± 0.02
Mean PPMC coefficient between injections day 2	0.985 ± 0.005	0.9986± 0.0006	0.993 ± 0.005	0.93 ± 0.04	0.974*	0.992 ± 0.007	0.988 ± 0.002
Mean PPMC coefficient between injections day 3	0.983 ± 0.005	0.997 ± 0.002	0.998 ± 0.002	0.901*	0.973 ± 0.003	0.99 ± 0.01	0.98 ± 0.01
Mean PPMC coefficient between days	0.97 ± 0.01	0.993 ± 0.004	0.990 ± 0.007	0.93 ± 0.05	0.97 ± 0.01	0.96 ± 0.03	0.98 ± 0.01

For mean PPMC coefficients between injections, n=3 except for \* where n=2 due to an outlier. For mean PPMC coefficients between days n=27 for gasolines A, B, C, G, and H, n=16 for gasoline E, and n=21 for gasoline F.

Gasoline E sets 2 and 3 had the lowest PPMC coefficients for instrument replicate comparisons. In the second injection of gasoline E set 3, the normalized abundances for many compounds including hexane, toluene, and a  $C_2$ -alkylbenzene had slightly higher normalized abundances (<0.1) than the first injection, while the first injection had higher normalized abundances (>0.1) for two  $C_2$ -alkylbenzene peaks and one  $C_3$ -alkylbenzene peak. For reference, the maximum normalized abundance of any compound for either injection was 1.4. Set 2 of gasoline E contains many discrepancies in abundance between the three injections. For example, the peak at retention index ( $I^T$ ) = 683 has a normalized abundance of 0.93 for injection 1, 1.06 for injection 2, and 0.74 for injection 3. Injection 1 has lower abundance than 2 or 3 for many compounds, with differences often >0.1. As a comparison, gasoline B set 1 has differences in

abundance of <0.05 for all compounds between injection replicates and a corresponding PPMC coefficient of  $0.9985 \pm 0.0008$ .

When unevaporated samples from the same source analyzed on three different days were compared to each other (within the same source), the mean PPMC coefficients ranged from  $0.93 \pm 0.05$  to  $0.993 \pm 0.004$ , depending on the source (Table 4.1, row 4). The high standard deviation observed for gasoline E comparisons between days is likely due to the smaller number of chromatograms being compared in this way, due to removal of two outlier injections, as well as the already low correlation between injections on the same day. Despite this, the correlation is still quite high, surpassing the 0.80 standard for strong correlation. Due to the strong correlation of chromatograms from the same source analyzed on different days, the second injection of the unevaporated sample analyzed on the first day for a given source was selected as the unevaporated chromatogram to be used for prediction purposes for that source in this chapter, with the exception of gasoline E, for which the first injection of the first unevaporated sample was used.

The chromatograms of unevaporated gasolines from different sources were also compared using PPMC coefficients (Table 4.2). For these comparisons, only the injection used for prediction purposes was investigated. Only 3 of the 21 comparisons resulted in PPMC coefficients below 0.90, with the lowest at 0.865, suggesting high similarity between the different gasoline samples.

Table 4.2. PPMC coefficients calculated for comparisons of unevaporated gasoline samples from different sources (Gasoline A-H).

	A	В	С	Е	F	G
В	0.987					
C	0.951	0.946				
Е	0.906	0.936	0.865			
F	0.933	0.959	0.903	0.968		
G	0.950	0.948	0.948	0.885	0.896	
Н	0.937	0.961	0.924	0.968	0.986	0.910

PPMC coefficients for comparisons of chromatograms of unevaporated gasoline samples from different sources are lower than instrument replicates of an individual sample. Lower values reflect true chemical differences between the gasoline samples as opposed to instrumental discrepancies. Gasoline G has the highest normalized abundance of toluene at 2.37, with gasoline A the next highest at a normalized abundance of 1.90 (Figure 4.1). Conversely, gasolines E, F, and H have normalized abundances of toluene of 1.17, 1.10, and 1.11, respectively. The large difference in abundances of toluene may contribute to gasolines A and G having poorer correlation with gasolines E, F, and H (Table 4.2). Relationships between gasolines were also investigated for other compounds, though toluene had the highest abundance and most variation in abundance among gasoline sources. The C2-alkylbenzenes were in higher abundance for gasolines A, B, C, and G (above 1.25 for the alkylbenzene eluting at  $I^T = 854$ ) when compared to the gasolines E, F, and H (normalized abundance < 1.0 for the same peak). C<sub>3</sub>-alkylbenzenes showed a more even spread in normalized abundances among different gasolines, ranging from 0.69-1.17 for  $I^T = 979$ . Methylnaphthalene at  $I^T = 1270$  showed a similar pattern in abundances as the C2-alkylbenzenes, with the exception of gasoline C grouping with gasolines of lower abundances. The abundances for methylnaphthalene are small but separate into two distinct groups, with the higher abundance group having abundances of 0.200.21 and the lower abundance group having abundances of 0.11-0.13. These comparisons all lend further credence to the separation of gasolines A and G from gasolines E, F, and H, as reflected in PPMC coefficients.

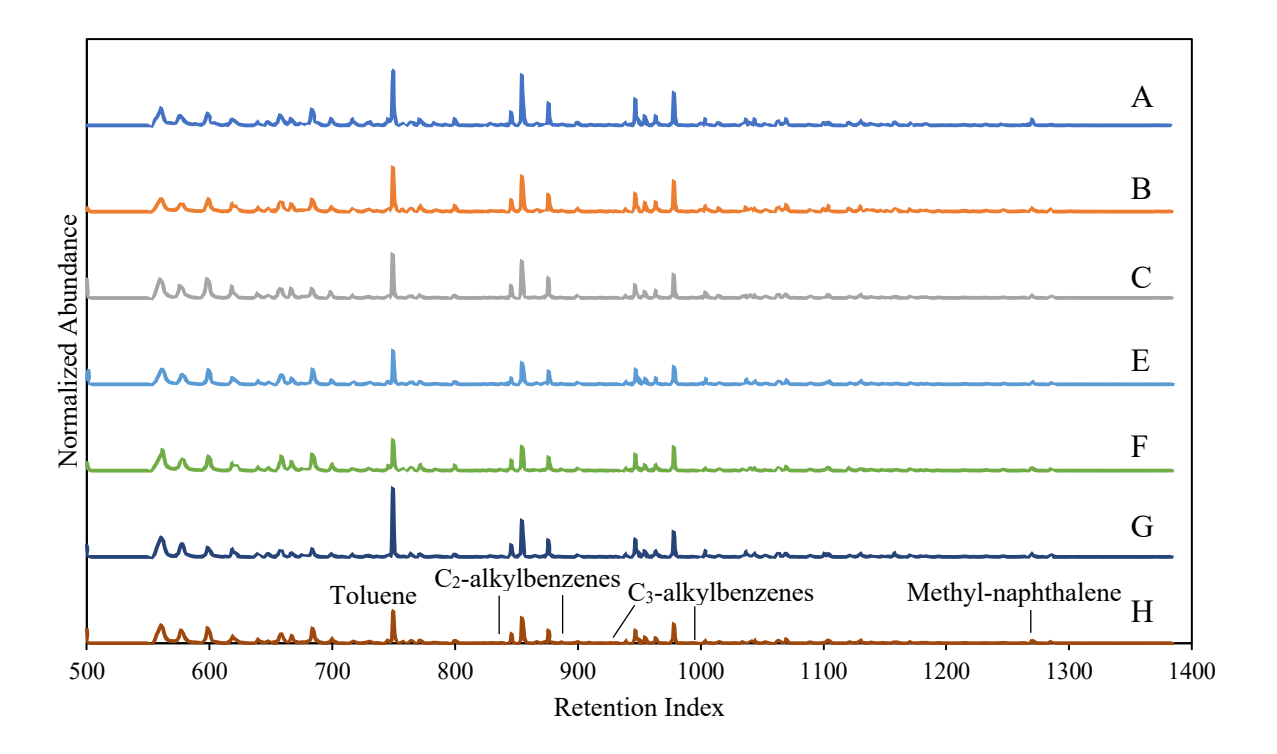


Figure 4.1. Chromatograms of unevaporated gasoline samples A-H.

4.2 Comparison of Chromatograms of Experimentally Evaporated Gasoline to Chromatograms Predicted Using Unevaporated Gasoline of the Same Source

Two methods were used to generate predicted chromatograms from an unevaporated gasoline for comparison to chromatograms of experimentally evaporated gasoline of the same source. In the first method, chromatograms were predicted from  $F_{total} = 0.1$  to 0.9 by area, in increments of 0.1, using a chromatogram of an unevaporated gasoline. The set of predicted chromatograms generated in this manner will be referred to as the gasoline reference collection, including a letter representing the gasoline source. Chromatograms were predicted for a given gasoline using the second injection of the unevaporated gasoline on the first day of analysis.

Each chromatogram in the reference collection was then compared to chromatograms of experimentally evaporated same-source gasoline with  $F_{total} = 0.5$ , 0.3, and 0.1 by mass, with three sets of evaporations performed and analyzed for each gasoline source. For a given experimentally evaporated sample, PPMC coefficients were calculated between the predicted chromatogram and experimental chromatograms from each of the triplicate injections, and the average PPMC coefficient is reported. The maximum PPMC coefficient between an experimental chromatogram and the reference collection was then determined (Figure 4.2).

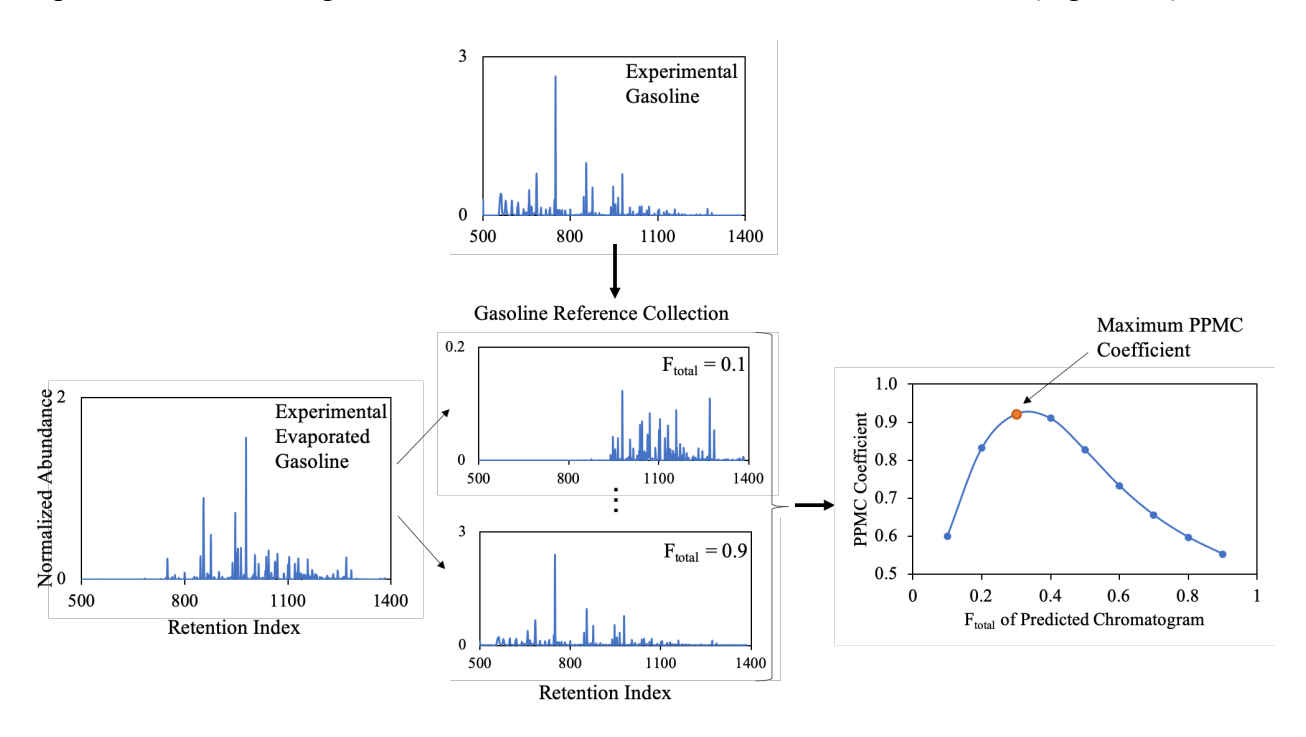


Figure 4.2. Workflow used to compare chromatograms of experimentally evaporated gasoline to reference collections.

As discussed in Section 3.4, there is a discrepancy between experimental  $F_{total}$  by mass and by area. Due to this discrepancy, the highest correlation to reference collection chromatograms was achieved at a  $F_{total}$  equal to or greater than the experimental  $F_{total}$  by mass. This is illustrated in Table 4.3, which shows a complete set of PPMC coefficients for the comparison of experimental gasoline A set 1 chromatograms to the gasoline A predicted

reference collection. The experimental  $F_{total} = 0.1$  by mass has the highest correlation with predicted  $F_{total} = 0.1$ , experimental  $F_{total} = 0.3$  with predicted  $F_{total} = 0.4$ , and experimental  $F_{total} = 0.5$  with predicted  $F_{total} = 0.7$ . The same method was applied to determine maximum correlation to the same-source reference collection for each gasoline and resulted in maximum PPMC coefficients ranging from 0.935-0.996 (Table 4.4). The corresponding predicted  $F_{total}$  values can be found in Table 4.5. All coefficients were above the  $\pm 0.8$  cutoff constituting strong correlation and were in fact all greater than 0.93, increasing the strength of correlation<sup>2</sup>.

Table 4.3. Mean PPMC coefficients calculated for comparisons of experimental chromatograms ( $F_{total} = 0.1, 0.3, \text{ and } 0.5 \text{ by mass}$ ) to a predicted reference collection developed using gasoline of the same source as the experimentally evaporated gasoline, gasoline A set 1 here.

	Experimental F <sub>total</sub> = 0.1 by mass	Experimental F <sub>total</sub> = 0.3 by mass	Experimental $F_{total} = 0.5$ by mass
Predicted $F_{\text{total}} = 0.1$	$0.961 \pm 0.003$	$0.445 \pm 0.008$	$0.290 \pm 0.007$
Predicted $F_{total} = 0.2$	$0.876 \pm 0.005$	$0.784 \pm 0.009$	$0.577 \pm 0.012$
Predicted $F_{total} = 0.3$	$0.7196 \pm 0.003$	$0.931 \pm 0.005$	$0.750 \pm 0.014$
Predicted $F_{total} = 0.4$	$0.590 \pm 0.002$	$0.986 \pm 0.002$	$0.863 \pm 0.012$
Predicted $F_{total} = 0.5$	$0.493 \pm 0.002$	$0.983 \pm 0.005$	$0.937 \pm 0.008$
Predicted $F_{total} = 0.6$	$0.4188 \pm 0.0015$	$0.948 \pm 0.007$	$0.976 \pm 0.004$
Predicted $F_{total} = 0.7$	$0.3621 \pm 0.0013$	$0.901 \pm 0.008$	$0.988 \pm 0.002$
Predicted $F_{total} = 0.8$	$0.3190 \pm 0.0012$	$0.853 \pm 0.009$	$0.982 \pm 0.003$
Predicted $F_{total} = 0.9$	$0.2846 \pm 0.0012$	$0.807 \pm 0.009$	$0.965 \pm 0.004$

Table 4.4. Maximum PPMC coefficients calculated for comparisons of experimental chromatograms ( $F_{total} = 0.1, 0.3, \text{ and } 0.5 \text{ by mass}$ ) to a predicted reference collection developed

using gasoline of the same source as the experimentally evaporated gasoline.

	Experimental E - Experimental E - Experimental E -		
	Experimental F <sub>total</sub> =	Experimental F <sub>total</sub> =	Experimental F <sub>total</sub> =
	0.1 by mass	0.3 by mass	0.5 by mass
Gas A Set 1	$0.961 \pm 0.004$	$0.986 \pm 0.002$	$0.988 \pm 0.002$
Gas A Set 2	$0.956 \pm 0.003$	$0.9882 \pm 0.0012$	$0.989 \pm 0.003$
Gas A Set 3	$0.9756 \pm 0.0012$	$0.986 \pm 0.002$	$0.986 \pm 0.004$
Gas B Set 1	$0.992 \pm 0.002$	$0.985 \pm 0.004$	$0.983 \pm 0.011$
Gas B Set 2	$0.980 \pm 0.002$	$0.993 \pm 0.002$	$0.988 \pm 0.006$
Gas B Set 3	$0.9490 \pm 0.0010$	$0.995 \pm 0.002$	$0.995 \pm 0.005$
Gas C Set 1	$0.964 \pm 0.004$	$0.9939 \pm 0.0006$	$0.983 \pm 0.008$
Gas C Set 2	$0.985 \pm 0.006$	$0.990 \pm 0.005$	$0.981 \pm 0.003$
Gas C Set 3	$0.9444 \pm 0.0015$	$0.989 \pm 0.011$	$0.987 \pm 0.010$
Gas E Set 1	$0.9614 \pm 0.0015$	$0.982 \pm 0.003$	$0.976 \pm 0.013$
Gas E Set 2	$0.937 \pm 0.007$	$0.95 \pm 0.02$	$0.95 \pm 0.02$
Gas E Set 3	$0.963 \pm 0.003$	$0.978 \pm 0.012$	$0.983 \pm 0.007$
Gas F Set 1	$0.978 \pm 0.002$	$0.983 \pm 0.003$	$0.971 \pm 0.015$
Gas F Set 2	$0.974 \pm 0.004$	$0.985 \pm 0.007$	$0.9651 \pm 0.0005$
Gas F Set 3	$0.975 \pm 0.002$	$0.985 \pm 0.003$	$0.977 \pm 0.011$
Gas G Set 1	$0.9954 \pm 0.0002$	$0.9954 \pm 0.0009$	$0.9940 \pm 0.0004$
Gas G Set 2	$0.991 \pm 0.002$	$0.9957 \pm 0.0011$	$0.995 \pm 0.002$
Gas G Set 3	$0.9761 \pm 0.0012$	$0.993 \pm 0.002$	$0.995 \pm 0.002$
Gas H Set 1	$0.9671 \pm 0.0005$	$0.991 \pm 0.003$	$0.98 \pm 0.02$
Gas H Set 2	$0.9790 \pm 0.0003$	$0.978 \pm 0.005$	$0.985 \pm 0.014$
Gas H Set 3	$0.963 \pm 0.002$	$0.97 \pm 0.02$	$0.96 \pm 0.02$
Range of PPMC coefficients	0.935-0.995	0.953-0.996	0.952-0.995

Table 4.5. Predicted reference collection  $F_{total}$  values corresponding to the maximum PPMC coefficients calculated for comparisons of experimental chromatograms ( $F_{total} = 0.1$ , 0.3, and 0.5 by mass) to a predicted reference collection developed using gasoline of the same source as the experimentally evaporated gasoline.

experimentary evaporat	Experimental $F_{total} =$	Experimental $F_{total} =$	Experimental $F_{total} =$
	0.1 by mass	0.3 by mass	0.5 by mass
Gas A Set 1	0.1	0.4	0.7
Gas A Set 2	0.1	0.4	0.7
Gas A Set 3	0.2	0.4	0.7
Gas B Set 1	0.2	0.5	0.8
Gas B Set 2	0.2	0.5	0.8
Gas B Set 3	0.1	0.5	0.8
Gas C Set 1	0.2	0.5	0.7
Gas C Set 2	0.2	0.5	0.7
Gas C Set 3	0.2	0.5	0.7
Gas E Set 1	0.2	0.5	0.7
Gas E Set 2	0.2	0.5	0.7
Gas E Set 3	0.2	0.5	0.7
Gas F Set 1	0.2	0.5	0.7
Gas F Set 2	0.2	0.5	0.8
Gas F Set 3	0.2	0.6	0.7
Gas G Set 1	0.2	0.5	0.8
Gas G Set 2	0.2	0.5	0.8
Gas G Set 3	0.2	0.5	0.7
Gas H Set 1	0.2	0.4	0.7
Gas H Set 2	0.2	0.5	0.8
Gas H Set 3	0.2	0.5	0.8
Range of Predicted F <sub>total</sub>	0.1 - 0.2	0.4 - 0.6	0.7 - 0.8

There are no trends in terms of relating PPMC coefficient to experimental  $F_{total}$  by mass that hold true for every set of evaporations (Table 4.4). There are some sets where the PPMC coefficient increases with  $F_{total}$  by mass, but this occurs in only 19% of cases. This is expected given the evenly distributed nature of the reference collection. There are nine evenly spaced  $F_{total}$  levels in the reference collection that span the range of possible experimental  $F_{total}$  used. The difference between the  $F_{total}$  that gives the highest PPMC coefficient and a reference collection  $F_{total}$ , therefore, is always < 0.05. This closeness of optimal  $F_{total}$  and reference

collection  $F_{total}$  leads to relatively high PPMC coefficients for comparisons to the reference collection. The extent of the  $F_{total}$  discrepancy is inconsistent across samples of the same approximate evaporation level due to slight differences in actual experimental evaporation level, as calculated by mass or area. For instance, with gasoline A at nominal  $F_{total} = 0.1$  for sets 1, 2, and 3, the actual  $F_{total}$  by mass are 0.0801, 0.0890, and 0.1107, respectively, and  $F_{total}$  by area are  $0.116 \pm 0.010$ ,  $0.101 \pm 0.010$ , and  $0.138 \pm 0.004$ , respectively. When compared to the reference collection, the highest PPMC coefficient was achieved with predicted  $F_{total}$  of 0.1, 0.1, and 0.2 for sets 1, 2, and 3. The higher  $F_{total}$  by mass and by area of set 3 as compared with sets 1 and 2 corresponds to the highest correlation with predicted  $F_{total}$  0.2 instead of 0.1. A complete list of  $F_{total}$  by mass and by area for all gasoline samples can be found in Appendix 3B.

Another method, discussed in Sections 2.5.2 and 3.4, is optimization of F<sub>total</sub> to generate the predicted chromatogram with the highest mean PPMC coefficient when compared to the corresponding experimental chromatograms. This method was applied to same-source comparisons in Chapter 3 and led to an overall range of maximum PPMC coefficients of 0.955-0.998 (Appendix 3A). PPMC coefficients resulting from optimization were greater than or equal to those resulting from comparison to reference collections, with increases ranging from 0-0.045. Given the nature of both methods, this result is expected. While the results of optimization were more highly correlated than comparison to reference collections, the high PPMC coefficients achieved using reference collection comparisons is encouraging.

4.3 Comparison of Chromatograms of Experimentally Evaporated Gasolines to Chromatograms Predicted Using Gasolines of Different Sources

To test the predictive abilities of the model more realistically, a reference collection of predicted chromatograms corresponding to  $F_{total} = 0.1 - 0.9$ , in increments of 0.1, was generated

using chromatograms of unevaporated gasolines from the seven sources discussed earlier (Table 2.1), leading to a reference collection with 63 total chromatograms. The reference collection chromatograms were then compared to experimentally derived chromatograms from different-source gasolines. Comparisons were performed between every predicted chromatogram from every gasoline source and all experimental chromatograms of gasolines from other sources. The maximum PPMC coefficient was identified for each comparison between experimental chromatograms and a portion of the reference collection corresponding to a single source.

A total of 378 comparisons were performed between an experimental chromatogram and a portion of the reference collection corresponding to a gasoline of a different source. Of these comparisons, 348, or 92%, resulted in a PPMC coefficient greater than 0.90 (Appendices A-G). This method can therefore be used to predict chromatograms from a gasoline of a single source for comparison to a gasoline sample of a different source, such as a liquid of unknown source found at a crime scene, with a high degree of correlation. There were some samples, 8% of the comparisons, which did result in PPMC coefficients of less than 0.90, and while in the minority, do merit discussion.

The gasoline resulting in the lowest PPMC coefficients for different-source predictions was gasoline E. All 30 comparisons resulting in PPMC coefficients < 0.90 (as low as 0.823) occurred when gasoline E was involved, either as the reference collection or the experimental chromatograms. An example shown in Table 4.6 highlights this trend with the comparison of the gasoline A reference collection to chromatograms of experimentally evaporated gasolines E and F. There is a stark difference in PPMC coefficients when the gasoline A reference collection is compared to experimental evaporated gasoline E samples as opposed to gasoline F. The gasoline F samples have PPMC coefficients above 0.97 while gasoline E samples result in PPMC

coefficients less than 0.91. The lowest PPMC coefficient of all samples ( $0.82 \pm 0.04$ ) occurred for the comparison of the gasoline C reference collection to experimental gasoline E,  $F_{total} = 0.5$  by mass, set 1. A possible explanation for this poorer correlation with gasoline E can be observed by examining comparisons of the unevaporated gasoline samples. Gasoline E was involved in two of the three comparisons of unevaporated gasoline samples resulting in PPMC coefficients below 0.90 (Table 4.2). This discrepancy between unevaporated chromatograms may be translating to discrepancies after evaporation.

Table 4.6. Maximum PPMC coefficients between gasolines E and F, set 1, and the gasoline A reference collection, with the  $F_{total}$  of the corresponding reference collection chromatogram.

	Maximum PPMC coefficient	F <sub>total</sub> of reference collection chromatogram: different source
Gas E-1-0.1	$0.881 \pm 0.012$	0.2
Gas E-1-0.3	$0.901 \pm 0.012$	0.6
Gas E-1-0.5	$0.89 \pm 0.04$	0.8
Gas F-1-0.1	$0.982 \pm 0.003$	0.2
Gas F-1-0.3	$0.985 \pm 0.006$	0.6
Gas F-1-0.5	$0.976 \pm 0.004$	0.9

The  $F_{total}$  of the reference collection chromatogram corresponding to the maximum PPMC coefficient was equal to or greater than the  $F_{total}$  by mass of the experimentally evaporated liquid of a different source, following a similar trend to that observed with same-source comparisons (Chapter 3 Appendix B). The ranges of  $F_{total}$  of reference collection chromatogram resulting in the maximum PPMC coefficient were 0.1-0.3 for  $F_{total} = 0.1$  by mass, 0.3-0.7 for  $F_{total} = 0.3$  by mass, and 0.6-0.9 for  $F_{total} = 0.5$  by mass. These ranges are wider than those observed with same-source comparisons, but that is expected given the nature of the comparisons. For comparisons to experimental gasoline samples with a  $F_{total} = 0.3$  or 0.5, there is often a range of reference collection chromatograms that resulted in PPMC coefficients above 0.9. Despite differences in unevaporated chromatograms, therefore, the reference collection chromatogram,

which by default has a  $F_{total}$  within 0.05 of the  $F_{total}$  by area of the experimental chromatogram, is still highly correlated with the experimental chromatogram. For example, while the maximum PPMC coefficient for comparison to Gas F-1-0.5 occurred for the reference collection chromatogram with a  $F_{total} = 0.9$ , all reference chromatograms with  $F_{total} = 0.6$ -0.9 resulted in PPMC coefficients above 0.9. In this case, the  $F_{total}$  by area of the experimental chromatogram is 0.75 and comparisons to both reference chromatograms with  $F_{total} = 0.7$  and 0.8 resulted in PPMC coefficients above 0.9.

The optimization technique discussed previously was also employed. As with same-source comparisons, some improvements were made for the correlation of individual gasoline samples, with increases in PPMC coefficients ranging from 0-0.05. The overall range of PPMC coefficients remained similar to same-source comparisons, however, at 0.823-0.995. Due to the similarity in ranges of PPMC coefficients, only reference collections will be used for comparisons to liquids of other ignitable liquid classes.

While the overall PPMC coefficient range calculated for different-source comparisons for gasoline spans 0.17, the lowest value calculated using optimization is close to 0.8, the cutoff for strong correlation. To determine if this low-end value (0.823) can be used as a boundary above which a sample can be considered to be gasoline, comparisons must be made to other ignitable liquid classes. If the PPMC coefficient range for comparisons of gasoline to non-gasoline sources has an upper limit less than the lower limit of comparisons of gasolines (0.823), then it is possible that 0.823 could preliminarily be used as a PPMC coefficient boundary for gasoline comparisons. If successful, this value could service as a boundary above which a sample could be considered gasoline.

4.4 Comparison of Chromatograms of Experimentally Evaporated Gasoline to Chromatograms Predicted Using Ignitable Liquids of Other ASTM Classes

To test if predicted chromatograms of a non-gasoline ASTM ignitable liquid class are sufficiently different from experimental chromatograms of gasoline, reference collections were created using ignitable liquids from non-gasoline ASTM classes (Table 2.2). Specifically, charcoal lighter (petroleum distillate), paint thinner (isoparaffinic), adhesive remover (aromatic), and marine fuel stabilizer (naphthenic-paraffinic) were used. The unevaporated liquids were analyzed by GC-MS and the resulting chromatograms were used to create reference collections with  $F_{total} = 0.1$  to 0.9 by area in increments of 0.1. Chromatograms of experimentally evaporated gasolines from all seven sources were then compared to the reference collections of non-gasoline samples. Maximum PPMC coefficients were identified for comparison of each experimentally evaporated gasoline to each reference collection, as well as an overarching maximum among all comparisons to non-gasoline reference collections.

Of the 252 comparisons performed, 217 (86%) resulted in a maximum PPMC coefficient of less than 0.5, defined as having weak correlation (Appendices H-K). This poor correlation is expected since the liquids being compared are of different ignitable liquid classes and generally consist of different classes of compounds. There were some however, 35 comparisons or 14%, which resulted in PPMC coefficients between 0.5 and 0.62. It should be noted that this range of higher PPMC coefficients still falls firmly in the lower end of moderate correlation.

The highest PPMC coefficient obtained through this method  $(0.617 \pm 0.011)$  resulted from the comparison of gasoline C, set 2,  $F_{total} = 0.3$  by mass to the aromatic product (adhesive remover) with a predicted  $F_{total} = 0.2$  (Figure 4.3). Other comparisons of the seven gasolines experimentally evaporated to nominal  $F_{total} = 0.1$ , 0.3, and 0.5 by mass to all non-gasoline reference collections resulted in maximum PPMC coefficients ranging from 0.150-0.617. All

comparisons involving gasoline with  $F_{total} = 0.3$  or 0.5 by mass had the highest PPMC coefficients when compared to the aromatic product, among non-gasoline reference collections. The aromatic product contains almost exclusively  $C_2$ -alkylbenzenes, compounds also present in gasoline at  $F_{total} = 0.3$  and 0.5 by mass. This overlap in compounds is likely the source of the higher PPMC coefficients.

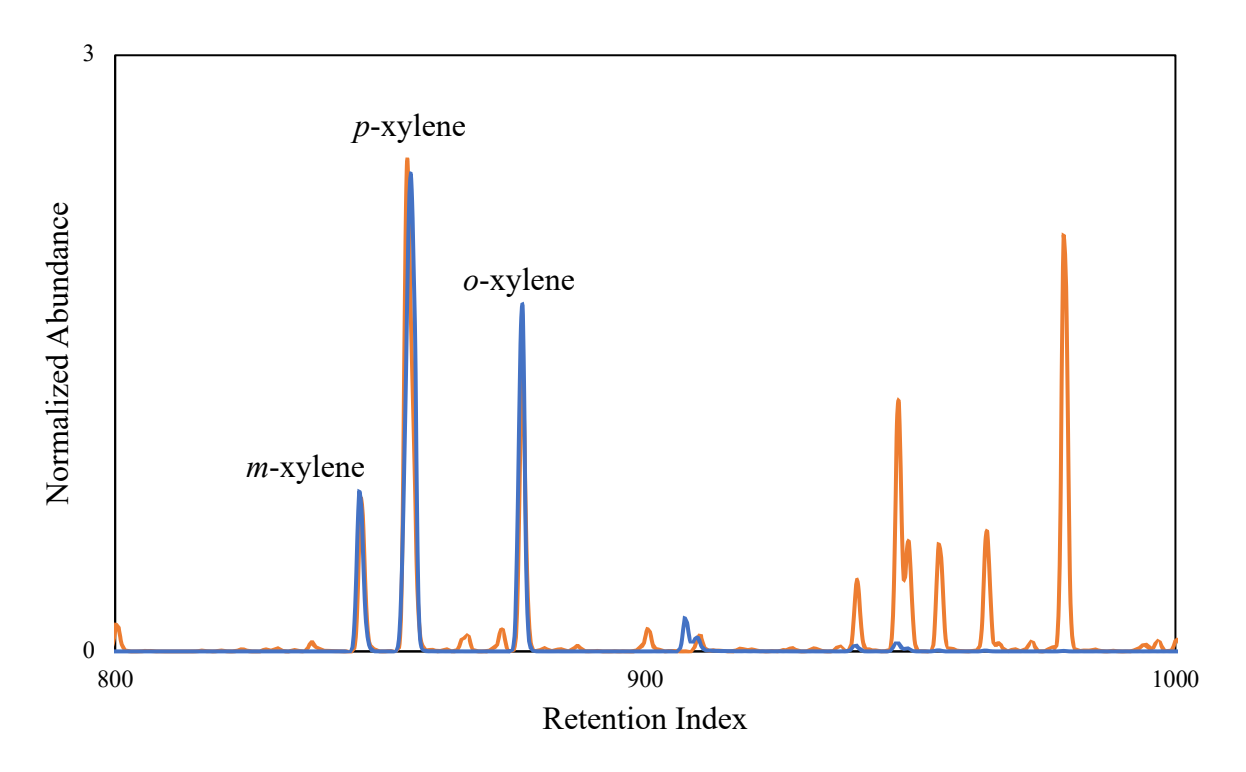


Figure 4.3. Overlay of the aromatic product predicted to  $F_{total} = 0.2$  (blue) and Gas C-2-0.3 (orange). The  $I^T$  range is such that all compounds in the aromatic product are shown.

For comparisons involving gasoline with  $F_{total} = 0.3$  by mass, the maximum PPMC coefficients (0.457-0.617) occurred on comparison to the aromatic reference collection chromatograms with  $F_{total} = 0.1$ -0.4. However, for  $F_{total} = 0.5$  by mass gasoline the maximum PPMC coefficients (0.490-0.599) occurred on comparison to the aromatic reference collection chromatograms with  $F_{total} = 0.3$ -0.8. This difference in range of reference collection  $F_{total}$  between  $F_{total}$  by mass samples is likely due to the differences in abundances of the  $C_2$ -alkylbenzenes in the gasoline samples. As the  $C_2$ -alkylbenzenes become more evaporated, the

ratios of the three compounds change, specifically the abundances of the earlier two eluting compounds (m,p-xylene) decrease relative to the last eluting compound (o-xylene). The ratios of these three compounds that most corresponds to the ratio in a given gasoline sample determines the reference collection  $F_{total}$  that will result in the highest PPMC coefficient. For gasoline samples with a higher  $F_{total}$  by mass, the  $C_2$ -alkylbenzenes would be less evaporated and so would correspond better to a high  $F_{total}$  of the aromatic reference standard.

While the other classes share some compounds with gasoline samples of  $F_{total} = 0.3$  and 0.5 by mass, there are also many compounds present in the non-gasoline liquid but not the gasoline, and vice versa. With gasoline and the aromatic liquid, the aromatic contains only one compound at low abundance not in gasoline. Accordingly, the vast majority of discrepancies occur with compounds present in gasoline but not the aromatic reference standard. This lower number of differing compounds and relatively high abundance of similar compounds likely led to the higher PPMC coefficients.

In all but one comparison of gasoline with  $F_{total} = 0.1$  by mass, the maximum PPMC coefficients (0.150-0.408) occurred when comparing to marine fuel stabilizer (MFS) predicted to  $F_{total} = 0.9$ . Both gasoline at  $F_{total} = 0.1$  by mass and MFS predicted to  $F_{total} = 0.9$  contain compounds over the same retention range ( $I^T = 900-1400$ ). At any further evaporation level of MFS, some of the early eluting compounds would have an abundance of zero, so the evaporation level of 0.9 had the highest correlation because of the largest number of compounds in common. The maximum PPMC coefficient for any comparison of gasoline with  $F_{total} = 0.1$  by mass was only 0.408 however, which is lower than maximum PPMC coefficients achieved for all samples with  $F_{total} = 0.3$  and 0.5 by mass. One comparison had the highest PPMC coefficient when compared to paint thinner, the isoparaffinic product. In general, samples with  $F_{total} = 0.1$  had

similar levels of correlation between the charcoal lighter and paint thinner reference collections but tended to have higher correlation to MFS. This is related to  $I^T$  ranges, as charcoal lighter contains compounds from  $I^T = 800$ -1200 and paint thinner contains compounds from  $I^T = 900$ -1200, while MFS contains compounds over the entire range of gasoline at  $F_{total} = 0.1$  by mass (Figure 4.5). PPMC coefficients for comparisons between the gasoline with  $F_{total} = 0.1$  by mass and the aromatic product were consistently low (<0.045) due to the lack of any similarity in  $I^T$  range and compounds contained.

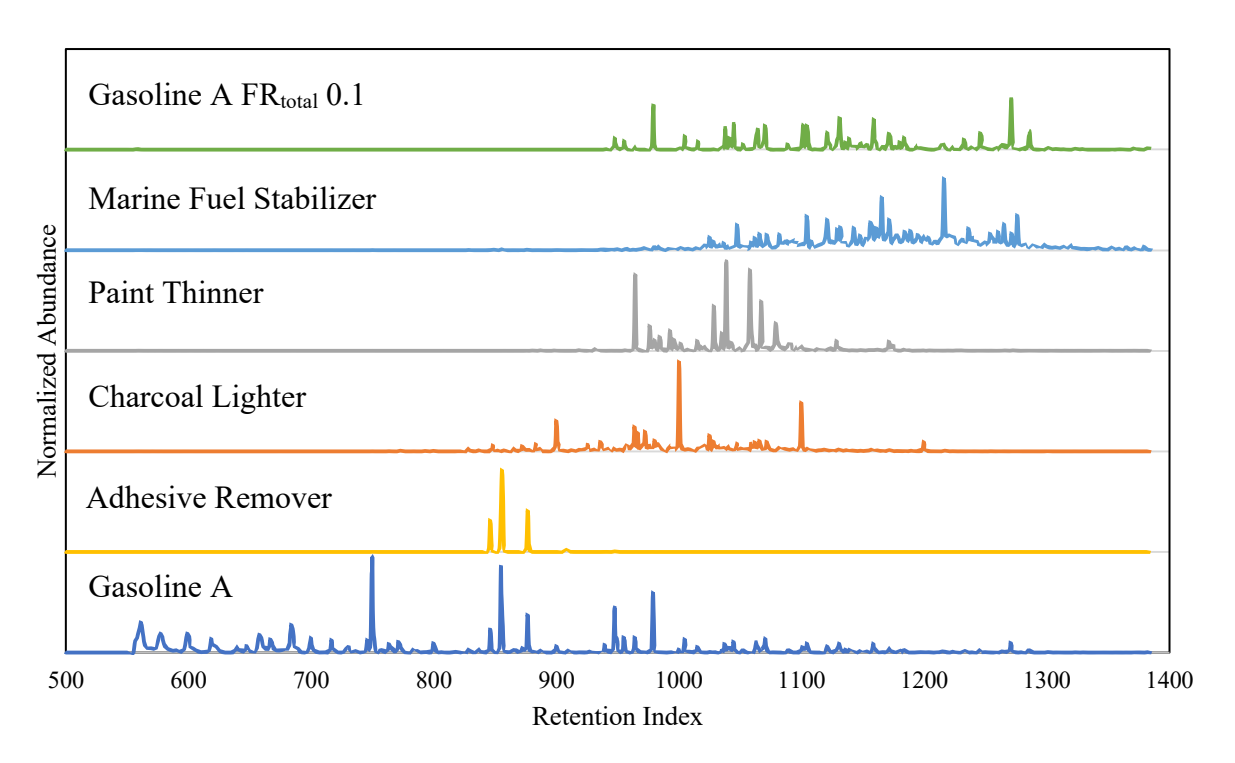


Figure 4.4. Chromatograms of unevaporated gasoline A, adhesive remover (aromatic class), charcoal lighter (petroleum distillate) marine fuel stabilizer (naphthenic-paraffinic), paint thinner (isoparaffinic), and gasoline A evaporated to  $F_{total}$  0.1 by mass.

## 4.5. Summary

Of the 252 comparisons performed between experimentally evaporated gasoline and a reference collection predicted using a liquid of a different ignitable liquid class, 217 (86%)

resulted in a maximum PPMC coefficient of less than 0.5, defined as a weak correlation (Appendices H-K). These low PPMC coefficients suggest that the model is working properly, since comparisons between liquids of different classes should not result in high PPMC coefficients. Specifically, the maximum PPMC coefficient for any such comparison was 0.617, a value on the low end of the range of moderate correlation coefficients. This maximum can be compared to the range of maximum PPMC coefficients calculated for comparisons between experimental chromatograms and reference chromatograms predicted using gasoline of a different source. The inter-class comparison maximum PPMC coefficient of 0.617 is lower than the lowest intra-class comparison PPMC coefficient of 0.823. This lends support to the idea of developing PPMC coefficient ranges for different classes of ignitable liquids for classification purposes.

APPENDICES

APPENDIX A. Maximum PPMC coefficients  $\pm$  standard deviation and the corresponding  $F_{total}$ , calculated between experimental chromatograms and (a) the gasoline A reference collection and (b) the optimized predicted chromatogram using unevaporated gasoline A.

(b) the optimized predicted chromatogram using dilevaporated gasonne A.				
	(a) Gasoline A Reference Collection		(b) Optimized Using Gasoline A	
	Maximum PPMC Coefficient ± Standard Deviation	F <sub>total</sub> of Predicted Reference Chromatogram	Maximum PPMC Coefficient ± Standard Deviation	F <sub>total</sub> of Predicted Optimized Chromatogram
Gas B-1-0.1	$0.943 \pm 0.002$	0.1	$0.9854 \pm 0.0007$	0.1386
Gas B-1-0.3	$0.990 \pm 0.002$	0.5	$0.9900 \pm 0.0019$	0.4967
Gas B-1-0.5	$0.985 \pm 0.005$	0.8	$0.985 \pm 0.005$	0.7948
Gas B-2-0.1	$0.962 \pm 0.003$	0.1	$0.9827 \pm 0.0003$	0.1264
Gas B-2-0.3	$0.985 \pm 0.005$	0.5	$0.986 \pm 0.004$	0.4748
Gas B-2-0.5	$0.988 \pm 0.003$	0.8	$0.988 \pm 0.003$	0.7798
Gas B-3-0.1	$0.980 \pm 0.0004$	0.1	$0.9804 \pm 0.0005$	0.1032
Gas B-3-0.3	$0.9910 \pm 0.0010$	0.5	$0.9921 \pm 0.0006$	0.4754
Gas B-3-0.5	$0.9896 \pm 0.0007$	0.8	$0.9904 \pm 0.0012$	0.7659
Gas C-1-0.1	$0.9546 \pm 0.0011$	0.2	$0.9824 \pm 0.0010$	0.1532
Gas C-1-0.3	$0.9814 \pm 0.0005$	0.6	$0.9814 \pm 0.0005$	0.6010
Gas C-1-0.5	$0.9815 \pm 0.0004$	0.8	$0.9815 \pm 0.0004$	0.8028
Gas C-2-0.1	$0.980 \pm 0.002$	0.2	$0.984 \pm 0.002$	0.1801
Gas C-2-0.3	$0.9842 \pm 0.0005$	0.6	$0.9852 \pm 0.0005$	0.5743
Gas C-2-0.5	$0.9847 \pm 0.0002$	0.8	$0.9853 \pm 0.0004$	0.8314
Gas C-3-0.1	$0.9370 \pm 0.0009$	0.2	$0.9788 \pm 0.0007$	0.1440
Gas C-3-0.3	$0.983 \pm 0.002$	0.6	$0.9833 \pm 0.0010$	0.5781
Gas C-3-0.5	$0.982 \pm 0.004$	0.8	$0.982 \pm 0.004$	0.7987
Gas E-1-0.1	$0.881 \pm 0.012$	0.2	$0.893 \pm 0.011$	0.1664
Gas E-1-0.3	$0.901 \pm 0.012$	0.6	$0.902 \pm 0.011$	0.5662
Gas E-1-0.5	$0.89 \pm 0.04$	0.8	$0.89 \pm 0.04$	0.8322
Gas E-2-0.1	$0.959 \pm 0.009$	0.2	$0.960 \pm 0.009$	0.2080
Gas E-2-0.3	$0.972 \pm 0.006$	0.5	$0.974 \pm 0.007$	0.5338
Gas E-2-0.5	$0.968 \pm 0.008$	0.8	$0.968 \pm 0.007$	0.7950
Gas E-3-0.1	$0.876 \pm 0.005$	0.2	$0.887 \pm 0.005$	0.1670
Gas E-3-0.3	$0.89 \pm 0.03$	0.5	$0.89 \pm 0.03$	0.5029
Gas E-3-0.5	$0.90 \pm 0.02$	0.8	$0.90 \pm 0.02$	0.8158
Gas F-1-0.1	$0.982 \pm 0.003$	0.2	$0.982 \pm 0.003$	0.2006
Gas F-1-0.3	$0.985 \pm 0.006$	0.6	$0.985 \pm 0.006$	0.5873
Gas F-1-0.5	$0.976 \pm 0.004$	0.9	$0.976 \pm 0.005$	0.8836
Gas F-2-0.1	$0.979 \pm 0.005$	0.2	$0.980 \pm 0.005$	0.1876
Gas F-2-0.3	$0.986 \pm 0.003$	0.6	$0.987 \pm 0.002$	0.5748

	(a) Gasoline A Refer	ence Collection	(b) Optimized Using Gasoline A	
	Maximum PPMC Coefficient ± Standard Deviation	F <sub>total</sub> of Predicted Reference Chromatogram	Maximum PPMC Coefficient ± Standard Deviation	F <sub>total</sub> of Predicted Optimized Chromatogram
Gas F-2-0.5	$0.9811 \pm 0.0010$	0.9	$0.9811 \pm 0.0010$	0.8981
Gas F-3-0.1	$0.982 \pm 0.003$	0.2	$0.984 \pm 0.002$	0.1861
Gas F-3-0.3	$0.9818 \pm 0.0013$	0.6	$0.9823 \pm 0.0011$	0.6212
Gas F-3-0.5	$0.974 \pm 0.008$	0.9	$0.974 \pm 0.007$	0.8671
Gas G-1-0.1	$0.9781 \pm 0.0003$	0.2	$0.9800 \pm 0.0003$	0.1858
Gas G-1-0.3	$0.9834 \pm 0.0004$	0.6	$0.9844 \pm 0.0003$	0.5723
Gas G-1-0.5	$0.9639 \pm 0.0006$	0.8	$0.9659 \pm 0.0006$	0.8502
Gas G-2-0.1	$0.9732 \pm 0.0007$	0.2	$0.9771 \pm 0.0002$	0.1800
Gas G-2-0.3	$0.9828 \pm 0.0013$	0.6	$0.9829 \pm 0.0015$	0.5921
Gas G-2-0.5	$0.967 \pm 0.002$	0.9	$0.968 \pm 0.002$	0.8545
Gas G-3-0.1	$0.9487 \pm 0.0006$	0.2	$0.9510 \pm 0.0006$	0.1847
Gas G-3-0.3	$0.979 \pm 0.002$	0.6	$0.981 \pm 0.003$	0.5644
Gas G-3-0.5	$0.968 \pm 0.005$	0.8	$0.969 \pm 0.005$	0.8318
Gas H-1-0.1	$0.9840 \pm 0.0010$	0.2	$0.9873 \pm 0.0005$	0.1820
Gas H-1-0.3	$0.987 \pm 0.002$	0.5	$0.987 \pm 0.002$	0.5123
Gas H-1-0.5	$0.983 \pm 0.005$	0.9	$0.984 \pm 0.003$	0.8773
Gas H-2-0.1	$0.9876 \pm 0.0003$	0.2	$0.9877 \pm 0.0003$	0.1983
Gas H-2-0.3	$0.9883 \pm 0.0004$	0.6	$0.9886 \pm 0.0003$	0.6165
Gas H-2-0.5	$0.984 \pm 0.003$	0.9	$0.984 \pm 0.003$	0.9054
Gas H-3-0.1	$0.967 \pm 0.002$	0.2	$0.9672 \pm 0.0015$	0.2044
Gas H-3-0.3	$0.983 \pm 0.002$	0.6	$0.984 \pm 0.003$	0.5730
Gas H-3-0.5	$0.984 \pm 0.002$	0.9	$0.984 \pm 0.003$	0.8895

APPENDIX B. Maximum PPMC coefficients  $\pm$  standard deviation and the corresponding  $F_{total}$ , calculated between experimental chromatograms and (a) the gasoline B reference collection and (b) the optimized predicted chromatogram using unevaporated gasoline B.

(b) the optimiz	(a) Gasoline B Reference Collection			(b) Optimized Using Gasoline B	
	Maximum PPMC Coefficient ± Standard Deviation	F <sub>total</sub> of Predicted Reference Chromatogram	Maximum PPMC Coefficient ± Standard Deviation	F <sub>total</sub> of Predicted Optimized Chromatogram	
Gas A-1-0.1	$0.951 \pm 0.003$	0.2	$0.968 \pm 0.004$	0.167	
Gas A-1-0.3	$0.989 \pm 0.002$	0.5	$0.989 \pm 0.002$	0.500	
Gas A-1-0.5	$0.982 \pm 0.005$	0.7	$0.984 \pm 0.004$	0.738	
Gas A-2-0.1	$0.968 \pm 0.004$	0.2	$0.976 \pm 0.003$	0.178	
Gas A-2-0.3	$0.989 \pm 0.007$	0.5	$0.989 \pm 0.003$	0.493	
Gas A-2-0.5	$0.983 \pm 0.004$	0.7	$0.984 \pm 0.004$	0.733	
Gas A-3-0.1	$0.982 \pm 0.015$	0.2	$0.988 \pm 0.002$	0.223	
Gas A-3-0.3	$0.984 \pm 0.002$	0.5	$0.989 \pm 0.002$	0.456	
Gas A-3-0.5	$0.9900 \pm 0.0010$	0.7	$0.9917 \pm 0.0005$	0.740	
Gas C-1-0.1	$0.9877 \pm 0.0010$	0.2	$0.9881 \pm 0.0010$	0.2050	
Gas C-1-0.3	$0.9717 \pm 0.0009$	0.6	$0.9745 \pm 0.0010$	0.6405	
Gas C-1-0.5	$0.982 \pm 0.004$	0.8	$0.983 \pm 0.004$	0.8215	
Gas C-2-0.1	$0.9749 \pm 0.0013$	0.2	$0.990 \pm 0.002$	0.2375	
Gas C-2-0.3	$0.983 \pm 0.003$	0.6	$0.983 \pm 0.003$	0.6174	
Gas C-2-0.5	$0.9869 \pm 0.0010$	0.8	$0.9885 \pm 0.0009$	0.8460	
Gas C-3-0.1	$0.9856 \pm 0.0010$	0.2	$0.9861 \pm 0.0010$	0.1939	
Gas C-3-0.3	$0.981 \pm 0.005$	0.6	$0.981 \pm 0.005$	0.6208	
Gas C-3-0.5	$0.981 \pm 0.010$	0.8	$0.982 \pm 0.010$	0.8168	
Gas E-1-0.1	$0.884 \pm 0.012$	0.2	$0.890 \pm 0.012$	0.223	
Gas E-1-0.3	$0.921 \pm 0.010$	0.6	$0.921 \pm 0.011$	0.619	
Gas E-1-0.5	$0.92 \pm 0.03$	0.9	$0.92 \pm 0.03$	0.856	
Gas E-2-0.1	$0.951 \pm 0.007$	0.3	$0.958 \pm 0.007$	0.269	
Gas E-2-0.3	$0.982 \pm 0.003$	0.6	$0.982 \pm 0.002$	0.586	
Gas E-2-0.5	$0.9780 \pm 0.0011$	0.8	$0.978 \pm 0.002$	0.818	
Gas E-3-0.1	$0.879 \pm 0.007$	0.2	$0.885 \pm 0.006$	0.223	
Gas E-3-0.3	$0.91 \pm 0.03$	0.6	$0.91 \pm 0.03$	0.563	
Gas E-3-0.5	$0.929 \pm 0.014$	0.8	$0.930 \pm 0.014$	0.841	
Gas F-1-0.1	$0.970 \pm 0.004$	0.3	$0.979 \pm 0.005$	0.260	
Gas F-1-0.3	$0.985 \pm 0.003$	0.6	$0.987 \pm 0.002$	0.634	
Gas F-1-0.5	$0.981 \pm 0.005$	0.9	$0.981 \pm 0.005$	0.892	
Gas F-2-0.1	$0.965 \pm 0.005$	0.3	$0.984 \pm 0.005$	0.246	
Gas F-2-0.3	$0.990 \pm 0.003$	0.6	$0.991 \pm 0.003$	0.622	

	(a) Gasoline B Refer	ence Collection	(b) Optimized Using Gasoline B	
	Maximum PPMC Coefficient ± Standard Deviation	F <sub>total</sub> of Predicted Reference Chromatogram	Maximum PPMC Coefficient ± Standard Deviation	F <sub>total</sub> of Predicted Optimized Chromatogram
Gas F-2-0.5	$0.9814 \pm 0.0005$	0.9	$0.9815 \pm 0.0006$	0.904
Gas F-3-0.1	$0.968 \pm 0.003$	0.3	$0.9868 \pm 0.0015$	0.245
Gas F-3-0.3	$0.9881 \pm 0.0016$	0.7	$0.9894 \pm 0.0012$	0.667
Gas F-3-0.5	$0.980 \pm 0.004$	0.9	$0.980 \pm 0.003$	0.880
Gas G-1-0.1	$0.9596 \pm 0.0007$	0.3	$0.9783 \pm 0.0005$	0.245
Gas G-1-0.3	$0.9894 \pm 0.0002$	0.6	$0.9899 \pm 0.0002$	0.617
Gas G-1-0.5	$0.963 \pm 0.002$	0.9	$0.967 \pm 0.002$	0.853
Gas G-2-0.1	$0.960 \pm 0.002$	0.2	$0.9753 \pm 0.0005$	0.238
Gas G-2-0.3	$0.981 \pm 0.007$	0.6	$0.982 \pm 0.006$	0.633
Gas G-2-0.5	$0.965 \pm 0.006$	0.9	$0.967 \pm 0.006$	0.857
Gas G-3-0.1	$0.925 \pm 0.002$	0.2	$0.9442 \pm 0.0013$	0.243
Gas G-3-0.3	$0.980 \pm 0.008$	0.6	$0.980 \pm 0.007$	0.610
Gas G-3-0.5	$0.965 \pm 0.010$	0.8	$0.966 \pm 0.010$	0.837
Gas H-1-0.1	$0.968 \pm 0.002$	0.2	$0.9859 \pm 0.0004$	0.240
Gas H-1-0.3	$0.9873 \pm 0.0010$	0.6	$0.9900 \pm 0.0008$	0.563
Gas H-1-0.5	$0.986 \pm 0.009$	0.9	$0.986 \pm 0.009$	0.885
Gas H-2-0.1	$0.9755 \pm 0.0002$	0.3	$0.9865 \pm 0.0006$	0.258
Gas H-2-0.3	$0.984 \pm 0.002$	0.7	$0.986 \pm 0.002$	0.659
Gas H-2-0.5	$0.991 \pm 0.003$	0.9	$0.991 \pm 0.003$	0.911
Gas H-3-0.1	$0.953 \pm 0.002$	0.3	$0.961 \pm 0.002$	0.264
Gas H-3-0.3	$0.977 \pm 0.010$	0.6	$0.978 \pm 0.009$	0.618
Gas H-3-0.5	$0.983 \pm 0.008$	0.9	$0.983 \pm 0.008$	0.896

APPENDIX C. Maximum PPMC coefficients  $\pm$  standard deviation and the corresponding  $F_{total}$ , calculated between experimental chromatograms and (a) the gasoline C reference collection and (b) the optimized predicted chromatogram using unevaporated gasoline C.

(b) the optimized predicted chromatogram using unevaporated gasonne C.				
	(a) Gasoline C Refer		(b) Optimized Using Gasoline C	
	Maximum PPMC Coefficient ± Standard Deviation	F <sub>total</sub> of Predicted Reference Chromatogram	Maximum PPMC Coefficient ± Standard Deviation	F <sub>total</sub> of Predicted Optimized Chromatogram
Gas A-1-0.1	$0.935 \pm 0.004$	0.1	$0.958 \pm 0.004$	0.1267
Gas A-1-0.3	$0.984 \pm 0.006$	0.4	$0.984 \pm 0.005$	0.3951
Gas A-1-0.5	$0.980 \pm 0.003$	0.6	$0.982 \pm 0.002$	0.6303
Gas A-2-0.1	$0.927 \pm 0.005$	0.1	$0.968 \pm 0.005$	0.1356
Gas A-2-0.3	$0.984 \pm 0.005$	0.4	$0.985 \pm 0.005$	0.3909
Gas A-2-0.5	$0.983 \pm 0.003$	0.6	$0.984 \pm 0.004$	0.6271
Gas A-3-0.1	$0.9674 \pm 0.0010$	0.2	$0.977 \pm 0.002$	0.1732
Gas A-3-0.3	$0.964 \pm 0.008$	0.4	$0.972 \pm 0.007$	0.3546
Gas A-3-0.5	$0.965 \pm 0.012$	0.6	$0.966 \pm 0.013$	0.6260
Gas B-1-0.1	$0.936 \pm 0.005$	0.2	$0.986 \pm 0.004$	0.1435
Gas B-1-0.3	$0.9889 \pm 0.0006$	0.4	$0.9936 \pm 0.0013$	0.4431
Gas B-1-0.5	$0.988 \pm 0.007$	0.7	$0.988 \pm 0.007$	0.7119
Gas B-2-0.1	$0.9508 \pm 0.0004$	0.1	$0.9826 \pm 0.0013$	0.1313
Gas B-2-0.3	$0.970 \pm 0.009$	0.4	$0.971 \pm 0.009$	0.4188
Gas B-2-0.5	$0.986 \pm 0.004$	0.7	$0.986 \pm 0.004$	0.6976
Gas B-3-0.1	$0.9842 \pm 0.0010$	0.1	$0.9868 \pm 0.0014$	0.1088
Gas B-3-0.3	$0.984 \pm 0.004$	0.4	$0.985 \pm 0.004$	0.4219
Gas B-3-0.5	$0.978 \pm 0.009$	0.7	$0.978 \pm 0.009$	0.6827
Gas E-1-0.1	$0.848 \pm 0.014$	0.2	$0.859 \pm 0.013$	0.1692
Gas E-1-0.3	$0.853 \pm 0.015$	0.5	$0.853 \pm 0.015$	0.4997
Gas E-1-0.5	$0.82 \pm 0.04$	0.7	$0.82 \pm 0.04$	0.7236
Gas E-2-0.1	$0.943 \pm 0.010$	0.2	$0.944 \pm 0.010$	0.2074
Gas E-2-0.3	$0.95 \pm 0.02$	0.5	$0.955 \pm 0.015$	0.4728
Gas E-2-0.5	$0.94 \pm 0.03$	0.7	$0.94 \pm 0.03$	0.6987
Gas E-3-0.1	$0.839 \pm 0.007$	0.2	$0.850 \pm 0.007$	0.1691
Gas E-3-0.3	$0.84 \pm 0.03$	0.4	$0.84 \pm 0.03$	0.4426
Gas E-3-0.5	$0.84 \pm 0.02$	0.7	$0.84 \pm 0.02$	0.7126
Gas F-1-0.1	$0.975 \pm 0.003$	0.2	$0.975 \pm 0.003$	0.2035
Gas F-1-0.3	$0.965 \pm 0.010$	0.5	$0.965 \pm 0.010$	0.5160
Gas F-1-0.5	$0.954 \pm 0.013$	0.8	$0.955 \pm 0.012$	0.7790
Gas F-2-0.1	$0.964 \pm 0.008$	0.2	$0.965 \pm 0.008$	0.1905
Gas F-2-0.3	$0.973 \pm 0.008$	0.5	$0.973 \pm 0.008$	0.5058

	(a) Gasoline C Refer	ence Collection	(b) Optimized Using Gasoline C	
	Maximum PPMC Coefficient ± Standard Deviation	F <sub>total</sub> of Predicted Reference Chromatogram	Maximum PPMC Coefficient ± Standard Deviation	F <sub>total</sub> of Predicted Optimized Chromatogram
Gas F-2-0.5	$0.967 \pm 0.002$	0.8	$0.967 \pm 0.0017$	0.7958
Gas F-3-0.1	$0.969 \pm 0.005$	0.2	$0.970 \pm 0.005$	0.1898
Gas F-3-0.3	$0.958 \pm 0.004$	0.5	$0.962 \pm 0.003$	0.5459
Gas F-3-0.5	$0.94 \pm 0.02$	0.8	$0.94 \pm 0.02$	0.7613
Gas G-1-0.1	$0.9782 \pm 0.0015$	0.2	$0.9794 \pm 0.0014$	0.1898
Gas G-1-0.3	$0.974 \pm 0.002$	0.5	$0.974 \pm 0.002$	0.5105
Gas G-1-0.5	$0.960 \pm 0.004$	0.8	$0.962 \pm 0.004$	0.7588
Gas G-2-0.1	$0.969 \pm 0.003$	0.2	$0.972 \pm 0.002$	0.1837
Gas G-2-0.3	$0.982 \pm 0.004$	0.5	$0.984 \pm 0.006$	0.5345
Gas G-2-0.5	$0.964 \pm 0.006$	0.8	$0.966 \pm 0.006$	0.7626
Gas G-3-0.1	$0.944 \pm 0.003$	0.2	$0.946 \pm 0.003$	0.1880
Gas G-3-0.3	$0.976 \pm 0.008$	0.5	$0.976 \pm 0.008$	0.5066
Gas G-3-0.5	$0.969 \pm 0.005$	0.7	$0.971 \pm 0.006$	0.7444
Gas H-1-0.1	$0.981 \pm 0.003$	0.2	$0.984 \pm 0.003$	0.1859
Gas H-1-0.3	$0.974 \pm 0.006$	0.5	$0.978 \pm 0.005$	0.4565
Gas H-1-0.5	$0.973 \pm 0.014$	0.8	$0.973 \pm 0.013$	0.7784
Gas H-2-0.1	$0.9855 \pm 0.0006$	0.2	$0.9855 \pm 0.0007$	0.2008
Gas H-2-0.3	$0.983 \pm 0.005$	0.6	$0.987 \pm 0.005$	0.5471
Gas H-2-0.5	$0.97 \pm 0.02$	0.8	$0.97 \pm 0.02$	0.8007
Gas H-3-0.1	$0.964 \pm 0.005$	0.2	$0.965 \pm 0.005$	0.2053
Gas H-3-0.3	$0.986 \pm 0.007$	0.5	$0.987 \pm 0.008$	0.5134
Gas H-3-0.5	$0.982 \pm 0.010$	0.8	$0.982 \pm 0.009$	0.7884

APPENDIX D. Maximum PPMC coefficients  $\pm$  standard deviation and the corresponding  $F_{total}$ , calculated between experimental chromatograms and (a) the gasoline E reference collection and (b) the optimized predicted chromatogram using unevaporated gasoline E.

(b) the optimize	ed predicted chromatog			
	(a) Gasoline E Refer		(b) Optimized Using Gasoline E	
	Maximum PPMC Coefficient ± Standard Deviation	F <sub>total</sub> of Predicted Reference Chromatogram	Maximum PPMC Coefficient ± Standard Deviation	F <sub>total</sub> of Predicted Optimized Chromatogram
Gas A-1-0.1	$0.91 \pm 0.02$	0.1	$0.91 \pm 0.02$	0.1133
Gas A-1-0.3	$0.918 \pm 0.009$	0.4	$0.920 \pm 0.008$	0.4242
Gas A-1-0.5	$0.919 \pm 0.008$	0.6	$0.921 \pm 0.008$	0.6351
Gas A-2-0.1	$0.888 \pm 0.008$	0.1	$0.902 \pm 0.006$	0.1223
Gas A-2-0.3	$0.921 \pm 0.012$	0.4	$0.922 \pm 0.011$	0.4174
Gas A-2-0.5	$0.915 \pm 0.009$	0.6	$0.916 \pm 0.009$	0.6303
Gas A-3-0.1	$0.903 \pm 0.002$	0.2	$0.920 \pm 0.002$	0.1589
Gas A-3-0.3	$0.940 \pm 0.012$	0.4	$0.941 \pm 0.013$	0.3831
Gas A-3-0.5	$0.951 \pm 0.014$	0.6	$0.952 \pm 0.013$	0.6343
Gas B-1-0.1	$0.884 \pm 0.011$	0.1	$0.910 \pm 0.012$	0.1307
Gas B-1-0.3	$0.901 \pm 0.009$	0.5	$0.902 \pm 0.009$	0.4708
Gas B-1-0.5	$0.91 \pm 0.03$	0.7	$0.91 \pm 0.03$	0.6966
Gas B-2-0.1	$0.907 \pm 0.004$	0.1	$0.918 \pm 0.004$	0.1190
Gas B-2-0.3	$0.949 \pm 0.009$	0.5	$0.953 \pm 0.009$	0.4549
Gas B-2-0.5	$0.919 \pm 0.015$	0.7	$0.919 \pm 0.015$	0.6879
Gas B-3-0.1	$0.901 \pm 0.006$	0.1	$0.901 \pm 0.006$	0.0957
Gas B-3-0.3	$0.929 \pm 0.009$	0.5	$0.934 \pm 0.010$	0.4536
Gas B-3-0.5	$0.94 \pm 0.02$	0.7	$0.94 \pm 0.02$	0.6748
Gas C-1-0.1	$0.875 \pm 0.011$	0.2	$0.910 \pm 0.010$	0.1440
Gas C-1-0.3	$0.891 \pm 0.003$	0.6	$0.895 \pm 0.003$	0.5499
Gas C-1-0.5	$0.932 \pm 0.013$	0.7	$0.932 \pm 0.013$	0.7019
Gas C-2-0.1	$0.909 \pm 0.012$	0.2	$0.916 \pm 0.012$	0.1712
Gas C-2-0.3	$0.919 \pm 0.011$	0.5	$0.921 \pm 0.012$	0.5301
Gas C-2-0.5	$0.938 \pm 0.005$	0.7	$0.938 \pm 0.005$	0.7212
Gas C-3-0.1	$0.881 \pm 0.001$	0.1	$0.9178 \pm 0.0011$	0.1367
Gas C-3-0.3	$0.92 \pm 0.03$	0.5	$0.92 \pm 0.02$	0.5320
Gas C-3-0.5	$0.92 \pm 0.03$	0.7	$0.92 \pm 0.03$	0.6934
Gas F-1-0.1	$0.897 \pm 0.007$	0.2	$0.898 \pm 0.008$	0.1912
Gas F-1-0.3	$0.940 \pm 0.010$	0.6	$0.944 \pm 0.010$	0.5483
Gas F-1-0.5	$0.940 \pm 0.014$	0.8	$0.941 \pm 0.015$	0.7752
Gas F-2-0.1	$0.942 \pm 0.007$	0.2	$0.946 \pm 0.007$	0.1797
Gas F-2-0.3	$0.939 \pm 0.012$	0.5	$0.942 \pm 0.011$	0.5388

	(a) Gasoline E Refer	rence Collection	(b) Optimized Using Gasoline E	
	Maximum PPMC Coefficient ± Standard Deviation	F <sub>total</sub> of Predicted Reference Chromatogram	Maximum PPMC Coefficient ± Standard Deviation	F <sub>total</sub> of Predicted Optimized Chromatogram
Gas F-2-0.5	$0.924 \pm 0.002$	0.8	$0.925 \pm 0.002$	0.7859
Gas F-3-0.1	$0.933 \pm 0.007$	0.2	$0.937 \pm 0.007$	0.1783
Gas F-3-0.3	$0.953 \pm 0.006$	0.6	$0.954 \pm 0.006$	0.5757
Gas F-3-0.5	$0.953 \pm 0.015$	0.8	$0.954 \pm 0.015$	0.7658
Gas G-1-0.1	$0.883 \pm 0.006$	0.2	$0.887 \pm 0.005$	0.1782
Gas G-1-0.3	$0.936 \pm 0.004$	0.5	$0.938 \pm 0.004$	0.5307
Gas G-1-0.5	$0.912 \pm 0.006$	0.7	$0.913 \pm 0.006$	0.7284
Gas G-2-0.1	$0.895 \pm 0.009$	0.2	$0.901 \pm 0.010$	0.1746
Gas G-2-0.3	$0.91 \pm 0.02$	0.5	$0.91 \pm 0.02$	0.5430
Gas G-2-0.5	$0.911 \pm 0.014$	0.7	$0.912 \pm 0.014$	0.7306
Gas G-3-0.1	$0.865 \pm 0.006$	0.2	$0.868 \pm 0.006$	0.1796
Gas G-3-0.3	$0.92 \pm 0.03$	0.5	$0.92 \pm 0.03$	0.5232
Gas G-3-0.5	$0.90 \pm 0.02$	0.7	$0.90 \pm 0.02$	0.7137
Gas H-1-0.1	$0.909 \pm 0.008$	0.2	$0.916 \pm 0.008$	0.1731
Gas H-1-0.3	$0.945 \pm 0.007$	0.5	$0.946 \pm 0.007$	0.4816
Gas H-1-0.5	$0.94 \pm 0.03$	0.8	$0.94 \pm 0.03$	0.7621
Gas H-2-0.1	$0.908 \pm 0.003$	0.2	$0.908 \pm 0.003$	0.1891
Gas H-2-0.3	$0.927 \pm 0.009$	0.6	$0.928 \pm 0.009$	0.5697
Gas H-2-0.5	$0.95 \pm 0.02$	0.8	$0.95 \pm 0.02$	0.7853
Gas H-3-0.1	$0.886 \pm 0.011$	0.2	$0.886 \pm 0.011$	0.1958
Gas H-3-0.3	$0.91 \pm 0.03$	0.5	$0.91 \pm 0.03$	0.5302
Gas H-3-0.5	$0.92 \pm 0.02$	0.8	$0.92 \pm 0.02$	0.7765

APPENDIX E. Maximum PPMC coefficients  $\pm$  standard deviation and the corresponding  $F_{total}$ , calculated between experimental chromatograms and (a) the gasoline F reference collection and (b) the optimized predicted chromatogram using unevaporated gasoline F.

(b) the optimize	ed predicted chromatog			- 41 <del>-</del>
	(a) Gasoline F Refer		(b) Optimized Using Gasoline F	
	Maximum PPMC Coefficient ± Standard Deviation	F <sub>total</sub> of Predicted Reference Chromatogram	Maximum PPMC Coefficient ± Standard Deviation	F <sub>total</sub> of Predicted Optimized Chromatogram
Gas A-1-0.1	$0.977 \pm 0.005$	0.1	$0.978 \pm 0.006$	0.1054
Gas A-1-0.3	$0.982 \pm 0.004$	0.4	$0.982 \pm 0.004$	0.3919
Gas A-1-0.5	$0.965 \pm 0.007$	0.6	$0.965 \pm 0.007$	0.6027
Gas A-2-0.1	$0.975 \pm 0.004$	0.1	$0.981 \pm 0.003$	0.1127
Gas A-2-0.3	$0.981 \pm 0.007$	0.4	$0.982 \pm 0.007$	0.3861
Gas A-2-0.5	$0.966 \pm 0.007$	0.6	$0.966 \pm 0.007$	0.5975
Gas A-3-0.1	$0.953 \pm 0.002$	0.2	$0.9890 \pm 0.0007$	0.1452
Gas A-3-0.3	$0.9822 \pm 0.0015$	0.4	$0.989 \pm 0.002$	0.3516
Gas A-3-0.5	$0.982 \pm 0.006$	0.6	$0.982 \pm 0.005$	0.6069
Gas B-1-0.1	$0.9729 \pm 0.0011$	0.1	$0.9878 \pm 0.0010$	0.1199
Gas B-1-0.3	$0.968 \pm 0.006$	0.4	$0.972 \pm 0.006$	0.4365
Gas B-1-0.5	$0.95 \pm 0.02$	0.7	$0.96 \pm 0.02$	0.6617
Gas B-2-0.1	$0.9831 \pm 0.0002$	0.1	$0.9870 \pm 0.0004$	0.1098
Gas B-2-0.3	$0.9896 \pm 0.0011$	0.4	$0.9911 \pm 0.0011$	0.4244
Gas B-2-0.5	$0.960 \pm 0.012$	0.7	$0.963 \pm 0.011$	0.6542
Gas B-3-0.1	$0.9802 \pm 0.0003$	0.1	$0.9843 \pm 0.0002$	0.0905
Gas B-3-0.3	$0.986 \pm 0.004$	0.4	$0.987 \pm 0.004$	0.4214
Gas B-3-0.5	$0.974 \pm 0.013$	0.6	$0.976 \pm 0.012$	0.6439
Gas C-1-0.1	$0.9477 \pm 0.0007$	0.1	$0.9842 \pm 0.0011$	0.1321
Gas C-1-0.3	$0.9507 \pm 0.0014$	0.5	$0.9514 \pm 0.0015$	0.5185
Gas C-1-0.5	$0.959 \pm 0.009$	0.7	$0.960 \pm 0.009$	0.6672
Gas C-2-0.1	$0.9649 \pm 0.0013$	0.2	$0.9853 \pm 0.0006$	0.1551
Gas C-2-0.3	$0.969 \pm 0.006$	0.5	$0.969 \pm 0.006$	0.5007
Gas C-2-0.5	$0.966 \pm 0.002$	0.7	$0.966 \pm 0.002$	0.6865
Gas C-3-0.1	$0.9607 \pm 0.0003$	0.1	$0.9830 \pm 0.0002$	0.1245
Gas C-3-0.3	$0.966 \pm 0.012$	0.5	$0.966 \pm 0.012$	0.5029
Gas C-3-0.5	$0.95 \pm 0.02$	0.7	$0.96 \pm 0.02$	0.6602
Gas E-1-0.1	$0.877 \pm 0.013$	0.2	$0.913 \pm 0.012$	0.1439
Gas E-1-0.3	$0.942 \pm 0.008$	0.5	$0.942 \pm 0.008$	0.5086
Gas E-1-0.5	$0.943 \pm 0.021$	0.7	$0.94 \pm 0.02$	0.7232
Gas E-2-0.1	$0.969 \pm 0.004$	0.2	$0.972 \pm 0.005$	0.1812
Gas E-2-0.3	$0.982 \pm 0.004$	0.5	$0.983 \pm 0.005$	0.4744

	(a) Gasoline F Refer	ence Collection	(b) Optimized Using Gasoline F	
	Maximum PPMC Coefficient ± Standard Deviation	F <sub>total</sub> of Predicted Reference Chromatogram	Maximum PPMC Coefficient ± Standard Deviation	F <sub>total</sub> of Predicted Optimized Chromatogram
Gas E-2-0.5	$0.976 \pm 0.009$	0.7	$0.977 \pm 0.010$	0.6771
Gas E-3-0.1	$0.871 \pm 0.006$	0.2	$0.906 \pm 0.006$	0.1442
Gas E-3-0.3	$0.93 \pm 0.03$	0.5	$0.93 \pm 0.03$	0.4576
Gas E-3-0.5	$0.952 \pm 0.008$	0.7	$0.952 \pm 0.008$	0.7040
Gas G-1-0.1	$0.9639 \pm 0.0012$	0.2	$0.9797 \pm 0.0010$	0.1599
Gas G-1-0.3	$0.979 \pm 0.002$	0.5	$0.979 \pm 0.002$	0.4984
Gas G-1-0.5	$0.932 \pm 0.004$	0.7	$0.932 \pm 0.004$	0.6946
Gas G-2-0.1	$0.9592 \pm 0.0005$	0.2	$0.9800 \pm 0.0009$	0.1552
Gas G-2-0.3	$0.963 \pm 0.011$	0.5	$0.963 \pm 0.011$	0.5089
Gas G-2-0.5	$0.932 \pm 0.010$	0.7	$0.932 \pm 0.010$	0.6963
Gas G-3-0.1	$0.941 \pm 0.002$	0.2	$0.9577 \pm 0.0003$	0.1596
Gas G-3-0.3	$0.969 \pm 0.014$	0.5	$0.969 \pm 0.014$	0.4895
Gas G-3-0.5	$0.929 \pm 0.015$	0.7	$0.930 \pm 0.015$	0.6778
Gas H-1-0.1	$0.971 \pm 0.002$	0.2	$0.9907 \pm 0.0005$	0.1569
Gas H-1-0.3	$0.982 \pm 0.002$	0.5	$0.987 \pm 0.002$	0.4538
Gas H-1-0.5	$0.97 \pm 0.02$	0.7	$0.97 \pm 0.02$	0.7342
Gas H-2-0.1	$0.9821 \pm 0.0003$	0.2	$0.9903 \pm 0.0005$	0.1711
Gas H-2-0.3	$0.972 \pm 0.004$	0.5	$0.975 \pm 0.005$	0.5396
Gas H-2-0.5	$0.979 \pm 0.011$	0.8	$0.981 \pm 0.011$	0.7585
Gas H-3-0.1	$0.9697 \pm 0.0009$	0.2	$0.975 \pm 0.002$	0.1771
Gas H-3-0.3	$0.97 \pm 0.02$	0.5	$0.97 \pm 0.02$	0.5005
Gas H-3-0.5	$0.96 \pm 0.02$	0.7	$0.96 \pm 0.02$	0.7450

APPENDIX F. Maximum PPMC coefficients  $\pm$  standard deviation and the corresponding  $F_{total}$ , calculated between experimental chromatograms and (a) the gasoline G reference collection and (b) the optimized predicted chromatogram using unevaporated gasoline G.

(b) the optimiz	(b) the optimized predicted chromatogram using unevaporated gasonne of				
	(a) Gasoline G Refer		(b) Optimized Using Gasoline G		
	Maximum PPMC Coefficient ± Standard Deviation	F <sub>total</sub> of Predicted Reference Chromatogram	Maximum PPMC Coefficient ± Standard Deviation	F <sub>total</sub> of Predicted Optimized Chromatogram	
Gas A-1-0.1	$0.943 \pm 0.005$	0.1	$0.967 \pm 0.004$	0.1270	
Gas A-1-0.3	$0.990 \pm 0.002$	0.4	$0.990 \pm 0.002$	0.4079	
Gas A-1-0.5	$0.984 \pm 0.002$	0.6	$0.985 \pm 0.002$	0.5782	
Gas A-2-0.1	$0.931 \pm 0.003$	0.1	$0.972 \pm 0.003$	0.1355	
Gas A-2-0.3	$0.990 \pm 0.002$	0.4	$0.990 \pm 0.002$	0.4033	
Gas A-2-0.5	$0.9829 \pm 0.0010$	0.6	$0.9843 \pm 0.0013$	0.5723	
Gas A-3-0.1	$0.9692 \pm 0.0008$	0.2	$0.977 \pm 0.002$	0.1741	
Gas A-3-0.3	$0.982 \pm 0.003$	0.4	$0.985 \pm 0.003$	0.3722	
Gas A-3-0.5	$0.978 \pm 0.007$	0.6	$0.979 \pm 0.006$	0.5737	
Gas B-1-0.1	$0.936 \pm 0.002$	0.2	$0.981 \pm 0.002$	0.1440	
Gas B-1-0.3	$0.986 \pm 0.002$	0.4	$0.994 \pm 0.002$	0.4473	
Gas B-1-0.5	$0.979 \pm 0.005$	0.6	$0.980 \pm 0.003$	0.6312	
Gas B-2-0.1	$0.9445 \pm 0.0011$	0.1	$0.9778 \pm 0.0014$	0.1321	
Gas B-2-0.3	$0.985 \pm 0.004$	0.4	$0.988 \pm 0.005$	0.4314	
Gas B-2-0.5	$0.981 \pm 0.002$	0.6	$0.982 \pm 0.002$	0.6211	
Gas B-3-0.1	$0.9714 \pm 0.0005$	0.1	$0.9752 \pm 0.0008$	0.1102	
Gas B-3-0.3	$0.9912 \pm 0.0005$	0.4	$0.9949 \pm 0.0012$	0.4322	
Gas B-3-0.5	$0.9823 \pm 0.0012$	0.6	$0.9823 \pm 0.0011$	0.6057	
Gas C-1-0.1	$0.962 \pm 0.002$	0.2	$0.985 \pm 0.002$	0.1578	
Gas C-1-0.3	$0.9853 \pm 0.0006$	0.5	$0.9864 \pm 0.0006$	0.5185	
Gas C-1-0.5	$0.9793 \pm 0.0011$	0.6	$0.982 \pm 0.002$	0.6412	
Gas C-2-0.1	$0.985 \pm 0.003$	0.2	$0.988 \pm 0.002$	0.1844	
Gas C-2-0.3	$0.9891 \pm 0.0008$	0.5	$0.9891 \pm 0.0008$	0.4995	
Gas C-2-0.5	$0.975 \pm 0.002$	0.7	$0.9771 \pm 0.0014$	0.6467	
Gas C-3-0.1	$0.9458 \pm 0.0007$	0.2	$0.9825 \pm 0.0003$	0.1485	
Gas C-3-0.3	$0.987 \pm 0.002$	0.5	$0.987 \pm 0.003$	0.5023	
Gas C-3-0.5	$0.978 \pm 0.003$	0.6	$0.979 \pm 0.002$	0.6327	
Gas E-1-0.1	$0.869 \pm 0.014$	0.2	$0.877 \pm 0.013$	0.1724	
Gas E-1-0.3	$0.898 \pm 0.015$	0.5	$0.899 \pm 0.014$	0.4904	
Gas E-1-0.5	$0.86 \pm 0.04$	0.6	$0.86 \pm 0.04$	0.6282	
Gas E-2-0.1	$0.968 \pm 0.008$	0.2	$0.969 \pm 0.008$	0.2081	
Gas E-2-0.3	$0.973 \pm 0.010$	0.5	$0.976 \pm 0.009$	0.4699	

	(a) Gasoline G Refer	rence Collection	(b) Optimized Using Gasoline G	
	Maximum PPMC Coefficient ± Standard Deviation	F <sub>total</sub> of Predicted Reference Chromatogram	Maximum PPMC Coefficient ± Standard Deviation	F <sub>total</sub> of Predicted Optimized Chromatogram
Gas E-2-0.5	$0.952 \pm 0.009$	0.6	$0.952 \pm 0.009$	0.5991
Gas E-3-0.1	$0.861 \pm 0.005$	0.2	$0.869 \pm 0.006$	0.1728
Gas E-3-0.3	$0.88 \pm 0.03$	0.5	$0.89 \pm 0.03$	0.4497
Gas E-3-0.5	$0.88 \pm 0.02$	0.6	$0.88 \pm 0.02$	0.6236
Gas F-1-0.1	$0.982 \pm 0.003$	0.2	$0.982 \pm 0.003$	0.2040
Gas F-1-0.3	$0.981 \pm 0.005$	0.5	$0.981 \pm 0.005$	0.4987
Gas F-1-0.5	$0.946 \pm 0.005$	0.7	$0.947 \pm 0.004$	0.6645
Gas F-2-0.1	$0.972 \pm 0.005$	0.2	$0.972 \pm 0.005$	0.1925
Gas F-2-0.3	$0.9858 \pm 0.0011$	0.5	$0.9859 \pm 0.0007$	0.4930
Gas F-2-0.5	$0.949 \pm 0.009$	0.7	$0.949 \pm 0.009$	0.6877
Gas F-3-0.1	$0.976 \pm 0.003$	0.2	$0.976 \pm 0.002$	0.1914
Gas F-3-0.3	$0.9770 \pm 0.0014$	0.5	$0.978 \pm 0.002$	0.5182
Gas F-3-0.5	$0.940 \pm 0.013$	0.7	$0.941 \pm 0.011$	0.6574
Gas H-1-0.1	$0.986 \pm 0.002$	0.2	$0.988 \pm 0.002$	0.1861
Gas H-1-0.3	$0.980 \pm 0.003$	0.5	$0.987 \pm 0.002$	0.4552
Gas H-1-0.5	$0.957 \pm 0.002$	0.7	$0.958 \pm 0.003$	0.6675
Gas H-2-0.1	$0.9895 \pm 0.0003$	0.2	$0.9895 \pm 0.0004$	0.2017
Gas H-2-0.3	$0.9869 \pm 0.0007$	0.5	$0.9884 \pm 0.0006$	0.5221
Gas H-2-0.5	$0.951 \pm 0.005$	0.7	$0.951 \pm 0.004$	0.6789
Gas H-3-0.1	$0.978 \pm 0.002$	0.2	$0.978 \pm 0.002$	0.2056
Gas H-3-0.3	$0.986 \pm 0.002$	0.5	$0.986 \pm 0.003$	0.4952
Gas H-3-0.5	$0.957 \pm 0.002$	0.7	$0.958 \pm 0.002$	0.6765

APPENDIX G. Maximum PPMC coefficients  $\pm$  standard deviation and the corresponding  $F_{total}$ , calculated between experimental chromatograms and (a) the gasoline H reference collection and (b) the optimized predicted chromatogram using unevaporated gasoline H.

(b) the optimize	ed predicted chromatog			
	(a) Gasoline H Refer		(b) Optimized Using Gasoline H	
	Maximum PPMC Coefficient ± Standard Deviation	F <sub>total</sub> of Predicted Reference Chromatogram	Maximum PPMC Coefficient ± Standard Deviation	F <sub>total</sub> of Predicted Optimized Chromatogram
Gas A-1-0.1	$0.979 \pm 0.003$	0.1	$0.979 \pm 0.003$	0.0997
Gas A-1-0.3	$0.977 \pm 0.003$	0.4	$0.980 \pm 0.005$	0.3661
Gas A-1-0.5	$0.962 \pm 0.006$	0.6	$0.962 \pm 0.006$	0.5964
Gas A-2-0.1	$0.981 \pm 0.002$	0.1	$0.9830 \pm 0.0011$	0.1070
Gas A-2-0.3	$0.977 \pm 0.008$	0.4	$0.981 \pm 0.008$	0.3601
Gas A-2-0.5	$0.960 \pm 0.007$	0.6	$0.960 \pm 0.007$	0.5904
Gas A-3-0.1	$0.9444 \pm 0.0007$	0.2	$0.989 \pm 0.002$	0.1399
Gas A-3-0.3	$0.987 \pm 0.005$	0.3	$0.990 \pm 0.005$	0.3266
Gas A-3-0.5	$0.982 \pm 0.007$	0.6	$0.982 \pm 0.007$	0.5995
Gas B-1-0.1	$0.981 \pm 0.002$	0.1	$0.989 \pm 0.002$	0.1145
Gas B-1-0.3	$0.968 \pm 0.006$	0.4	$0.968 \pm 0.006$	0.4120
Gas B-1-0.5	$0.95 \pm 0.02$	0.7	$0.95 \pm 0.02$	0.6636
Gas B-2-0.1	$0.9885 \pm 0.0005$	0.1	$0.9892 \pm 0.0003$	0.1043
Gas B-2-0.3	$0.994 \pm 0.003$	0.4	$0.994 \pm 0.003$	0.3995
Gas B-2-0.5	$0.956 \pm 0.012$	0.7	$0.958 \pm 0.012$	0.6533
Gas B-3-0.1	$0.9754 \pm 0.0003$	0.1	$0.9856 \pm 0.0007$	0.0846
Gas B-3-0.3	$0.987 \pm 0.005$	0.4	$0.987 \pm 0.005$	0.3961
Gas B-3-0.5	$0.973 \pm 0.015$	0.6	$0.975 \pm 0.014$	0.6429
Gas C-1-0.1	$0.9668 \pm 0.0011$	0.1	$0.991 \pm 0.002$	0.1263
Gas C-1-0.3	$0.956 \pm 0.002$	0.5	$0.956 \pm 0.002$	0.5038
Gas C-1-0.5	$0.971 \pm 0.011$	0.7	$0.972 \pm 0.011$	0.6732
Gas C-2-0.1	$0.9639 \pm 0.0015$	0.2	$0.991 \pm 0.002$	0.1493
Gas C-2-0.3	$0.975 \pm 0.008$	0.5	$0.976 \pm 0.008$	0.4845
Gas C-2-0.5	$0.977 \pm 0.003$	0.7	$0.977 \pm 0.003$	0.6954
Gas C-3-0.1	$0.9779 \pm 0.0003$	0.1	$0.9907 \pm 0.0001$	0.1189
Gas C-3-0.3	$0.973 \pm 0.015$	0.5	$0.97 \pm 0.02$	0.4868
Gas C-3-0.5	$0.97 \pm 0.02$	0.7	$0.97 \pm 0.02$	0.6654
Gas E-1-0.1	$0.885 \pm 0.011$	0.2	$0.927 \pm 0.010$	0.1398
Gas E-1-0.3	$0.956 \pm 0.008$	0.5	$0.956 \pm 0.008$	0.4870
Gas E-1-0.5	$0.95 \pm 0.02$	0.7	$0.96 \pm 0.02$	0.7176
Gas E-2-0.1	$0.972 \pm 0.003$	0.2	$0.980 \pm 0.004$	0.1740
Gas E-2-0.3	$0.981 \pm 0.005$	0.5	$0.985 \pm 0.006$	0.4524

	(a) Gasoline H Refer	rence Collection	(b) Optimized Usin	ng Gasoline H
	Maximum PPMC Coefficient ± Standard Deviation	F <sub>total</sub> of Predicted Reference Chromatogram	Maximum PPMC Coefficient ± Standard Deviation	F <sub>total</sub> of Predicted Optimized Chromatogram
Gas E-2-0.5	$0.976 \pm 0.013$	0.7	$0.976 \pm 0.014$	0.6767
Gas E-3-0.1	$0.880 \pm 0.004$	0.2	$0.921 \pm 0.005$	0.1403
Gas E-3-0.3	$0.95 \pm 0.02$	0.4	$0.95 \pm 0.02$	0.4327
Gas E-3-0.5	$0.964 \pm 0.007$	0.7	$0.964 \pm 0.007$	0.7011
Gas F-1-0.1	$0.971 \pm 0.004$	0.2	$0.982 \pm 0.005$	0.1668
Gas F-1-0.3	$0.982 \pm 0.006$	0.5	$0.982 \pm 0.006$	0.5012
Gas F-1-0.5	$0.97 \pm 0.02$	0.7	$0.969 \pm 0.015$	0.7496
Gas F-2-0.1	$0.971 \pm 0.003$	0.2	$0.992 \pm 0.002$	0.1572
Gas F-2-0.3	$0.984 \pm 0.008$	0.5	$0.984 \pm 0.008$	0.4902
Gas F-2-0.5	$0.95784 \pm 0.00008$	0.8	$0.9593 \pm 0.0012$	0.7603
Gas F-3-0.1	$0.9706 \pm 0.0002$	0.2	$0.9915 \pm 0.0015$	0.1559
Gas F-3-0.3	$0.984 \pm 0.004$	0.5	$0.986 \pm 0.004$	0.5329
Gas F-3-0.5	$0.976 \pm 0.012$	0.7	$0.978 \pm 0.011$	0.7393
Gas G-1-0.1	$0.958 \pm 0.002$	0.2	$0.980 \pm 0.002$	0.1538
Gas G-1-0.3	$0.981 \pm 0.002$	0.5	$0.982 \pm 0.002$	0.4836
Gas G-1-0.5	$0.943 \pm 0.005$	0.7	$0.943 \pm 0.005$	0.7038
Gas G-2-0.1	$0.9552 \pm 0.0008$	0.2	$0.983 \pm 0.002$	0.1495
Gas G-2-0.3	$0.963 \pm 0.013$	0.5	$0.963 \pm 0.013$	0.4951
Gas G-2-0.5	$0.942 \pm 0.011$	0.7	$0.942 \pm 0.011$	0.7062
Gas G-3-0.1	$0.9338 \pm 0.0005$	0.2	$0.958 \pm 0.002$	0.1528
Gas G-3-0.3	$0.97 \pm 0.02$	0.5	$0.97 \pm 0.02$	0.4735
Gas G-3-0.5	$0.94 \pm 0.02$	0.7	$0.94 \pm 0.02$	0.6865

APPENDIX H. Maximum PPMC coefficients and standard deviation comparing experimental chromatograms to reference chromatogram predicted from unevaporated charcoal lighter.

chromatograms to reference chromatogram predicted from unevaporated charcoal lighter.  Maximum PPMC Coefficient ± F <sub>total</sub> of Predicted Reference		
	Standard Deviation	Chromatogram
Gas A-1-0.1	$0.156 \pm 0.004$	0.1
Gas A-1-0.3	$0.102 \pm 0.003$	0.9
Gas A-1-0.5	$0.051 \pm 0.005$	0.9
Gas A-2-0.1	$0.163 \pm 0.002$	0.1
Gas A-2-0.3	$0.101 \pm 0.003$	0.9
Gas A-2-0.5	$0.0598 \pm 0.0015$	0.9
Gas A-3-0.1	$0.1680 \pm 0.0007$	0.1
Gas A-3-0.3	$0.1189 \pm 0.0010$	0.9
Gas A-3-0.5	$0.069 \pm 0.004$	0.9
Gas B-1-0.1	$0.1709 \pm 0.0011$	0.1
Gas B-1-0.3	$0.0985 \pm 0.0007$	0.9
Gas B-1-0.5	$0.0532 \pm 0.0008$	0.9
Gas B-2-0.1	$0.1682 \pm 0.0014$	0.1
Gas B-2-0.3	$0.1024 \pm 0.0003$	0.9
Gas B-2-0.5	$0.0681 \pm 0.0006$	0.9
Gas B-3-0.1	$0.1695 \pm 0.0006$	0.1
Gas B-3-0.3	$0.0999 \pm 0.0016$	0.9
Gas B-3-0.5	$0.0657 \pm 0.0012$	0.9
Gas C-1-0.1	$0.149 \pm 0.003$	0.1
Gas C-1-0.3	$0.0553 \pm 0.0002$	0.9
Gas C-1-0.5	$0.0250 \pm 0.0004$	0.9
Gas C-2-0.1	$0.135 \pm 0.002$	0.2
Gas C-2-0.3	$0.0595 \pm 0.0012$	0.9
Gas C-2-0.5	$0.0346 \pm 0.0004$	0.9
Gas C-3-0.1	$0.1482 \pm 0.0011$	0.1
Gas C-3-0.3	$0.0591 \pm 0.0012$	0.9
Gas C-3-0.5	$0.0300 \pm 0.0003$	0.9
Gas E-1-0.1	$0.113 \pm 0.004$	0.2
Gas E-1-0.3	$0.0693 \pm 0.0008$	0.9
Gas E-1-0.5	$0.030 \pm 0.004$	0.9
Gas E-2-0.1	$0.115 \pm 0.003$	0.4
Gas E-2-0.3	$0.078 \pm 0.002$	0.9
Gas E-2-0.5	$0.040 \pm 0.002$	0.9
Gas E-3-0.1	$0.118 \pm 0.002$	0.2
Gas E-3-0.3	$0.0816 \pm 0.0014$	0.9

	Maximum PPMC Coefficient ± Standard Deviation	F <sub>total</sub> of Predicted Reference Chromatogram
Gas E-3-0.5	$0.0365 \pm 0.0004$	0.9
Gas F-1-0.1	$0.122 \pm 0.003$	0.3
Gas F-1-0.3	$0.071 \pm 0.002$	0.9
Gas F-1-0.5	$0.0302 \pm 0.0015$	0.9
Gas F-2-0.1	$0.143 \pm 0.101$	0.2
Gas F-2-0.3	$0.073 \pm 0.003$	0.9
Gas F-2-0.5	$0.031 \pm 0.007$	0.9
Gas F-3-0.1	$0.146 \pm 0.005$	0.2
Gas F-3-0.3	$0.069 \pm 0.031$	0.9
Gas F-3-0.5	$0.034 \pm 0.020$	0.9
Gas G-1-0.1	$0.113 \pm 0.002$	0.2
Gas G-1-0.3	$0.0595 \pm 0.0004$	0.9
Gas G-1-0.5	$0.0202 \pm 0.0003$	0.9
Gas G-2-0.1	$0.1122 \pm 0.0006$	0.2
Gas G-2-0.3	$0.055 \pm 0.002$	0.9
Gas G-2-0.5	$0.0255 \pm 0.0010$	0.9
Gas G-3-0.1	$0.078 \pm 0.003$	0.2
Gas G-3-0.3	$0.045 \pm 0.002$	0.9
Gas G-3-0.5	$0.0287 \pm 0.0014$	0.9
Gas H-1-0.1	$0.126 \pm 0.002$	0.2
Gas H-1-0.3	$0.0726 \pm 0.0004$	0.9
Gas H-1-0.5	$0.024 \pm 0.002$	0.9
Gas H-2-0.1	$0.118 \pm 0.002$	0.2
Gas H-2-0.3	$0.0526 \pm 0.0013$	0.9
Gas H-2-0.5	$0.0254 \pm 0.0008$	0.9
Gas H-3-0.1	$0.084 \pm 0.002$	0.2
Gas H-3-0.3	$0.045 \pm 0.002$	0.9
Gas H-3-0.5	$0.0269 \pm 0.0010$	0.9

APPENDIX I. Maximum PPMC coefficients and standard deviation comparing experimental chromatograms to reference chromatogram predicted from unevaporated paint thinner.

chromatograms to reference chromatogram predicted from unevaporated paint thinner.			
	Maximum PPMC Coefficient ±	F <sub>total</sub> of Predicted Reference	
	Standard Deviation	Chromatogram	
Gas A-1-0.1	$0.172 \pm 0.006$	0.1	
Gas A-1-0.3	$0.095 \pm 0.002$	0.9	
Gas A-1-0.5	$0.051 \pm 0.003$	0.9	
Gas A-2-0.1	$0.1785 \pm 0.0011$	0.1	
Gas A-2-0.3	$0.100 \pm 0.004$	0.9	
Gas A-2-0.5	$0.0534 \pm 0.0013$	0.9	
Gas A-3-0.1	$0.1774 \pm 0.0006$	0.1	
Gas A-3-0.3	$0.117 \pm 0.004$	0.9	
Gas A-3-0.5	$0.061 \pm 0.003$	0.9	
Gas B-1-0.1	$0.186 \pm 0.002$	0.1	
Gas B-1-0.3	$0.0937 \pm 0.0007$	0.9	
Gas B-1-0.5	$0.051 \pm 0.002$	0.9	
Gas B-2-0.1	$0.189 \pm 0.002$	0.1	
Gas B-2-0.3	$0.103 \pm 0.002$	0.9	
Gas B-2-0.5	$0.0601 \pm 0.0011$	0.9	
Gas B-3-0.1	$0.193 \pm 0.003$	0.1	
Gas B-3-0.3	$0.100 \pm 0.002$	0.9	
Gas B-3-0.5	$0.0605 \pm 0.0014$	0.9	
Gas C-1-0.1	$0.1563 \pm 0.0008$	0.1	
Gas C-1-0.3	$0.0601 \pm 0.0002$	0.9	
Gas C-1-0.5	$0.0359 \pm 0.0009$	0.9	
Gas C-2-0.1	$0.1394 \pm 0.0006$	0.1	
Gas C-2-0.3	$0.067 \pm 0.002$	0.9	
Gas C-2-0.5	$0.0382 \pm 0.0008$	0.9	
Gas C-3-0.1	$0.1607 \pm 0.0003$	0.1	
Gas C-3-0.3	$0.066 \pm 0.003$	0.9	
Gas C-3-0.5	$0.038 \pm 0.002$	0.9	
Gas E-1-0.1	$0.157 \pm 0.007$	0.1	
Gas E-1-0.3	$0.104 \pm 0.003$	0.9	
Gas E-1-0.5	$0.067 \pm 0.003$	0.9	
Gas E-2-0.1	$0.174 \pm 0.007$	0.9	
Gas E-2-0.3	$0.100 \pm 0.004$	0.9	
Gas E-2-0.5	$0.062 \pm 0.004$	0.9	
Gas E-3-0.1	$0.162 \pm 0.002$	0.1	
Gas E-3-0.3	$0.1168 \pm 0.0005$	0.9	

	Maximum PPMC Coefficient ± Standard Deviation	F <sub>total</sub> of Predicted Reference Chromatogram
Gas E-3-0.5	$0.0692 \pm 0.0010$	0.9
Gas F-1-0.1	$0.134 \pm 0.008$	0.9
Gas F-1-0.3	$0.0858 \pm 0.0011$	0.9
Gas F-1-0.5	$0.0492 \pm 0.0012$	0.9
Gas F-2-0.1	$0.17 \pm 0.08$	0.9
Gas F-2-0.3	$0.0896 \pm 0.0013$	0.9
Gas F-2-0.5	$0.0464 \pm 0.0020$	0.9
Gas F-3-0.1	$0.171 \pm 0.004$	0.1
Gas F-3-0.3	$0.09 \pm 0.05$	0.9
Gas F-3-0.5	$0.05 \pm 0.02$	0.9
Gas G-1-0.1	$0.1181 \pm 0.0004$	0.1
Gas G-1-0.3	$0.0679 \pm 0.0009$	0.9
Gas G-1-0.5	$0.0296 \pm 0.0005$	0.9
Gas G-2-0.1	$0.120 \pm 0.003$	0.1
Gas G-2-0.3	$0.063 \pm 0.003$	0.9
Gas G-2-0.5	$0.032 \pm 0.002$	0.9
Gas G-3-0.1	$0.085 \pm 0.004$	0.1
Gas G-3-0.3	$0.054 \pm 0.004$	0.9
Gas G-3-0.5	$0.033 \pm 0.002$	0.9
Gas H-1-0.1	$0.141 \pm 0.004$	0.1
Gas H-1-0.3	$0.0922 \pm 0.0012$	0.9
Gas H-1-0.5	$0.0434 \pm 0.0016$	0.9
Gas H-2-0.1	$0.1356 \pm 0.0012$	0.9
Gas H-2-0.3	$0.0702 \pm 0.0010$	0.9
Gas H-2-0.5	$0.043 \pm 0.002$	0.9
Gas H-3-0.1	$0.095 \pm 0.002$	0.9
Gas H-3-0.3	$0.061 \pm 0.005$	0.9
Gas H-3-0.5	$0.042 \pm 0.003$	0.9

APPENDIX J. Maximum PPMC coefficients and standard deviation comparing experimental chromatograms to reference chromatogram predicted from the unevaporated adhesive remover.

em emacegrame e	Maximum PPMC Coefficient ±	F <sub>total</sub> of Predicted Reference
	Standard Deviation	Chromatogram
Gas A-1-0.1	$-0.0297 \pm 0.0007$	0.9
Gas A-1-0.3	$0.494 \pm 0.004$	0.2
Gas A-1-0.5	$0.534 \pm 0.011$	0.3
Gas A-2-0.1	$-0.0302 \pm 0.0003$	0.9
Gas A-2-0.3	$0.50 \pm 0.02$	0.1
Gas A-2-0.5	$0.533 \pm 0.004$	0.4
Gas A-3-0.1	$-0.0159 \pm 0.0002$	0.9
Gas A-3-0.3	$0.4570 \pm 0.0011$	0.1
Gas A-3-0.5	$0.563 \pm 0.012$	0.4
Gas B-1-0.1	$-0.0244 \pm 0.0005$	0.9
Gas B-1-0.3	$0.516 \pm 0.008$	0.2
Gas B-1-0.5	$0.52 \pm 0.02$	0.4
Gas B-2-0.1	$-0.0310 \pm 0.0003$	0.9
Gas B-2-0.3	$0.544 \pm 0.007$	0.2
Gas B-2-0.5	$0.513 \pm 0.008$	0.4
Gas B-3-0.1	$-0.0363 \pm 0.0003$	0.4
Gas B-3-0.3	$0.528 \pm 0.006$	0.2
Gas B-3-0.5	$0.53 \pm 0.02$	0.4
Gas C-1-0.1	$-0.0167 \pm 0.0005$	0.9
Gas C-1-0.3	$0.5973 \pm 0.0013$	0.2
Gas C-1-0.5	$0.599 \pm 0.013$	0.4
Gas C-2-0.1	$0.045 \pm 0.002$	0.1
Gas C-2-0.3	$0.617 \pm 0.011$	0.2
Gas C-2-0.5	$0.594 \pm 0.007$	0.4
Gas C-3-0.1	$-0.0153 \pm 0.0003$	0.9
Gas C-3-0.3	$0.61 \pm 0.02$	0.2
Gas C-3-0.5	$0.59 \pm 0.02$	0.4
Gas E-1-0.1	$-0.0133 \pm 0.0014$	0.9
Gas E-1-0.3	$0.5845 \pm 0.0011$	0.4
Gas E-1-0.5	$0.553 \pm 0.011$	0.8
Gas E-2-0.1	$0.034 \pm 0.004$	0.1
Gas E-2-0.3	$0.56 \pm 0.02$	0.3
Gas E-2-0.5	$0.55 \pm 0.02$	0.5
Gas E-3-0.1	$-0.0111 \pm 0.0006$	0.9
Gas E-3-0.3	$0.5657 \pm 0.0007$	0.3

	Maximum PPMC Coefficient ± Standard Deviation	F <sub>total</sub> of Predicted Reference Chromatogram
Gas E-3-0.5	$0.550 \pm 0.006$	0.6
Gas F-1-0.1	$0.030 \pm 0.004$	0.1
Gas F-1-0.3	$0.558 \pm 0.013$	0.4
Gas F-1-0.5	$0.51 \pm 0.03$	0.6
Gas F-2-0.1	$0.0150 \pm 0.0014$	0.1
Gas F-2-0.3	$0.561 \pm 0.004$	0.4
Gas F-2-0.5	$0.490 \pm 0.007$	0.5
Gas F-3-0.1	$0.0287 \pm 0.0006$	0.1
Gas F-3-0.3	$0.57 \pm 0.02$	0.4
Gas F-3-0.5	$0.52 \pm 0.02$	0.7
Gas G-1-0.1	$0.0328 \pm 0.0012$	0.1
Gas G-1-0.3	$0.560 \pm 0.003$	0.3
Gas G-1-0.5	$0.495 \pm 0.002$	0.6
Gas G-2-0.1	$0.0225 \pm 0.0011$	0.1
Gas G-2-0.3	$0.539 \pm 0.014$	0.3
Gas G-2-0.5	$0.490 \pm 0.010$	0.6
Gas G-3-0.1	$0.0120 \pm 0.0012$	0.1
Gas G-3-0.3	$0.55 \pm 0.02$	0.3
Gas G-3-0.5	$0.494 \pm 0.013$	0.6
Gas H-1-0.1	$0.014 \pm 0.002$	0.1
Gas H-1-0.3	$0.605 \pm 0.003$	0.3
Gas H-1-0.5	$0.56 \pm 0.03$	0.5
Gas H-2-0.1	$0.0394 \pm 0.0014$	0.1
Gas H-2-0.3	$0.598 \pm 0.005$	0.3
Gas H-2-0.5	$0.57 \pm 0.02$	0.5
Gas H-3-0.1	$0.025 \pm 0.002$	0.1
Gas H-3-0.3	$0.59 \pm 0.03$	0.3
Gas H-3-0.5	$0.55 \pm 0.03$	0.5

APPENDIX K. Maximum PPMC coefficients and standard deviation comparing experimental chromatograms to reference chromatogram predicted from unevaporated marine fuel stabilizer.

chromatograms to reference chromatogram predicted from unevaporated marine fuel stabilizer.  Maximum PPMC Coefficient ± F <sub>total</sub> of Predicted Reference		
	Standard Deviation	r <sub>total</sub> of Fredicted Reference Chromatogram
Gas A-1-0.1	$0.332 \pm 0.005$	0.9
Gas A-1-0.3	$0.0404 \pm 0.0013$	0.9
Gas A-1-0.5	$-0.06957 \pm 0.00004$	0.1
Gas A-2-0.1	$0.328 \pm 0.002$	0.9
Gas A-2-0.3	$0.047 \pm 0.002$	0.9
Gas A-2-0.5	$-0.0752 \pm 0.0009$	0.1
Gas A-3-0.1	$0.2866 \pm 0.0010$	0.9
Gas A-3-0.3	$0.0627 \pm 0.0007$	0.9
Gas A-3-0.5	$-0.076 \pm 0.007$	0.1
Gas B-1-0.1	$0.3482 \pm 0.0015$	0.9
Gas B-1-0.3	$0.0476 \pm 0.0004$	0.9
Gas B-1-0.5	$-0.0703 \pm 0.0008$	0.1
Gas B-2-0.1	$0.368 \pm 0.002$	0.9
Gas B-2-0.3	$0.0514 \pm 0.0005$	0.9
Gas B-2-0.5	$-0.0751 \pm 0.0006$	0.1
Gas B-3-0.1	$0.408 \pm 0.003$	0.9
Gas B-3-0.3	$0.0536 \pm 0.0008$	0.9
Gas B-3-0.5	$-0.076 \pm 0.002$	0.1
Gas C-1-0.1	$0.2955 \pm 0.0010$	0.9
Gas C-1-0.3	$0.0033 \pm 0.0002$	0.9
Gas C-1-0.5	$-0.0706 \pm 0.0011$	0.1
Gas C-2-0.1	$0.253 \pm 0.002$	0.9
Gas C-2-0.3	$0.0099 \pm 0.0005$	0.9
Gas C-2-0.5	$-0.084 \pm 0.002$	0.1
Gas C-3-0.1	$0.313 \pm 0.002$	0.9
Gas C-3-0.3	$0.0091 \pm 0.0012$	0.9
Gas C-3-0.5	$-0.0751 \pm 0.0007$	0.1
Gas E-1-0.1	$0.242 \pm 0.004$	0.9
Gas E-1-0.3	$0.0030 \pm 0.0014$	0.9
Gas E-1-0.5	$-0.078 \pm 0.004$	0.1
Gas E-2-0.1	$0.160 \pm 0.007$	0.9
Gas E-2-0.3	$-0.0591 \pm 0.0014$	0.1
Gas E-2-0.5	$-0.079 \pm 0.002$	0.1
Gas E-3-0.1	$0.246 \pm 0.002$	0.9
Gas E-3-0.3	$0.016 \pm 0.003$	0.9

	Maximum PPMC Coefficient ± Standard Deviation	F <sub>total</sub> of Predicted Reference Chromatogram
Gas E-3-0.5	$-0.0777 \pm 0.0007$	0.1
Gas F-1-0.1	$0.198 \pm 0.008$	0.9
Gas F-1-0.3	$-0.0630 \pm 0.0014$	0.1
Gas F-1-0.5	$-0.0809 \pm 0.0011$	0.1
Gas F-2-0.1	$0.2 \pm 0.2$	0.9
Gas F-2-0.3	$-0.0584 \pm 0.0005$	0.1
Gas F-2-0.5	$-0.083 \pm 0.009$	0.1
Gas F-3-0.1	$0.254 \pm 0.006$	0.9
Gas F-3-0.3	$-0.07 \pm 0.07$	0.1
Gas F-3-0.5	$-0.082 \pm 0.008$	0.1
Gas G-1-0.1	$0.2091 \pm 0.0014$	0.9
Gas G-1-0.3	$-0.0482 \pm 0.0003$	0.1
Gas G-1-0.5	$-0.0676 \pm 0.0003$	0.1
Gas G-2-0.1	$0.211 \pm 0.005$	0.9
Gas G-2-0.3	$-0.0478 \pm 0.0006$	0.1
Gas G-2-0.5	$-0.0709 \pm 0.0012$	0.1
Gas G-3-0.1	$0.1655 \pm 0.0015$	0.9
Gas G-3-0.3	$-0.0479 \pm 0.0008$	0.1
Gas G-3-0.5	$-0.0693 \pm 0.0009$	0.1
Gas H-1-0.1	$0.217 \pm 0.004$	0.9
Gas H-1-0.3	$-0.0601 \pm 0.0004$	0.1
Gas H-1-0.5	$-0.0888 \pm 0.0007$	0.1
Gas H-2-0.1	$0.1925 \pm 0.0045$	0.9
Gas H-2-0.3	$-0.0662 \pm 0.0006$	0.1
Gas H-2-0.5	$-0.096 \pm 0.003$	0.1
Gas H-3-0.1	$0.150 \pm 0.006$	0.9
Gas H-3-0.3	$-0.0619 \pm 0.0009$	0.1
Gas H-3-0.5	$-0.092 \pm 0.004$	0.1

## V. Conclusions and Future Directions

## 5.1. Conclusions

Current practices for the analysis of fire debris involve the comparison of chromatograms of extracted ignitable liquid residues to a library of reference chromatograms<sup>1</sup>. The reference chromatograms are typically chromatograms of ignitable liquids that have been experimentally evaporated to different levels. However, experimental evaporation of liquids is time consuming, so a mathematical model that could accurately predict the evaporation of ignitable liquids would provide a more time-efficient option.

This work focused on improving predictive accuracy, with respect to gasoline, of a previously developed kinetic model and further applying that model to create reference collections of accurately predicted gasoline. The reference collections were then used, in combination with reference collections of non-gasoline ignitable liquids, to determine the feasibility of using correlation coefficients to assist in the classification of ignitable liquid residues. Predictive accuracy in this case is determined through comparison of a chromatogram of experimentally evaporated gasoline to a chromatogram predicted using unevaporated gasoline of the same source to the same total fraction remaining (F<sub>total</sub>) level as the experimentally evaporated gasoline. The comparison is quantified using Pearson product-moment correlation (PPMC) coefficients. Source is defined here as a single dispensation from a single service station pump.

Improvement in predictive accuracy with respect to gasoline samples was achieved as a result of modifications to the instrument parameters and the method for calculating the fraction remaining. The solvent delay was eliminated to extend the retention index ( $I^{T}$ ) range visible, background subtraction was performed to eliminate peaks resulting from solvent impurities, and

 $F_{total}$  of the experimentally evaporated liquid was calculated based on chromatographic area rather than mass lost. The most significant change occurred with the change of  $F_{total}$  calculation method. Originally,  $F_{total}$  of the experimentally evaporated liquid was calculated using mass, the mass of gasoline after evaporation divided by the mass of gasoline before evaporation. The predicted chromatogram was then calculated to have a  $F_{total}$  equal to the  $F_{total}$  by mass. However,  $F_{total}$  for predicted chromatograms is calculated using abundance. For petroleum distillates such as torch fuel, there is no significant difference between  $FR_{total}$  by mass and  $F_{total}$  by area. For gasoline, however, the difference is significant and impacted the apparent predictive ability of the model.

When chromatograms were predicted to the experimental F<sub>total</sub> by area, the PPMC coefficient calculated between the experimental and predicted chromatograms increased, with increases ranging from 0.006 to 0.258. The new PPMC coefficient range is above the 0.8 cutoff for strong correlation, and more closely corresponds with that found for petroleum distillates with all PPMC coefficients calculated to be greater than 0.90. The mathematical model is therefore capable of accurately predicting the evaporation of gasoline. This proven accuracy allows the model to be employed to create reference collections of predicted chromatograms for gasoline.

Currently, comparisons between chromatograms of questioned samples and reference collections involve visual comparison of chromatographic pattern as well as comparison of specific compound types and ratios, with no statistical component. A possible statistical method could employ comparisons using PPMC coefficients. These coefficients and comparisons will only be valuable if there are clear PPMC coefficient limits above which a chromatogram can be positively identified as belonging to a certain ignitable liquid class or subclass. These clear

limits can be developed through intra- and inter-class comparisons of predicted and experimental chromatograms, with a limit only possible when the lowest intra-class comparison PPMC coefficient is higher than the higher inter-class comparison PPMC coefficient.

In this research, experimental chromatograms from one gasoline were compared to reference chromatograms from six other gasoline samples. The experimental chromatograms were also compared to reference collections generated for ignitable liquids representative of four other ASTM classes. The maximum PPMC coefficient was determined for each comparison to a reference collection. The range of maximum PPMC coefficients for comparisons of experimentally evaporated gasoline to a predicted gasoline reference chromatogram was greater than the range of maximum coefficients found for comparisons of experimentally evaporated gasoline to predicted non-gasoline reference chromatograms. This suggests that it may be possible, at least with gasoline, to develop limits above which a sample can be positively identified as gasoline based on the PPMC coefficient.

## 5.2. Future Directions

In this research the equation used for prediction purposes was developed by McIlroy et al. for the retention index range 800-2200. In this work, however, the model was used for prediction purposes for retention indices as low as  $I^T = 500$ . This work presumed the trend observed by McIlroy et al. would continue at lower retention indices and therefore used the model with no modifications at these lower retention indices<sup>2</sup>. It is possible, however, that the relation between retention index and rate constant does not remain constant at retention indices less than 800. To ensure the most accurate model is being used for predictive purposes, a similar process to that originally performed by McIlroy et al. should be employed. Compounds of

multiple compound classes (*n*-alkanes, polycyclic aromatic hydrocarbons, etc.) should be experimentally evaporated for different periods of time and decay curves determined. The rate constants calculated from these decay curves can be plotted against retention index in order to determine an equation that relates the two. If the equation developed with the earlier retention index range is sufficiently similar to that developed by McIlroy *et al.*, the data from the two retention index ranges can be combined to calculate an inclusive model. If the equations for the two retention index ranges are different, however, it may be necessary to use different models when predicting the evaporation of different retention index ranges.

In this work, source was defined as a single dispensation from a gasoline service station pump on a specific day. While useful, this definition does not address the complexities of source definitions. Multiple service stations in a similar location may receive gasoline from the same supplier, meaning they share a source defined a different way. Additionally, samples collected from the same service station from a different pump, different day, or even different time could be considered the same source. Despite these common origins, however, there may be slight differences in terms of fill level of the holding tank from which the gasoline is drawn. A lower fill level in the tank may lend itself to greater evaporation of more volatile compounds, slightly changing the composition of the sample removed. Comparison of chromatograms predicted using an "unevaporated" sample from a day when the fill level of the tank was low to chromatograms of experimentally evaporated gasoline from a day when the fill level of the tank was high may lead to the maximum PPMC coefficient occurring at a different F<sub>total</sub> level than comparison to chromatograms predicted from "unevaporated" gasoline from the same day. The change will likely not be enough to cause the sample to not be classified as gasoline, but the issue should still be discussed.

More relevant to this work, all samples were collected from service stations within a 5mile radius, and in two cases two gasoline samples were collected on the same day. These samples may not actually be different enough to be considered as originating from a different source, therefore. Comparisons were made between reference collections and experimental chromatograms of samples from different service stations in order to determine an intra-class PPMC coefficient range. However, since these service stations were so close together and samples were collected on similar days, these gasoline samples may not be sufficient to determine an intra-class PPMC coefficient range. Expansion of this testing should include gasolines collected from service stations from a wider radius, over a longer period of time, and including multiple octane ratings. Comparison of reference and experimental chromatograms from gasoline samples differing in all the aforementioned variables will provide a more robust intra-class PPMC coefficient range. Additionally, it may be discovered that different locations, seasons, or octane ratings are sufficiently different that the intra- and inter-class PPMC coefficient ranges overlap. If this is determined, it may be possible to separate gasoline into subclasses within which PPMC coefficient ranges are sufficiently high to be distinguishable from other ignitable liquid classes or subclasses.

Intra-class comparisons should also be conducted for other ignitable liquid classes and subclasses. Most likely, subclasses will need to include different alkane ranges (light, medium, and heavy), as well as potentially further sub-classification based on intended use. Concurrently with intra-class comparisons, inter-class comparisons should be conducted between experimental chromatograms of one class or subclass and reference chromatograms of all other classes or subclasses, and vice versa. Maximum PPMC coefficients calculated from inter-class comparisons can be used with the maximum PPMC coefficient range for intra-class comparisons

to determine if a class is sufficiently different from all other classes to be classified based on PPMC coefficients.

While evaporation is an important contribution to changing composition of an ignitable liquid during a fire, substrate interference and pyrolysis products from both the ignitable liquid and the substrate can also affect the composition. Previous work by Smith *et al.* described PPMC coefficients of approximately 0.2 when comparing a gasoline reference collection to a chromatogram of a gasoline sample burned on a substrate<sup>3</sup>. It may be possible to determine chromatographic peaks (and corresponding compounds) characteristic of burned substrates that are not present in ignitable liquids. If identified, these peaks could be subtracted from chromatograms when present. It may also be possible to analyze an ignitable liquid that was ignited on a relatively inert surface, so as to note specific pyrolysis products originating from the ignitable liquid. By analyzing burned substrates alone, burned ignitable liquids alone, and burned substrates spiked with ignitable liquids, a method may be able to be developed to result in chromatograms more representative of the ignitable liquid from a fire debris sample.

Through incorporation of suggestions discussed in this section, this model has the potential for application in fire debris analysis. Validations with other ignitable liquid classes is certainly required to ensure the model is capable of accurately predicting the evaporation of all ignitable liquid samples. Additionally, development of PPMC coefficient ranges require a larger, more varied sample set to ensure ranges encompass the variety of samples that might be encountered in fire debris analysis. With this further research, however, this model certainly could be a valuable asset to fire debris analysts.

**REFERENCES** 

## **REFERENCES**

- 1. ASTM E1618-14, Standard Test Method for Ignitable Liquid Residues in Extracts from Fire Debris Samples by Gas Chromatography–Mass Spectrometry. ASTM International, West Conshohocken, PA, 2014.
- 2. McIlroy, J.W., Jones, A.D., McGuffin, V.L., Gas Chromatographic Retention Index as a Basis for Predicting Evaporation Rates of Complex Mixtures. Anal. Chim. Acta 2014, Sep; 852: 257-66
- 3. Smith, R.W., Brehe, R.J., McIlroy, J.W., McGuffin, V.L., Mathematically Modeling Chromatograms of Evaporated Ignitable Liquids for Fire Debris Applications. Forensic Chemistry 2016, Jan; 2: 37-45.